

NRL Report 6300

UNCLASSIFIED

# Review of Concepts and Status of Procedures for Fracture-Safe Design of Complex Welded Structures Involving Metals of Low to Ultra-High Strength Levels

W. S. PELLINI, R. J. GOODE, P. P. PUZAK,  
E. A. LANGE AND R. W. HUBER

*Metallurgy Division*

June 1965



U.S. NAVAL RESEARCH LABORATORY  
Washington, D.C.

## CONTENTS

Abstract	iii
Problem Status	iv
Authorization	iv
Acknowledgments	v
INTRODUCTION	1
GENERAL DESCRIPTION OF THE USE AND INTERPRETATION OF THE DROP-WEIGHT TEAR TEST	7
SIMPLIFIED PROCEDURES FOR "CAT" CURVE DETERMINATIONS	11
EVOLUTION OF FRACTURE TOUGHNESS INDEX DIAGRAM FOR HIGH STRENGTH STEELS	17
Effect of Anisotropy	22
DWT T Tests in the Transition Temperature Range of High Strength Steels	25
Fracture Toughness Index Diagram for High Strength Steel	27
Applicability of $C_v$ Test	30
Consideration of Fatigue Crack Modified $C_v$ Tests	30
EVOLUTION OF FRACTURE TOUGHNESS INDEX DIAGRAM FOR TITANIUM ALLOYS	34
EVOLUTION OF FRACTURE TOUGHNESS INDEX DIAGRAM FOR ALUMINUM ALLOYS	42
CONSIDERATION OF THICKNESS EFFECTS	48
EVALUATION AND CONTROL OF WELD METAL PROPERTIES	52
EVALUATION AND CONTROL OF HEAT-AFFECTED-ZONE PROPERTIES	55
MICROMECHANISMS OF FRACTURE PROCESSES	57
IMPLICATIONS OF STRESS-CORROSION-CRACKING ASPECTS	62
IMPLICATIONS OF LOW CYCLE FATIGUE CRACK PROPAGATION ASPECTS	67
STATISTICAL PROBLEMS IN APPLICATIONS OF LOW FRACTURE TOUGHNESS METALS	77
SUMMARIZATION OF TECHNOLOGICAL IMPLICATIONS	80
REFERENCES	83

## ABSTRACT

This report presents integrated analyses and substantiating data on problems of metallurgical optimization and solutions to fracture-safe design and fabrication of large welded structures, utilizing high strength metals. The apparent complexities of attaining practical engineering use of high strength metals derive primarily from lack of appreciation of the close interrelationships that exist between the intrinsic susceptibilities of these metals to various failure modes and the intrinsic structural mechanics features of the structures. Metals of high intrinsic resistance to failure may be matched to structures of high intrinsic design complexity and ordinary fabrication techniques, with assurance of structural safety. Metals of low intrinsic resistance to failure must be matched only to structures that are exactly stress analyzable and thereby are restricted to designs of the utmost attainable simplicity and to fabrication by techniques of utmost precision. Such separations are basic to the theme of this report and provide the "starting point" for analyses of the potentials of utilizing various metals, within the range of metallurgically attainable strength levels. The metallurgical problems of optimizing the base metals, welds and heat-affected zones have been complicated by the absence of parametric "frames of reference" required as bases of comparison. The absence of such broad-base guide lines arises from the failure to evolve an adequate understanding of the significance of conventional engineering tests and from the previous absence of definitive tests that provide assessment of failure mode sensitivities across the full spectrum of materials and attainable strength levels. The development of such test procedures has been one of the principal aims of the investigations conducted by the authors and their associates. The spectrum view that has emerged clearly defines metals and specific strength ranges that provide for matching to applications involving conventional fabrication of complex structures as compared to those that require exact design and fabrication. Thus, applications that may provide fracture-safe design based on the use of simple engineering test methods may be separated from applications that require the exact mathematical analyses of fracture mechanics.

## PROBLEM STATUS

This is a special summary progress report covering the results of a wide spectrum of integrated investigations within the Metallurgy Division of NRL, aimed at the general problem of metallurgical optimization and fracture-safe design use of high strength metals in welded structures. The major portions of the studies are continuing under the general "core effort" informal categorization of "Principles of Fracture-Safe Design," including various officially established problem and sub-task categories, defined below.

## AUTHORIZATION

NRL Problem F01-17; Project SP-00405  
NRL Problem M01-05; Projects SF 020-01-01-0724,  
RR 007-01-46-5405, and WW-041 (R05-24A)  
NRL Problem M01-18; Projects SF 020-01-05-0731,  
RR 007-01-46-5420, WW-041 (R05-24B), and MIPR Eng-Nav-65-12  
NRL Problem M03-01; Projects SF 020-01-01-0850 and  
SF 020-01-01-0854

Manuscript submitted May 24, 1965.

### ACKNOWLEDGMENTS

In addition to the specialized professional contributions of members of the Metallurgy Division of the Naval Research Laboratory cited in the text, the authors gratefully recognize independent contributions of major professional importance on the part of associates that have been closely involved in the fracture and fatigue studies—these include: R. W. Judy, Jr., T. W. Crooker, C. N. Freed, D. G. Howe, and R. E. Morey.

The authors are particularly grateful for the financial assistance provided for the past and continuing aspects of these studies by Mr. George Sorkin and Mr. T. Griffin of the Bureau of Ships; Mr. H. Bernstein of the Navy Special Projects Office; Mr. M. L. Martin of the Army Corps of Engineers, and by our parent organization, the Office of Naval Research.

REVIEW OF CONCEPTS AND STATUS OF PROCEDURES  
FOR FRACTURE-SAFE DESIGN OF COMPLEX WELDED STRUCTURES  
INVOLVING METALS OF LOW TO ULTRA-HIGH STRENGTH LEVELS

UNCLASSIFIED

INTRODUCTION

If we stand off far enough from the multitudinous details and litigations of specimen designs and interpretations and survey the general field of fracture-safe design with reasonable detachment, it becomes clear that there is need for a variety of approaches to the problem and that there are no "one method" panacea. This conclusion derives from recognition of a simple, yet fundamental fact that structural design problems cover a wide spectrum – this fact may be appreciated by considering a broad split of the spectrum in terms of two generic classes of "structures" requiring fracture-safe design consideration:

(1) Structures that are rigorously stress analyzable at all locations. Such analyses are not within the state of the art of ordinary computational design procedures and are attainable only by strain gaging and/or photoelastic stress analysis of representative models. Such structures generally feature the utmost attainable geometric simplicity and require exacting retention of the design features by fabrication with "watchmaking" finesse. Rocket cases and aircraft components fall into this class.

(2) Structures that are stress analyzable in the usual "rough" sense, particularly, only in regions of relative geometric simplicity. Many regions of such structures are simply considered "stress indeterminate," and the natural plasticity of the metal is counted upon to provide for adjustment and redistribution of loads at points of geometric complexity. Ordinary fabrication practices (out of roundness, slight mismatch at points of connection, residual stresses, etc.) further compound the stress-indeterminate nature of the complex regions and degrade the accuracy of computational stress analyses even for the remaining regions of relatively simple geometry.

Now, any fracture-safe analysis method that depends on exact knowledge of flaw size and stress level in the elastic range must necessarily relate to structures that are "in fact" rigorously stress determinate at all positions. The virtue of the linear elastic analysis (fracture mechanics) approach lies in its potential capability for mathematically defining critical levels of flaw size and stress. For relatively brittle materials that may be considered critically sensitive to the presence of flaws in the elastic range, safe structures may be constructed by such procedures, provided exact knowledge of the stress level and the flaw size at all positions of interest is available. We endorse and use this approach as the only feasible route by which such metals may be used.

To illustrate this case, we may consider Fig. 1 which presents the "upper bound" (best values) limits of plane strain fracture toughness ( $K_{Ic}$ ) for two broad groupings of steels in the 1/2 to 1-in. thickness range. This figure represents a summary compilation by the authors of the highest recorded values resulting from tests of these two groups of steels by various qualified laboratories. Note that critical flaw sizes calculated by fracture mechanics procedures for yield stress and one-half yield stress levels are presented in connection with the higher of the two "upper bound" limit curves. These critical sizes are for flaws of relatively long dimension with respect to depth (10-1 ratio), commonly known as the "worst" case. It is obvious from this figure that as the  $K_{Ic}$  value approaches

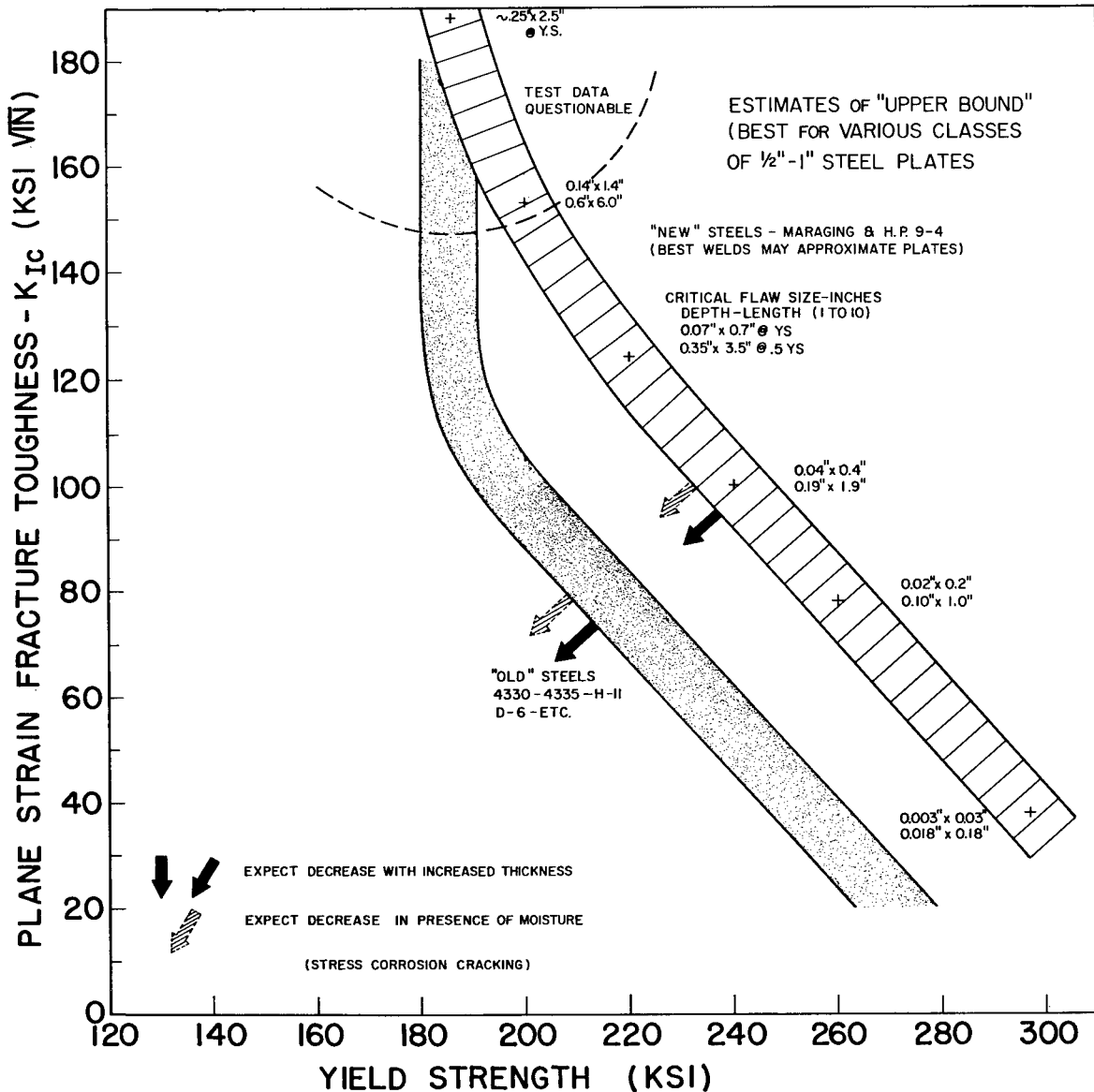


Fig. 1 - Upper bound, best value, limits of plane strain fracture toughness ( $K_{Ic}$ ) for 1/2- to 1-in. plates of high strength steels, as reported by various qualified laboratories

180 ksi  $\sqrt{\text{in}}$ , the critical flaw size for steels of the respective strength level increases to the order of 0.25-in. depth for yield point stresses. In general the accuracy of measurement of  $K_{Ic}$  values in the range of 150-180 ksi  $\sqrt{\text{in}}$ , for the specified thickness, becomes questionable because of the development of an excessive plastic zone size at the crack tip. The implication of the almost vertical "upswing" of the curves in the 180-200 ksi yield strength (YS) range, for the subject "best" steels of this thickness, is that further decrease in YS level would result in very high increase in fracture toughness. Thus, at strength levels below 180 ksi YS, the high order of metallurgically attainable fracture toughness may be measurable readily by simple test methods - this fact is discussed in greater detail in the sections to follow. Another point to note is that by increasing the strength level to above 240 ksi YS, the critical flaw size decreases to exceedingly small values depending on the level of applied elastic stress. In the range of roughly 200 to 250 ksi YS (depending on stress level) it is absolutely necessary to have exact knowledge of

stress level and of flaw sizes; this implies use of flaw inspection techniques which would make such definition certain. Above the 240-250 ksi YS range, flaw inspectability becomes essentially impossible because of the minuteness of the critical flaw sizes, even for stresses considerably below yield levels.

As indicated by the bold arrows in Fig. 1, metallurgical effects due to increased thickness will result in decrease of the  $K_{Ic}$  levels of the two "upper bound" curves. Effects due to environment, such as the presence of water (stress corrosion cracking) are known to additionally decrease the  $K_{Ic}$  levels, as will be discussed. Thus, from an optimum materials point of view and for steels of the cited thickness range for which data are available, there is a relatively narrow range of strength for which the exact techniques of fracture mechanics may be applied with confidence, provided environmental effects are additionally considered. To disregard such exactness is to court disaster in the use of the best attainable steels of the cited thickness at strength levels in excess of 200 ksi YS. In a broader sense, this statement applies to any steel or other metal that falls roughly in the 50 to 150  $K_{Ic}$  fracture toughness range. Again, it should be emphasized that exactness is necessary not only in measurement of the  $K_{Ic}$  value, but also with respect to knowledge of stress levels and flaw sizes - these requirements must be met simultaneously. The evolution of fracture mechanics analyses procedures may be credited with making feasible the use of metals in the ultra-high strength range. Investigators in this field are therefore to be commended for attainments of critical importance to fracture-safe design.

Now, a problem arises in that the application of fracture mechanics in the treatment of fracture-safe design is considered by many as the only potentially certain method for coping with all fracture-safe design problems. Other approaches lacking the sophistication of mathematical calculation are too often considered crudity - we challenge such attitudes and consider such thinking of a singular approach to the general problem as basically unrealistic. The major tonnages of engineering structures are designed and fabricated by methods that defy the application of such exact stress and flaw size analyses. Moreover, a large bulk of available structural materials in the intermediate and high strength range can be melted, processed and heat treated to develop fracture toughness levels that presently defy valid measurement by linear elastic analysis techniques. Simple engineering tests can be used to determine, specify, and quality-control materials of fracture toughness properties that fall outside the province of presently established fracture mechanics definition. To the extent that such simple test procedures may be used, it is then possible to design and fabricate ordinary structures with complete safety. In other words, materials of high fracture toughness do not require and do not allow for ultra-refined, mathematically based, fracture-safe design procedures. The validity of this fact must be recognized and accepted on the same basis as it is recognized and accepted that metals of low fracture toughness cannot be used without the application of the utmost finesse in all respects and that fracture mechanics procedures are essential. There is a place for a simple "tinkers job" as well as for a refined "tailors job," both are honorable professions. Thus, we should not impose unrealistically uniform procedures of rigorous stress analysis and fabrication finesse on structures built of materials that do not require such treatment. The basic question then becomes how to identify a material as falling in the class of being fracture-safe for use in complex structures or falling into the class that it can only be used with the utmost of design and fabrication finesse. The delineation between the two categories is not difficult and is readily definable by the use of relatively simple procedures. This point is often missed and is not generally understood. A few introductory examples will suffice to explain this situation at this point and the body of this report will further highlight the reality of this statement.

As a first example, let us consider low strength steels having sharply defined transition temperature features. For such materials the temperature range of nil-ductility transition (NDT) to  $NDT + 30^{\circ}F$  marks the separation between material of relatively low fracture toughness and material of relatively high fracture toughness. If we carry the

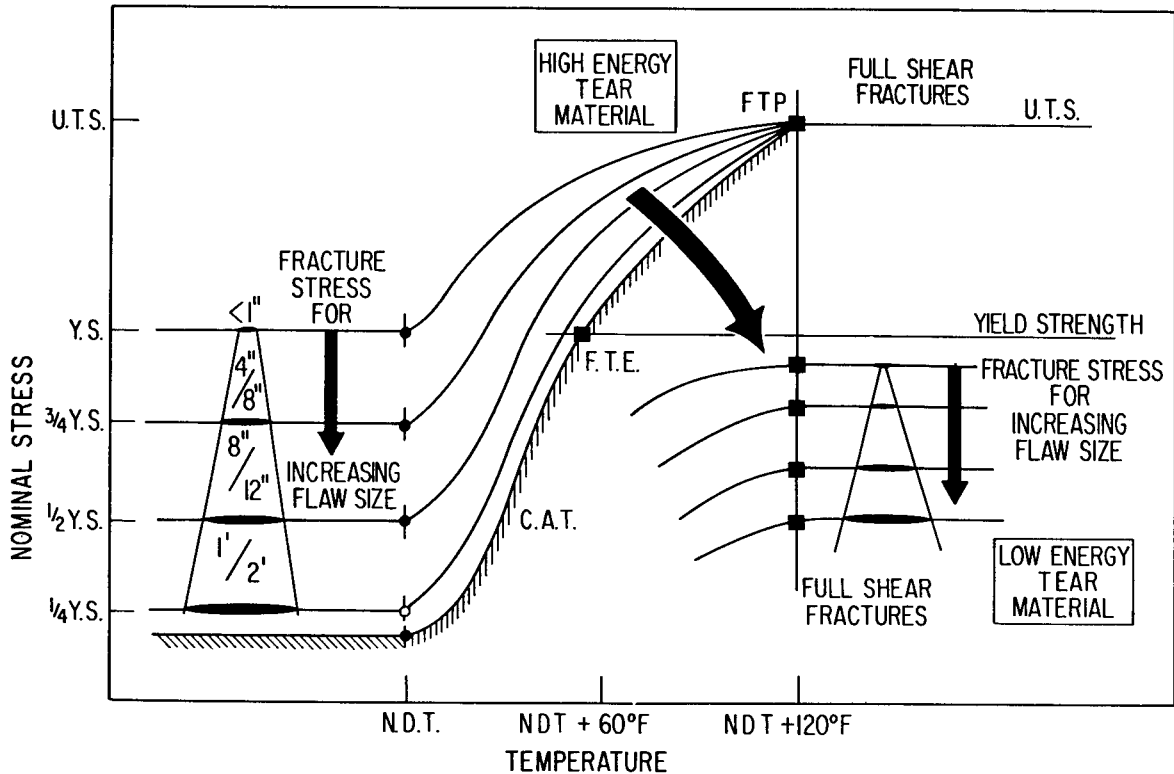
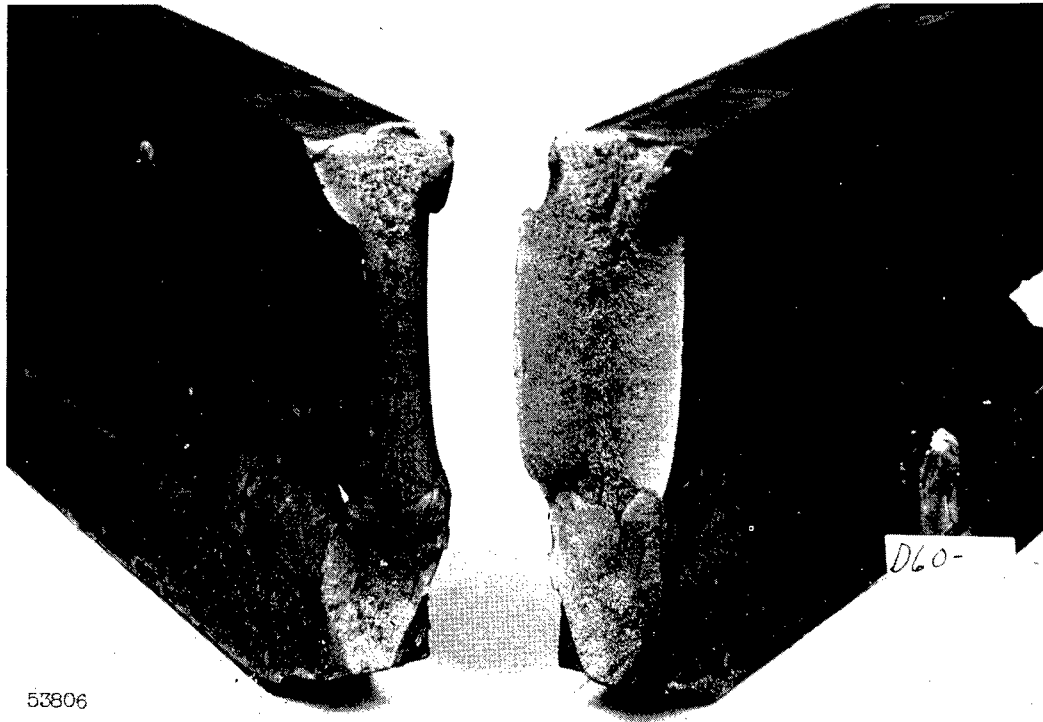


Fig. 2 - Fracture Analysis Diagram and conceptual modifications for steels of decreasing levels of fracture toughness in the fully ductile mode - noted as "low energy tear" for the low levels.

temperature to  $NDT + 60^{\circ}F$ , a much higher level of fracture toughness is obtainable. The Fracture Analysis Diagram, Fig. 2, clearly illustrates the stress level-indexed increase in critical flaw size and crack arrest temperature (CAT), with increasing temperature above the NDT temperature; references (1, 2, and 3) provide detailed description of the derivation and use of the NDT indexed, Fracture Analysis Diagram. It is a simple and adequate engineering, fracture-safe design procedure for low strength steels that have a sharply defined transition temperature and high fracture toughness in the fully ductile (ductile tearing fracture) state. A perfectly logical question would be - do we need an exact procedure for complex structures that are stress analyzable and flaw size inspectable only within crude limits? Moreover, for ordinary steels of low strength level, for which this method is clearly applicable, there are no other developed and proven methods available at this time or in the foreseeable near future.

As a second example, let us consider metals that do not develop definite temperature transition features; or that develop a gradual "fading out" of such features with increasing strength level, such as steels that ultimately fall to very low levels of "upper shelf" (ductile tearing) energy. Figure 2 illustrates schematically the basic effect of decreasing ductile tear energy in terms of the Fracture Analysis Diagram (4). From the known "downward rotation" of the CAT curve of the diagram, there emerges the possibility of developing and utilizing a simple test method which defines whether or not a steel can propagate fractures at levels of general stress below yield, at "shelf" temperatures of maximum fracture toughness. Such a test method could then be used in designating high strength steels (or other metals) of ductile tear energy levels that do not require sophisticated flaw size and stress analyses as compared to those that would require such analysis. Such a simple "first cut" separation is of considerable value and if we had such a test method, we should use it.



53806

Fig. 3 - Fracture appearance of a drop-weight tear test (DWTT) specimen representing a 1-in.-thick steel plate of high fracture toughness; brittle bar type test specimen

The crux of the exposition to this point is - why attempt to develop highly sophisticated fracture-safe design procedures for a metal that does not require it? Also, it poses a metallurgical challenge for evolving metals that are of this class to the highest possible strength level. Such metallurgical attainment provides a most valuable flexibility to designers and fabricators. Specifically, such flexibility relates to the privilege of designing and fabricating with assurance that stress level errors at points of design complexity will not place the structure in danger. Designers and fabricators of "ordinary" structures require such assurance - for the simple reason that without metals of such inherent tolerance for plastic flow, the "ordinary" must be discarded with resort to the difficulties and costs of ultra-precise design and fabrication practices.

Such thinking has led us to proceed beyond the DWT (drop-weight test) evolution of the NDT indexed, Fracture Analysis Diagram, in the direction of new tests and fracture toughness index diagrams of similar simplicity but with the potential of application "across the board" to all types of metals and specifically including the non-transition and low energy tear types. This test approach was first conceived by Pellini, late in 1961, immediately following the evolution of concepts that led to publication of the Fracture Analysis Diagram (5). In order to cover the full spectrum of materials, it was decided that the test should measure energy absorption in the process of propagation of a fracture. The original concept of the DWT (NDT) was to use a brittle weld crack to determine the temperature point of nil ductility in the presence of a natural sharp crack. The basic concept of the new test was to measure fracture propagation energy starting with a similar, natural (brittle) crack as the flaw condition. As a first approach, the DWT (NDT) specimen turned on its side with the added feature of a brittle bar welded to the tension side, appeared to serve the purpose of the concept. Figure 3 illustrates such a specimen after fracture, for a steel of high fracture toughness. On drop-weight loading, the brittle bar fractures

and transmits a brittle crack through a brittle weld connection to the test material. For a metal of high fracture toughness in the propagating mode, this results in high energy absorption in the process of tearing through the test element and a high value of breaking energy is recorded – for a metal of low fracture toughness characteristics a low value of breaking energy is recorded. Because of the initial use of drop-weight test equipment to determine the value of energy absorption, the test method was identified as the drop-weight tear test (DWTT). Extensive testing of a wide variety of metals has been conducted at NRL since 1962 based on this test; with development of experience in its use, modifications of the basic design were evolved aimed at the simplification of specimen preparation. It is one of the principal purposes of this report to present the status of development of the DWTT in its various modifications and of the interpretation of the resulting data in terms of novel Fracture Toughness Index Diagrams for fracture-safe design. It should be understood that while there has been substantial accomplishments of these aims, both aspects cited are in a stage of continuing development and refinement. In relation to these aspects, the following sections of this document must be considered in the nature of a progress report aimed at indicating the long range practical potentialities of such an approach. Other test techniques and subject matter bearing on the fracture-safe design subject are also covered in keeping with the broad objectives of the report.

Inasmuch as the micromechanisms of fracture are important in establishing the level of energy absorption in fracture propagation, a brief summary will be presented of this aspect. Also, there are discussions of low cycle fatigue and stress corrosion cracking which may result in the enlargement of flaw sizes (slow crack growth) for metals of both high and low fracture propagation resistance. The importance of these additional discussions is to emphasize that what are ordinarily considered “slow” crack growth processes may be relatively rapid from engineering points of view, under certain conditions and for specific materials – even for metals of high fracture toughness and therefore high resistance to fast fracture propagation. For metals of low resistance to fracture propagation, minor enlargement of flaw sizes by “slow” growth processes may have catastrophic results.

GENERAL DESCRIPTION OF THE USE AND INTERPRETATION  
OF THE DROP-WEIGHT TEAR TEST

UNCLASSIFIED

The drop-weight tear test (DWTT) may be used to define the temperature region of sharp rise of the crack arrest temperature (CAT) curve from the lower shelf, commonly known as the "Robertson" lower shelf. This is the 5-8 ksi, minimum stress level for fracture propagation that is applicable to temperatures at and below the Fracture Analysis Diagram, nil-ductility transition (NDT) temperature. It should be understood that a rapidly rising CAT curve in the temperature range above the NDT is specific to steels characterized by relatively "sharp" transition temperature characteristics. The rate of rise with temperature for CAT curves is believed to be relatively invariant for low strength, steels of the common structural variety and has been explored primarily for 3/4 to 1-in. plates. The CAT curve rise features may be expected (conceptually) to depend to some degree on the relative sharpness of the transition temperature of other types of steels. Also, there are indications in the literature that for plates of (3 - 4-in. thickness) the rate of rise is affected (CAT curve moved 20°-30° F to right at the low end) by the increased plate thickness. In other words, the CAT curve "fix" deduced from the NDT temperature point of the Fracture Analysis Diagram is somewhat open to discussion on points of "fine" differences. For general engineering use, it is believed to represent an adequate representation for the common grades of low strength steels that feature "through thickness" fracture toughness uniformity. Metallurgical effects of increased thickness are properly accounted for by increase in the NDT temperature and thereby a temperature shift of the Fracture Analysis Diagram.

The DWTT is believed to offer considerable promise in predicting the specific CAT curve rise features of steels without recourse to complex, large scale, crack arrest tests. The complexities of such large scale tests have been the basic reason for the lack of information relative to CAT curves for thick materials, and for the wide variety of new Q&T (quench and temper) low alloy steels. Unless much simpler methods for developing this information are found, it is unlikely that extensive CAT curve data will be evolved in the near future, despite its evident need.

The DWTT test is not capable of following the full course of the CAT curve (to its highest limits) because of the relatively low level of elastic bending stresses in the advance of the crack front which generally results in "arrests" at temperatures of 30° - 40° F above the NDT. This is specifically predictable from the Fracture Analysis Diagram CAT curve. At the "toe" portion of the CAT curve, adequate stress levels for DWTT fracture propagation without arrests are available, and the toe region thus is definable, as will be documented in a section to follow. This concept led to the proposal in early 1962 by NRL investigators that steels of less than 5/8-in. thickness could effectively be evaluated by the DWTT to determine the toe region of the CAT curve and in effect could indicate the NDT position, despite the fact that the standard DWT (NDT) test could not be used for "thin" steels. Subsequent NRL experimentation proved this was the case. In 1962, a prediction of exact equivalence in DWTT fracture appearance with gas-line burst tests, at temperatures close to the NDT, was made first to Bethlehem Steel Corp. Laboratory (BSCL) personnel, and then to the Battelle Memorial Institute (BMI) investigators of gas-line steels. In early 1963, the DWTT was again recommended for this application when a review of the NRL studies was given to the AISI Subcommittee on Line Pipe Research which included representatives from all major line pipe producers (6).

We must credit BMI and the BSCL investigators for development of proof of the value of the DWTT for thin sections (7,8). It was found independently by NRL, BMI, and BSCL that a brittle crack starting element was not needed for the simple purpose of determination of the toe region temperature location of the CAT curve. A sharp notch, such as the pressed knife edge type, suffices. It was also determined that the CAT curve toe region could be defined by energy absorption measurements or simply by observation of the fracture appearance. With the latter criterion, studies by Battelle and Bethlehem investigators have shown that the full scale fracture propagation characteristics of gas line pipe can be predicted from laboratory DWTT test results. Thus, it is now firmly established that the DWTT provides accurate predictions of the CAT curve, toe region temperature range for "thin" steels.

We believe, but have not yet proven, that similar, simple CAT curve toe region determinations may be made for the more complex problem of transition temperature steels having fracture toughness gradients through the thickness, irrespective of plate thickness. This requires that a full thickness test be conducted. In effect, this prediction is based on the reasonable concept that the test should integrate the composite fracture toughness through the thickness. Accordingly, the DWTT method should be of considerable interest for the rapidly evolving family of spray-cooled, low alloy steels which generally feature marked Charpy V ( $C_v$ ) and DWT determined NDT fracture toughness gradients from surface to center of the section. These steels are presently being used without the benefit of exact definition of their "composite" fracture toughness and are generally indexed by  $1/4T$  (thickness)  $C_v$  values of debatable significance. It may also be predicted that the DWTT would allow for evaluating the effects of very severe cold work - a condition for which the use of DWT is not recommended because of the change in HAZ properties adjoining the brittle weld in a direction of improved toughness. Again, this is an unexplored area and the use is offered as a suggestion of potential value.

The NRL efforts following the initial exploratory tests of thin section steels were directed primarily to problems of evaluating high strength steels, steels of suspected low tear energy properties irrespective of strength level, and essentially non-transition metals such as titanium and aluminum. The foremost aim was to develop (as a first step) the DWTT test to a point that it would predict whether or not a particular metal required stresses above yield for fracture propagation. Also, to determine the degree of plastic overload that was required for fracture propagation of metals featuring very high fracture toughness.

To accomplish the above aims, it was necessary to conduct interpretive, correlating tests on a reasonably large section of plate that could be considered as a structure prototype element. For this purpose, NRL developed the explosion tear test (ETT) which features a  $2T$  (2 times the thickness) through-crack in a brittle weld "patch" region. Loading is accomplished by bulging to a cylindrical configuration so as to maintain a nearly constant stress field ahead of the propagating fracture - ductile or brittle. Figure 4 illustrates "flat break" fracture performance (fracture propagated below yield stresses) and Fig. 5, a fracture which required a level of 5% plastic strain for propagation. A large number of such tests were conducted to determine the level of plastic strain (measured by a grid) that was required for propagation of the fracture across the test plate. The general features of this structural prototype test will be discussed in detail in a section to follow.

The strain levels of fracture propagation resistance indicated by the ETT are highly reproducible and thus provided for correlation with the likewise highly reproducible DWTT energy values. At the present stage of development, the DWTT energy value is obtained first and is used to closely predict the ETT fracture propagation resistance. All such

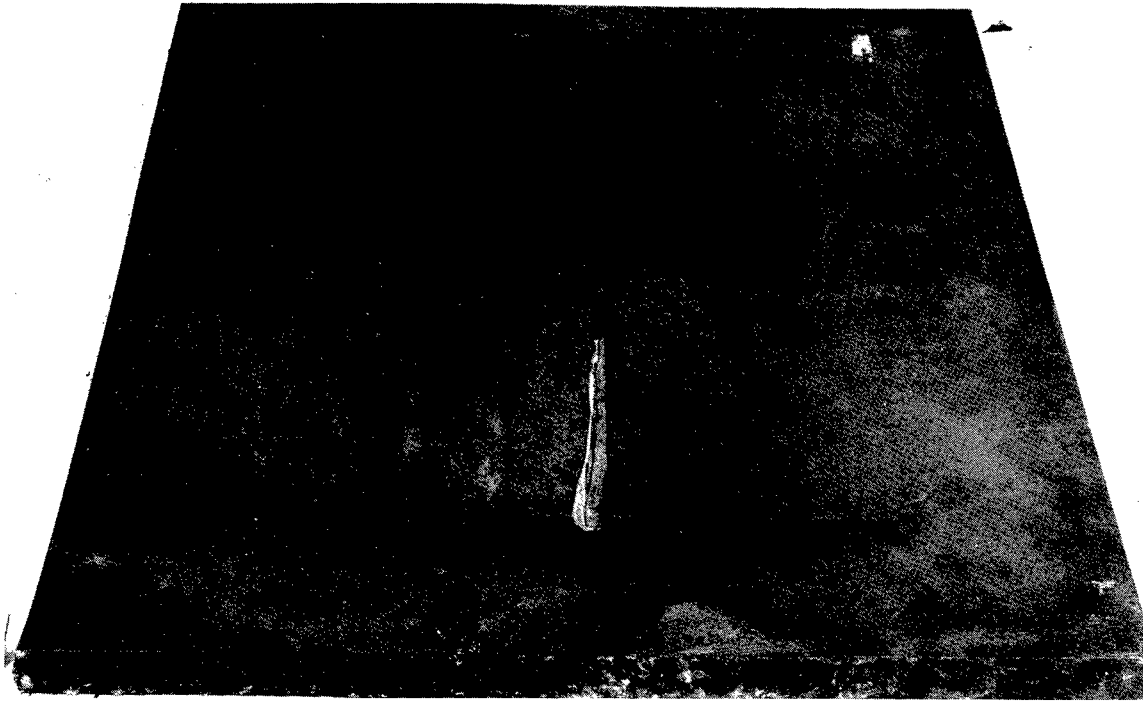


Fig. 4 - Explosion tear test (ETT) of 1-in. steel plate, illustrating "flat break" performance indicative of fracture propagation at nominal stresses below yield strength level

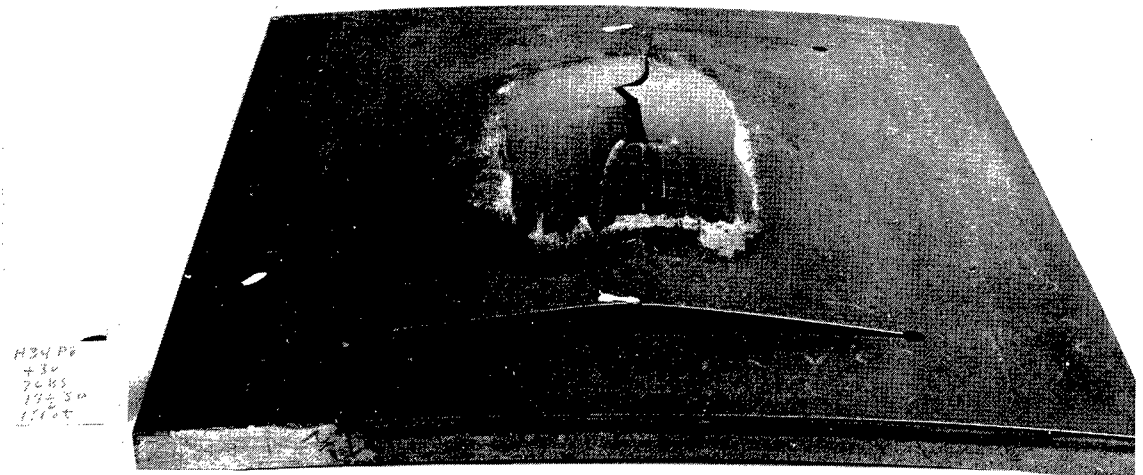


Fig. 5 - Explosion tear test (ETT) of 1-in. steel plate, illustrating performance indicative of plastic strain requirement for fracture propagation

correlation or "indexing" tests for transition temperature type steels have been conducted at temperatures of maximum energy absorption - i.e., at temperatures of the upper shelf of the DWTT vs temperature curve. For non-transition temperature metals, such precautions are not necessary.

The above correlation approach permits comparison of fracture characteristics of a broad spectrum of metals and strength levels at any specific stage of their development. As the particular metal is improved the summary charts clearly indicate the degree of improvement. The significance of DWTT energy vs metal yield strength plots which define "upper bound" i.e., presently best attainable properties (plots to be presented) is that above a specific and rather narrow "critical" range of yield strength it is not possible to procure a given metal with properties such that fracture propagation would be resisted to above yield stress loading. Below this "critical" strength range level, the best steels or other metals cited can be expected propagate to fractures only if plastic overload stress levels are applied. We have taken this "critical" range as the point of separation between metals of a given family that require fracture mechanics design methods and metals that do not require such refined procedures. The logic of this separation is that fracture propagation through elastic load regions is not possible for the latter type, irrespective of flaw sizes.

Throughout this test program, attempts were made to correlate  $C_v$  test data and fatigue cracked  $C_v$  test data with DWTT values and ETT performance. Within limits, the  $C_v$  test may be used as a reasonable index; however, there are limitations that will be discussed.

## SIMPLIFIED PROCEDURES FOR "CAT" CURVE DETERMINATIONS

CLASSIFIED

As described previously, the drop-weight tear test (DWTT) may be utilized to define the temperature region of sharp rise of the crack arrest temperature (CAT) curve from the "Robertson" lower shelf. We shall now present data to document that the DWTT exactly indexes the CAT curve indicated by the Fracture Analysis Diagram for the relatively simple case of steels featuring through-thickness uniformity; even if conducted as a sub-size design version (small size test piece) using a pressed knife edge, sharp notch. The importance of conducting full thickness DWTT for determinations of the more mechanically complex, non-homogeneous steels and for otherwise unexplored thick steels is illustrated by through-thickness sub-size DWTT and by Charpy V ( $C_v$ ) data for such steels.

The course of evolution of the notch configuration of the DWTT specimen used as a CAT curve index by BMI, BSCL and NRL followed independent courses, but finally focused collectively on the use of a simple mechanical notch. The NRL "brittle bar" type of specimen first used (see detailed description in section on high strength steels) was independently found not to be necessary for the CAT curve "toe region" determination of thin steels featuring a sharp fracture toughness rise in the transition temperature range.

The two types of notch design evolved by the NRL investigators are illustrated in Fig. 6; both types are practical and the choice is simply a matter of preference in preparation. The notch in the top specimen of the figure features brittle TIG weld crack starting, using brittle "feed" wire. It also features "V" side grooving to provide a "point" starting source to minimize initiation energy. More recently, we have favored the design shown at the bottom of the figure. This involves a slot of 1/16-in. width made with circular slitting milling cutter. The bottom of the notch is sharpened to less than 0.001-in. radius by pressing in a knife edge tool to a depth of 0.015-in. This notch differs from the BMI design which involves a notch totally formed by the pressing in of a knife edge tool. The dimensions of the "standard" reference specimen for CAT curve determinations are 5/8 × 1-5/8 × 7 inches with a net width of 1-1/8 inches for the fracture depth. We define this as the standard, "subsize" DWTT specimen for use whenever a sample is cut from a plate or forging of greater thickness. The 5/8-in. thickness can be reduced to the plate thickness of thinner steels; however, NRL has not devoted appreciable effort to investigating "thin" steels. Our major concern has been with the potentials of the sub-size test and the nature of correlation with the CAT curve of the Fracture Analysis Diagram.

Figure 7 (top), illustrates such a correlation for A201B steel (taken from PVRC Vessel No. 1 of 2-in. thickness (9,10,11)) for which the DWT indicated a 0°F NDT value and thereby provided for charting the Fracture Analysis Diagram at the illustrated position on the temperature axis. The DWTT correspondence shown in Fig. 7 (bottom) is most striking. The tests were conducted with the NRL pendulum (Charpy-like) machine, now generally utilized for conducting DWTT studies. The data in the figure are for the 5/8-in. sub-size DWTT. Note the sharp rise in energy absorption above the NDT temperature; also, note that at NDT +40°F and NDT +60°F, the specimens showed arrests as deduced by examination of the fractured specimens. The arrests are clearly evident on the fracture surfaces and are indicated by the arrows in Fig. 8.

We are in the process of exploring features of the CAT curve rise, as deduced by the 5/8-in. DWTT, for a wide variety of steels. Selected, characteristically different curves

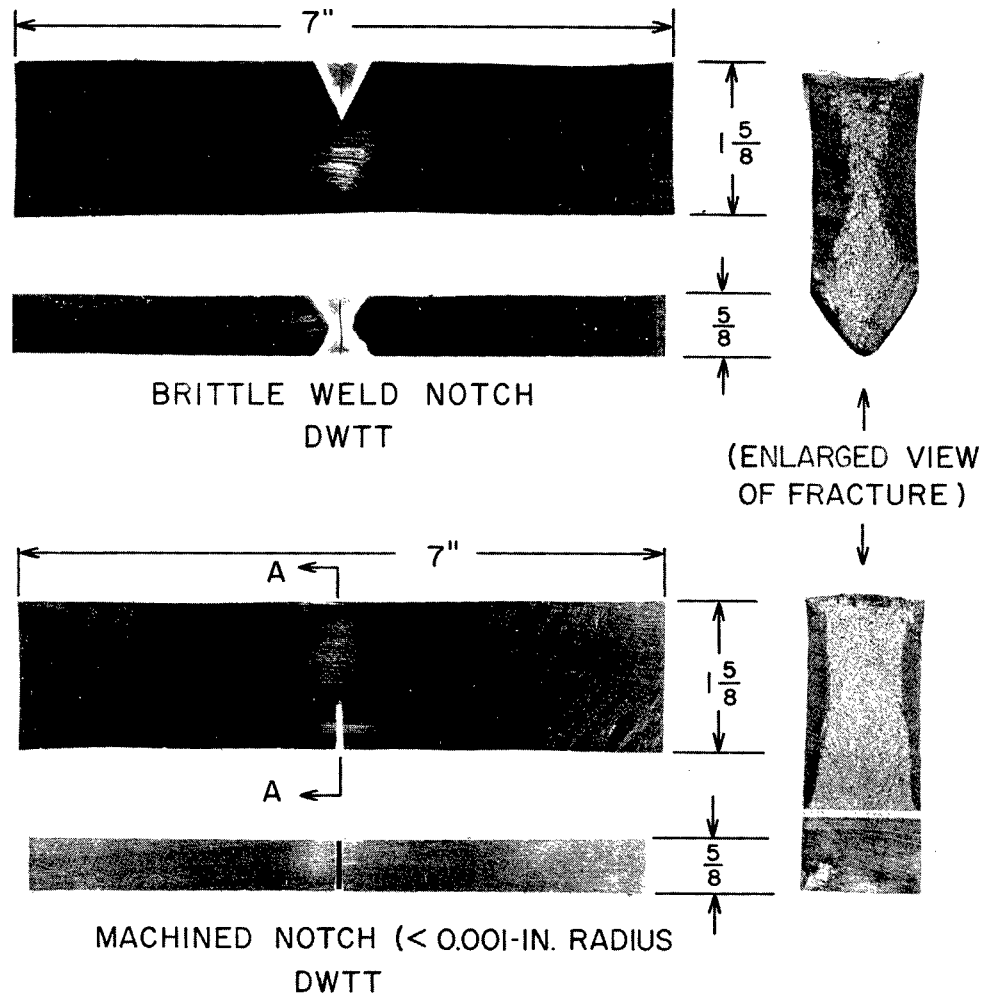


Fig. 6 - Dimensions and notch details of sub-size (5/8-in. thick) Drop Weight Tear Test (DWTT) specimens used for CAT curves, "toe region" determinations. Top specimen has "V" side grooves with a brittle weld; bottom specimen has a machined notch with pressed knife edge sharpening.

are presented in Fig. 9 to illustrate the variety of forms of CAT curve rise that may be obtained. There is a great deal of information that may be "read out" of these curves, with additional examination of the fracture surfaces. The rate of the CAT curve rise above the NDT and the maximum (shelf) energy attained are obviously different - these features are evident from the curves in Fig. 9. For example, the low energy value features of the upper shelf (for ductile tearing) of 4340 are readily understandable and expected (see section on high strength steels). In all cases, arrests have been evident in the fracture surfaces at temperatures of NDT + 40° to 60° F. A wide selection of steels are to be investigated by this technique in order to evolve a more complete picture of the DWTT test potentials as a CAT curve determinant. The results shown in Fig. 9 demonstrate that the test can predict the low elastic stress fracture propagation temperature region for a wide variety of steels that show transition temperature effects; i.e., the "toe region" of the CAT curve. It should be noted that the energy measurement method coupled with fracture appearance examination for arrests is the logical and most definitive method of using this test. Fracture appearance evaluation of DWTT performance may be a satisfactory simplified procedure in some cases; however, as examples, it

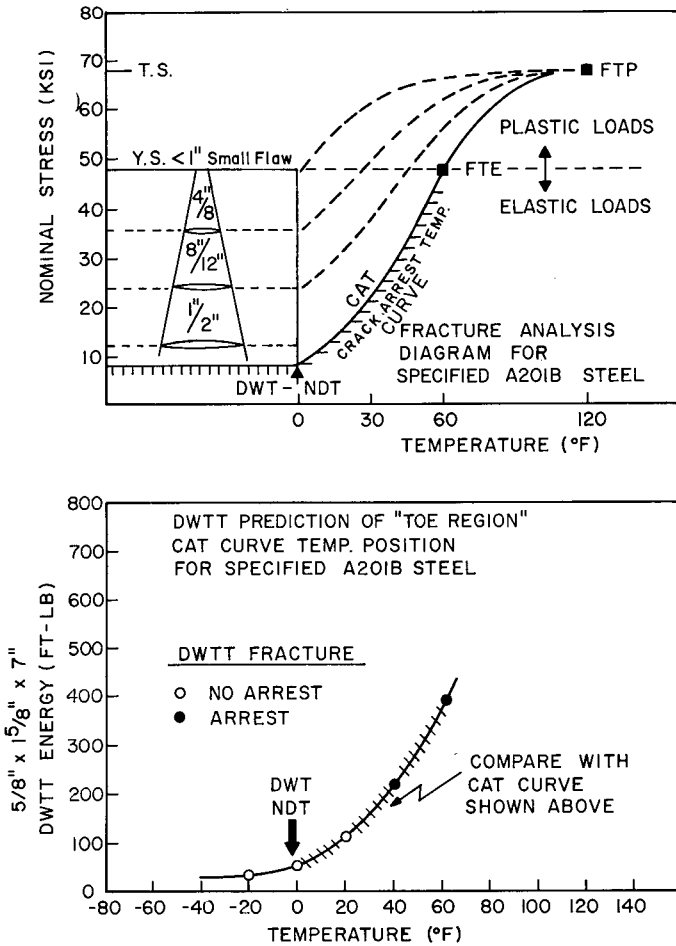


Fig. 7 - Illustrating the correspondence between the CAT curve of a A201B steel defined by the Fracture Analysis Diagram and the CAT curve temperature location indicated by the sub-size Drop Weight Tear Test

would not disclose the dramatic difference in ductile tear energy shown by the 4340 steel as compared to the A302B, or the difference in slopes (more gradual rise of the CAT curve) between the A201B and A302B steels. In general, it appears that steels which show a more gradual initial DWTT rise develop a much steeper subsequent rise on reaching arrest temperatures.

Next we shall illustrate the case for use of the DWTT test for steels that show very broad scatter of  $C_v$  data - also steels that have abnormal  $C_v$  curve relationship to the NDT temperature. A dramatic illustration of this latter limitation of the  $C_v$  test was described in reference (2) where the NDT temperature of the 2.25%Cr-1%Mo, Q&T steel fell on the upper shelf of the  $C_v$  curve. The reference cited clearly illustrated that the NDT deduced Fracture Analysis Diagram was in exact conformance with burst test results of slit flawed air flasks constructed of this material and with CAT data obtained by the isothermal Robertson test of the steels.

We may illustrate both points by presenting data for A387D (2.25%Cr-1%Mo) Q&T steel rolled to 4-in. plate thickness. Limitations of the  $C_v$  test to indicate a precise

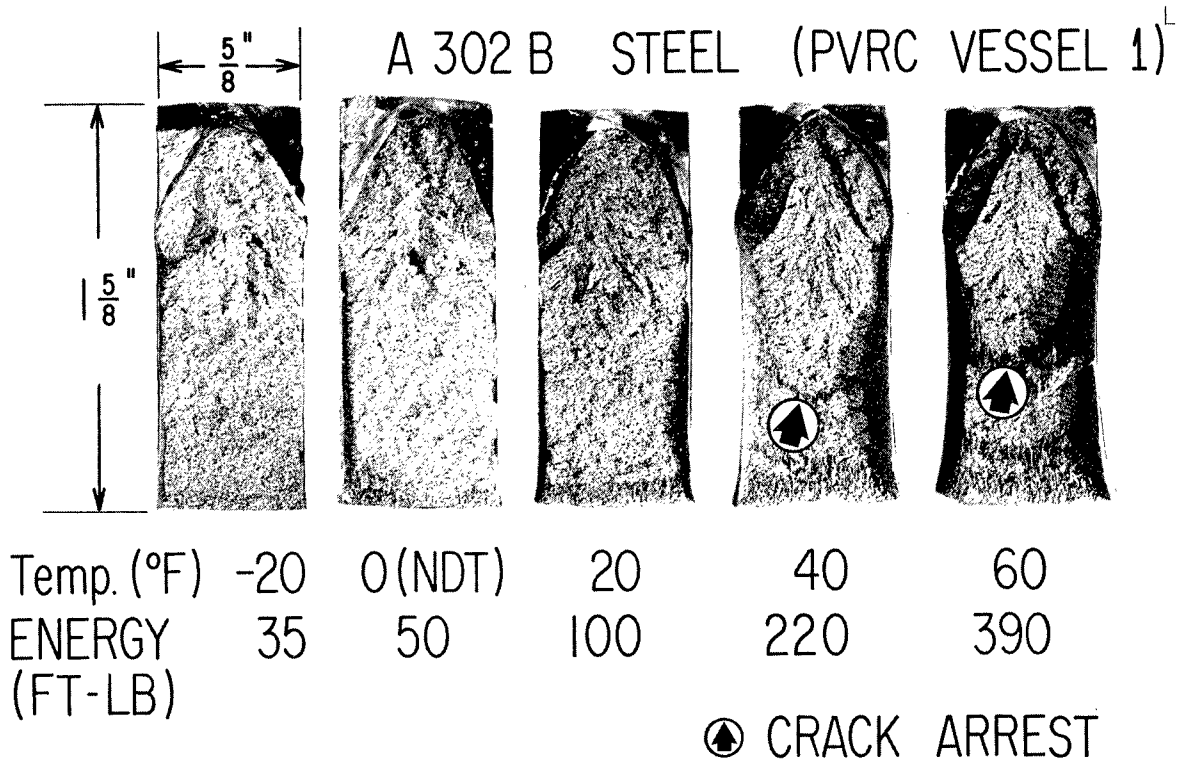


Fig. 8 - Fracture appearance of the 5/8-in. DWTT specimens of A201B steel corresponding to the data presented in Fig. 7. Note crack arrests developed in the specimens tested at NDT + 40°F and NDT + 60°F.

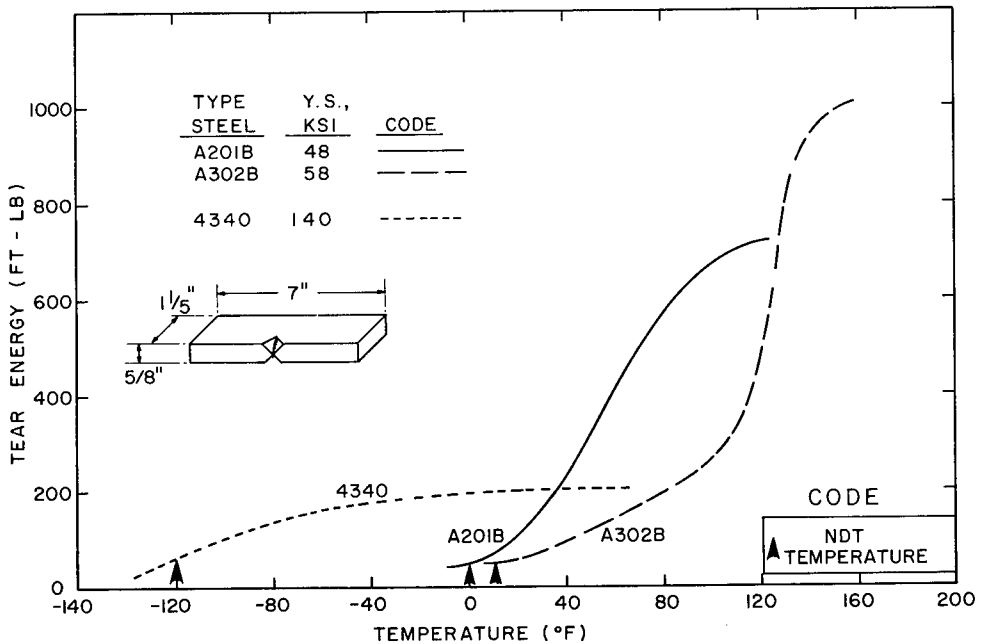


Fig. 9 - Illustrating 5/8-in. DWTT energy data definition of CAT curve features for a variety of steels - A201B, A302B, and 4340. Drop Weight Test (DWT) determined NDT temperatures are indicated by the arrows.

transition temperature index for this steel (even for a single test location in the plate thickness) are readily apparent from the data presented in Fig. 10. Only a diffused picture of fracture toughness transition is obtained due to the scatter in results for  $C_v$  specimens which were taken in the standard orientation and at the usually specified  $1/4 T$  (thickness) position. The energy-temperature relationship from the  $C_v$  test for this steel would indicate that the 4-in. thick steel has significant levels of fracture toughness (20-25 ft-lb) at the  $1/4 T$  position for temperatures as low as  $-140^\circ F$ , and that full shear  $C_v$  fractures are attained at  $20^\circ F$ . Despite the scatter, similar data have been widely considered as representing high fracture toughness characteristics for such steels at sub-zero temperatures. We are alarmed by such broad-brush use of  $C_v$  data for steels that have not been properly indexed as to the significance of the  $C_v$  test and particularly for practices of estimating  $C_v$  curves from bands involving such extreme scatter. To document the basis for this alarm, we illustrate NDT and the DWTT data for this steel at the same  $1/4 T$  position, Fig. 11. The NDT is established at  $20^\circ F$  for this position and the CAT curve deduction derived by the DWTT is in accordance with this index - crack arrest properties at this position are not attained until temperatures of  $50^\circ$  to  $60^\circ F$  are reached. Now, there are additional complications in analyzing such a steel - note that the NDT of the surface and center materials are  $-40^\circ F$  and  $50^\circ F$ , respectively. Also, that the DWTT indexed CAT curve temperature location is in conformance with the NDT prediction for these locations. For the surface position, crack arrest characteristics begin to show at approximately  $0^\circ F$  and for the center at approximately  $80^\circ$  to  $90^\circ F$ . Obviously, the question that arises is: how does this steel behave as a natural composite, considering the severe nature of the through-thickness, fracture toughness gradients? It may be (or not) that the surface properties will impart a controlling effect rather than the center or the  $1/4 T$  positions. The answer to this question in a CAT curve sense must be related to both the specific nature of the metallurgically dependent gradient and the mechanical integration effects of such gradients. The example cited appears to indicate a rather "shallow" surface of low transition temperature material - the  $1/4 T$  and center curves are rather close together. Until we have the answer as to how to evaluate such a composite of gradient properties, it is difficult to analyze such a steel on a fracture-safe design basis. The industrial practice of analysis based on  $C_v$  properties, usually a few test specimens taken at  $1/4 T$  position and at a pre-specified temperature, is almost meaningless.

The next obvious step in these explorations is to test such a material using a full, 4-in. thickness DWTT to establish a mechanically integrated CAT curve temperature location. Unfortunately, there was insufficient material from this specific steel to conduct the full thickness test. The data shown in Fig. 11 were obtained recently; to pursue this matter, samples of the same type of steel and similar types (of other compositions of the expected gradient type) are being procured to conduct the gradient  $5/8$ -in. thickness tests plus full thickness tests. This is a critically important area of exploration - considering the increasingly expanding use of such materials in recent years for thick sections and very large, highly stressed structures of considerable complexity.

It is obvious that explorations of the use of the DWTT for the above-described purposes are yet in the initial phase. However, it is equally obvious that a very exciting potential exists for the use of this simple test and that it provides information that is readily translatable to engineering analysis for fracture-safe design, as has been done by the Battelle and the Bethlehem investigators for specific types of "thin" line pipe steels (7,8). There is considerable urgency for studies related to thick steels, as well as to studies to prevent indiscriminate use of the  $C_v$  test for thick or thin steels that have not been examined as to the interpretability of  $C_v$  test data.

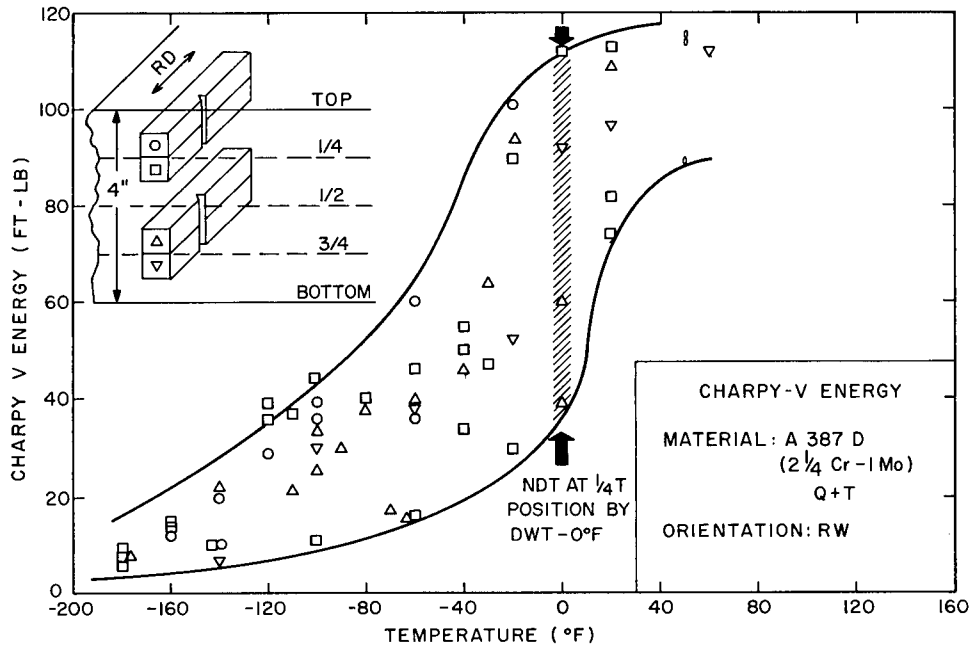


Fig. 10 - Broad band of  $C_v$  test data obtained for opposite, quarter thickness positions of a 4-in.-thick plate of A387D (2.25% Cr-1% Mo), Q&T steel. Note position with respect to the  $C_v$  band of the 0°F, NDT temperature determined by the DWT at the same position.

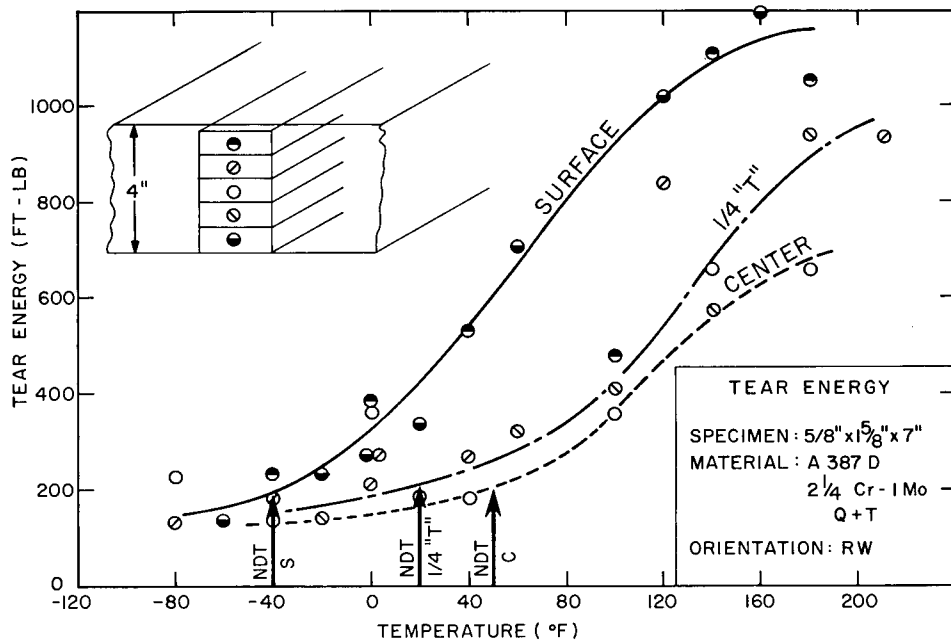


Fig. 11 - Sub-size DWTT energy data for various locations in the subject 4-in.-thick A387D steel plate, indicating relative locations of the respective CAT curves. Note that the NDT temperatures correspond to the toe regions of the indicated CAT curves. Fracture arrests develop at 40° to 60°F above the respective NDT temperatures.

## EVOLUTION OF FRACTURE TOUGHNESS INDEX DIAGRAM FOR HIGH STRENGTH STEELS

As explained in the introduction, one of the major problems in evaluating the fracture toughness of high strength steels is the marked decrease in the level of energy absorption that may be developed at temperatures involving a fully ductile fracture mode. The development of very low levels of fracture toughness at temperatures above the transition range poses problems that cannot be resolved simply by limiting the lowest range of service temperatures, as is the case for steels featuring a transition to high levels of fracture toughness. Decreases of fracture toughness above the transition range may result from increasing strength to high levels or as the result of the presence of improper microstructural aggregations for Q&T steels of intermediate or low strength. Such decreases are indicated by Charpy V ( $C_v$ ) curve upper shelf levels and are translatable to a "downward rotation" of the Fracture Analysis Diagram, as illustrated in Fig. 2. It should be noted that at strength levels above 220 ksi yield strength (YS) the  $C_v$  curves become almost "flat" and are undecipherable with respect to transition temperature features. In the interest of near-term possibilities for the utilization of high strength steels in complex structures, it became imperative to evolve fracture-safe design principles of the same relative simplicity as the transition temperature related Fracture Analysis Diagram approach, but of specific applicability to the case of temperature invariant differences in fracture toughness.

From a Navy interest point of view, a decade of evolutionary test development is not permissible. Some immediate method, even if relatively unsophisticated, is required for the present and immediate future so as to provide fracture-safe design guidance for complex structures having stress indeterminate regions. Also, to serve as a guide for the development of optimized metals for structural applications of near-term Navy interest—the long lead time for such developments require definition of practical routes at the earliest possible time. The DWTT, coupled with the explosion tear test (ETT), as a correlating structural prototype, were therefore evolved concurrently for this purpose and extensive use of the prototype correlation approach was made during the period 1962 to the present.

The features of the ETT test, which serves as the flaw-containing structural prototype, are illustrated in Fig. 12. The first concept of the use of this test was to evaluate the effects of flaws of different sizes—and we continue to have this long term objective. However, more deliberate consideration of "first things first" and experience with the test led us to considering it in a more restrictive but yet more readily analyzable manner that would provide near-term answers to engineering design problems. This was the concept that the simplest "first cut" in evaluating fracture toughness of metals for use in complex structures was obtaining the answer to the simplest "first" question—does a given metal allow fracture propagation at or below yield point stresses, or does it require plastic overload stresses to propagate the fracture? Also, if the latter is the case—how high a plastic overload is required? The significance of such answers to a design engineer faced with the development of yield point or higher stresses at points of geometric complexity, for a structure that is designed to operate at below yield levels of nominal stress, are quite obvious. If fractures cannot propagate out of the zones of high stress concentration, the structure will remain "positively" safe. If he is faced with military application questions involving a major area of the structure being plastically overloaded, he may readily access how high an overload is tolerable before fractures may be expected to propagate.

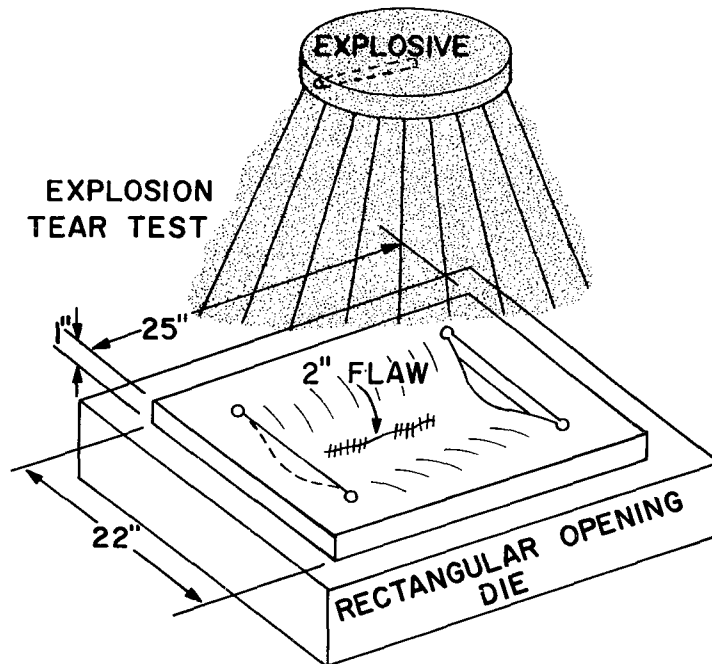


Fig. 12 - Features of the explosion tear test (ETT)

The ETT is ideally suited to provide such answers because of the "long run" of fracture that is available for evaluation of fracture propagation resistance. Correlation with the DWTT to predict the ETT performance is considered equivalent to predicting the characteristic fracture resistance of the metal in a structure. This is a "simple-minded" - but straightforward and readily analyzable concept and we shall proceed to illustrate this with facts and numbers.

The ETT features a through-the-thickness, sharp crack of length equal to  $2T$  (twice the thickness), developed in the plate by a brittle weld "patch" technique. In effect, a short groove is machined in the plate and refilled with a brittle weld. More recently, with the advent of electron beam welding equipment, it was found that the brittle crack may be produced with less effort by the use of an electron beam, brittle weld technique, to be described.

The ETT is used for purposes of "indexing" the significance of DWTT energy vs YS summary plots (to be presented). As points of reference, three levels of 1-in.-thick steel plate ETT performance are illustrated in Fig. 13. The bottommost ETT sample illustrates "flat break" fracture propagation at levels of elastic loading; see also Fig. 4 as another example of "flat break" with shattering eliminated by the use of a very "light" explosive blow. The center ETT sample shows a steel that "half-ran" the fracture across the plate at 3-5% strain but did not run the fracture significantly at 2-3% strain. Thus, 5-7% strain for this steel is about the required limit for fracture propagation. The topmost ETT sample (HY-80 steel) shows extreme fracture toughness resistance - five blows caused incremental 1/2 to 1 in. propagation on each blow with resulting 10-12% (plus) deformation. The ETT tests are generally conducted with explosive offset load conditions (determined by grid method) that will provide essentially: 1. - zero deformation (elastic loading), 2. - 1-2% deformation, 3. - 5-7% deformation, and 4. - 10% (plus) deformation. With the evolution of correlation experience it was found possible to conduct DWTT first and rather

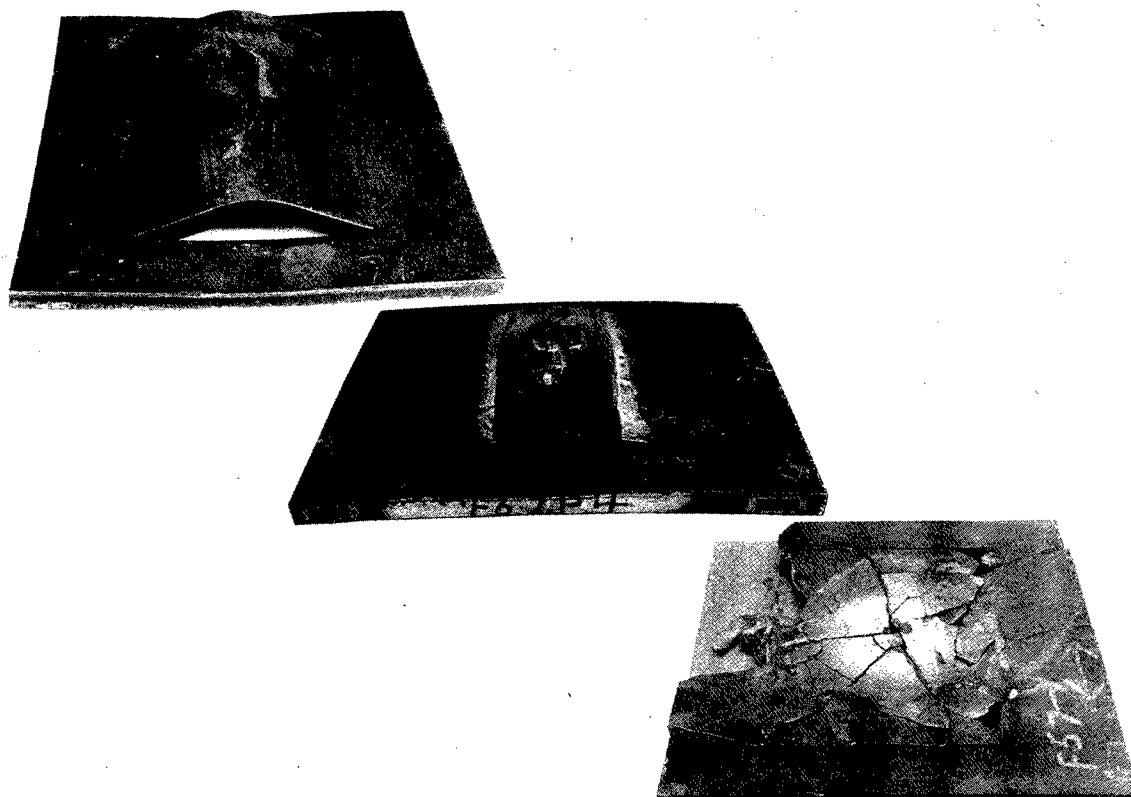


Fig. 13 - Illustrating the wide range of fracture propagation resistance observed in ETT of 1-in.-thick plate specimens. Top, extreme resistance to propagation; center, fracture propagation requiring approximately 5-7 percent strain; bottom, shattering at elastic stress levels (flat break).

accurately predetermine the minimum deformation level that should be applied to cause the fracture to propagate extensively across the section. This procedure conserves scarce material and allows for developing more extensive documentation of the index features of the diagrams to be presented.

To date, the ETT correlation work has been concentrated primarily on 1-in.-thick plate materials and tests at 30°F. However, it was ensured that all of the steels considered in the correlations to be presented were tested at their maximum energy (fully ductile) state at this test temperature. This precaution was necessary to avoid complications of the transition range. In other words, the main interest was in assessing the characteristics of the metal in its state of highest attainable fracture toughness. The effects of transition temperature will be described separately for purposes of clarification.

The value of the DWTT in the work to be described is that: 1. - it provides for inexpensive, "mass-production" testing required for broad field explorations, 2. - it minimizes the amount of energy absorbed in initiation of the fracture to a closely similar, low level, for all metals tested, and 3. - it is both feasible and practical for later use for specification and quality control purposes. These aims were achieved with the ultimate design of the DWTT specimens shown at the bottom of Fig. 14 which is readily applicable "across the board" for evaluations of steels, titanium, and aluminum alloys, and is expected to serve for other materials.

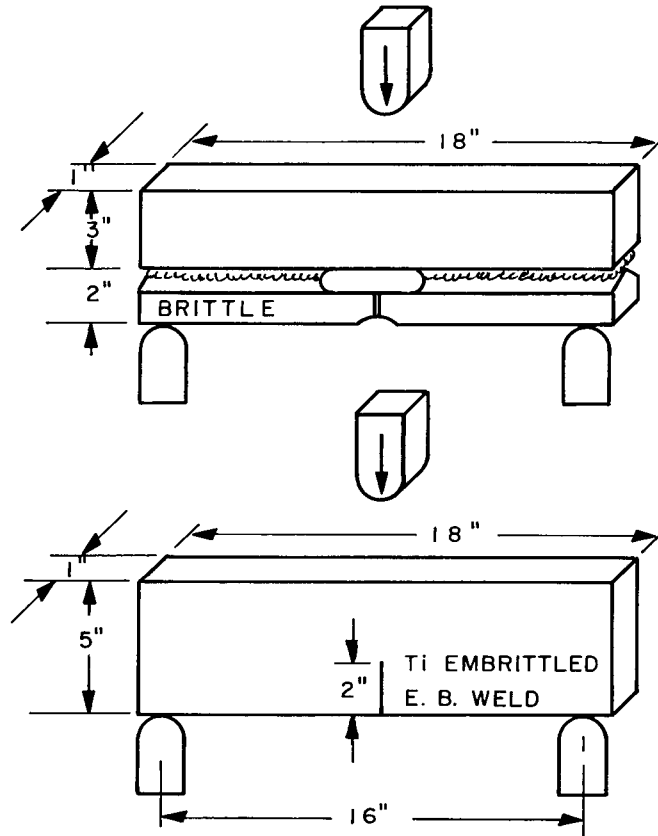


Fig. 14 - DWTT specimen designs for tests at temperatures of maximum fracture energy; (top) welded brittle bar assembly design; (bottom) electron beam embrittled weld design

The initial DWTT specimen used for steels featured a composite weldment, Fig. 14 top, formed by joining a  $1 \times 3 \times 18$ -in. test plate to a notched, brittle, cast steel bar. To provide a brittle crack path extending to the test plate, a brittle electrode (Hardex N—the same as ordinarily used for DWT) was used to deposit a full-thickness weld approximately 4-in. long opposite the notch in the cast bar. The rest of the weld joint consisted of two root passes made with conventional electrodes normally employed for welding of the particular test steels.

After test temperature conditioning in liquid baths, the DWTT specimen was tested initially by loading as a simple beam by the action of a falling weight. The DWTT energy value for complete fracture of the specimen was obtained by “bracketing” (within an increment of 250 ft-lb) tests of several specimens of the same steel. The relatively simple “bracketing” techniques were originally employed for DWTT in order to take advantage of existing drop-weight equipment. Such techniques, however, did result in a considerable expenditure of scarce test material, as well as an excessive amount of time in preparation of the number of specimens required for the determination of each data point. Consequently, a large (5,000 ft-lb capacity) pendulum-type impact machine, Fig. 15, was designed and constructed by NRL for continuing DWTT studies of full thickness (1 and 2 inches) high strength materials. This new equipment (basically a large Charpy machine) also provides for more exact determinations of the DWTT energy values.

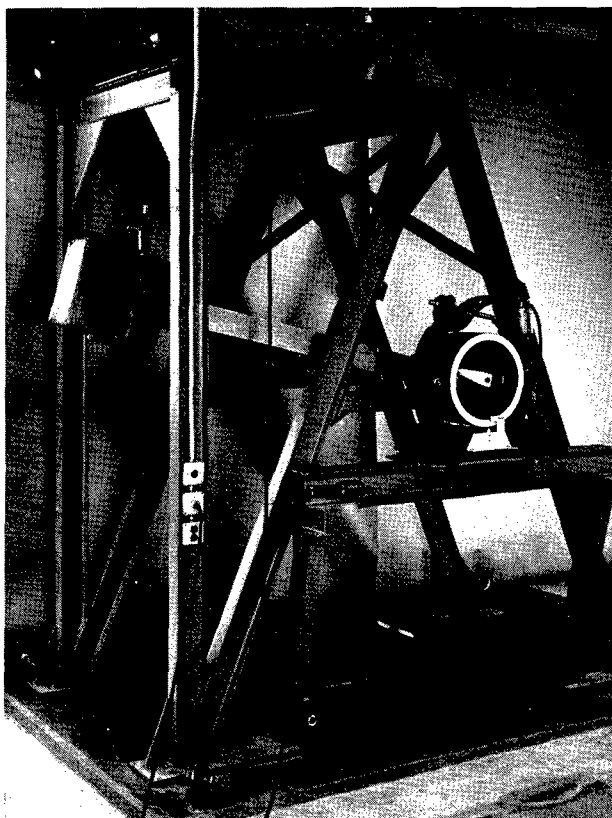


Fig. 15 - Pendulum machine for DWTT of 1-in. and 2-in.-thick specimens—5000 ft-lb capacity

For the composite, brittle bar type of DWTT specimen, some difficulties were experienced in determining fracture energy values for certain steels. Fictitiously high values occasionally resulted from (evident) underbead weld cracks that precluded a continuous crack path from the brittle region into the test section of high-carbon content Q&T steels. It has also been determined that the brittle bar specimen may cause significant errors in energy measurement when heat-treatment of the test steel was conducted with fabricated DWTT specimens, due to simultaneous heat-treatment of the brittle weld. These difficulties were generally identified and eliminated from consideration—steels of low fracture toughness provided the problems in these respects. Because of the above experiences with the brittle bar type, the DWTT specimen was redesigned as shown in Fig. 14, bottom. The brittle, crack-starter portion of the specimen is confined to a narrow, embrittled, through-the-plate electron beam weld. An unalloyed titanium wire (1/16-in. dia.  $\times$  2-in. long) is peened into a shallow groove and diffused through the steel plate by a single pass electron beam weld, forming a hard and brittle alloy. The “V” notch side grooves are saw-cut along the embrittled weld to reduce initiation energy of the fracture to a reproducible low level of approximately 400 ft-lb. A broken DWTT specimen, which illustrates the use of the embrittled electron beam weld for crack-starter purposes, is shown for a fracture tough steel, Fig. 16, top, and for a brittle steel, Fig. 16, bottom.

Prior to discussing the results of a broad-scale survey of high strength steels and of the ETT index correlations, we shall discuss first the general effects of processing as related to anisotropy and also the features of DWTT data for high strength steels involving tests conducted in the transition temperature range.

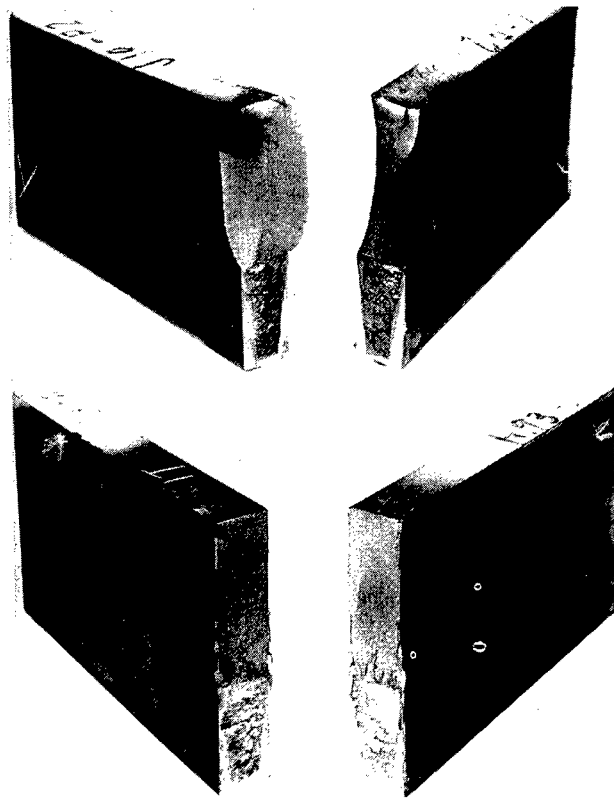


Fig. 16 - Fractures of electron beam embrittled weld design DWTT, representing 1-in.-thick plates of evident fracture tough and brittle steels. Note brittle weld region with side notches.

#### EFFECT OF ANISOTROPY

One of the important early findings of these studies was the determination of wide differences in fracture toughness that could be measured by the DWTT for conventionally cross-rolled steel plate as a function of specimen orientation. Conventionally processed steel plates feature approximately 3 - 1 cross-rolling ratios. For purposes of investigating anisotropy effects as a function of rolling variables, a heat of steel was procured with special handling to obtain five degrees of prescribed cross-rolling ratios. The steel was conventionally melted (single oxidizing slag, electric furnace, air melt practice), and the various plates were rolled from the single heat conforming to chemical requirements of the high chemistry (thick section) HY-80 analysis, as follows:

<u>%C</u>	<u>%Mn</u>	<u>%Si</u>	<u>%P</u>	<u>%S</u>	<u>%Ni</u>	<u>%Cr</u>	<u>%Mo</u>
0.20	0.35	0.32	0.008	0.013	3.20	1.62	.72

Special handling by the mill in slab cutting and rolling to 1-in. plates provided material for studies of the anisotropy effects that could be developed by a wide range of production cross-rolling.

The effects of test specimen fracture orientation and degree of cross-rolling on fracture toughness properties are illustrated by the data shown in Fig. 17 for two extreme cases of cross-rolling. The top and bottom curves depict the extreme differences in fracture toughness that may be developed in the fiber (weak) direction and in the trans-fiber (strong) direction for straight-away rolling (essentially no cross-rolling). The two directions defined as "weak" and "strong" may be recognized by the ASTM\* method as respectively the WR and RW directions. The effects were explored over a range of strength levels indicated in the figure. It is apparent that straight-away rolling of steel plate results in a relatively low fracture toughness in the fiber (weak) direction and much higher fracture toughness in the trans-fiber (strong) direction. As depicted by the center curve in Fig. 17, essentially equivalent (isotropic) fracture toughness properties are developed in both directions for highly (1 - 1) cross-rolled plate. In general, the results of these tests (not all cross-rolling ratios are presented herein) showed that for any given strength level, an increase in weak direction and a decrease in strong direction fracture toughness occurs with increasing degrees of cross-rolling. Full (1 - 1) cross-rolling is required for the attainment of the maximum possible level of fracture toughness in a biaxial sense - i.e., to eliminate a weak direction. The relative importance of attaining 1 - 1 cross-rolling to maximize fracture toughness depends on the strength level. For example, the high level of tearing energy inherent to commercially processed HY-80 at the 80-90 ksi YS level causes no concern with respect to the weak direction of poorly cross-rolled material, because even the weak direction features a relatively high fracture toughness. However, the same may not be said for steels of higher strength levels—for these there is little tearing energy to spare and the presence of a weak direction is highly detrimental.

In heat-treatment studies conducted for a wide variety of steels, all were shown to exhibit decreasing levels of fracture toughness with increasing strength. The general effect is such that as the strength level of a given material is increased, a point is reached where the weak direction of a poorly cross-rolled material drops to low toughness levels correlating to fracture propagation at elastic load levels at much lower strength levels than for the strong direction. Accordingly, practical considerations dictate that the weak direction of fracture resistance of a material should be taken as the criteria of reference relating to the suitability of the steel for structures involving multi-directional loading.

For special design cases, the high fracture toughness inherent of the transverse direction may be a desirable factor and straight-away rolled steels may be desired for such purposes. For example, consider an insert section in a gas line pipe for fracture arrest purposes—the most economical approach would be to utilize a straight-away rolled Q&T steel with the fiber direction in the hoop orientation. Thus, the fracture is forced to propagate through material of higher fracture toughness than would be attainable by 1 - 1 cross rolling. Highly cross-rolled steel would not be desired for special applications involving unique restrictions of fracture paths.

---

\*It is recognized that the ASTM suggested method for describing specimen orientation and fracture directions in rolled plate provides for exact definition of all possible situations and is to be preferred. The method described in Materials Research and Standards, Vol. 1, No. 5, May 1961, uses the letter R (direction of principal rolling), W (plate width), and T (plate thickness) to describe the six possible orthogonal fracture directions. We support and ordinarily use this method. However, throughout this report we are concerned with only two fracture directions—the "weak" direction, where the fracture propagation is parallel to the principal rolling direction (WR), and the "strong" direction (RW), where the fracture propagation is perpendicular to the principal rolling direction. For descriptive simplicity and additionally for purposes of emphasis, the terminology of "weak" and "strong" fracture directions are used in this report.

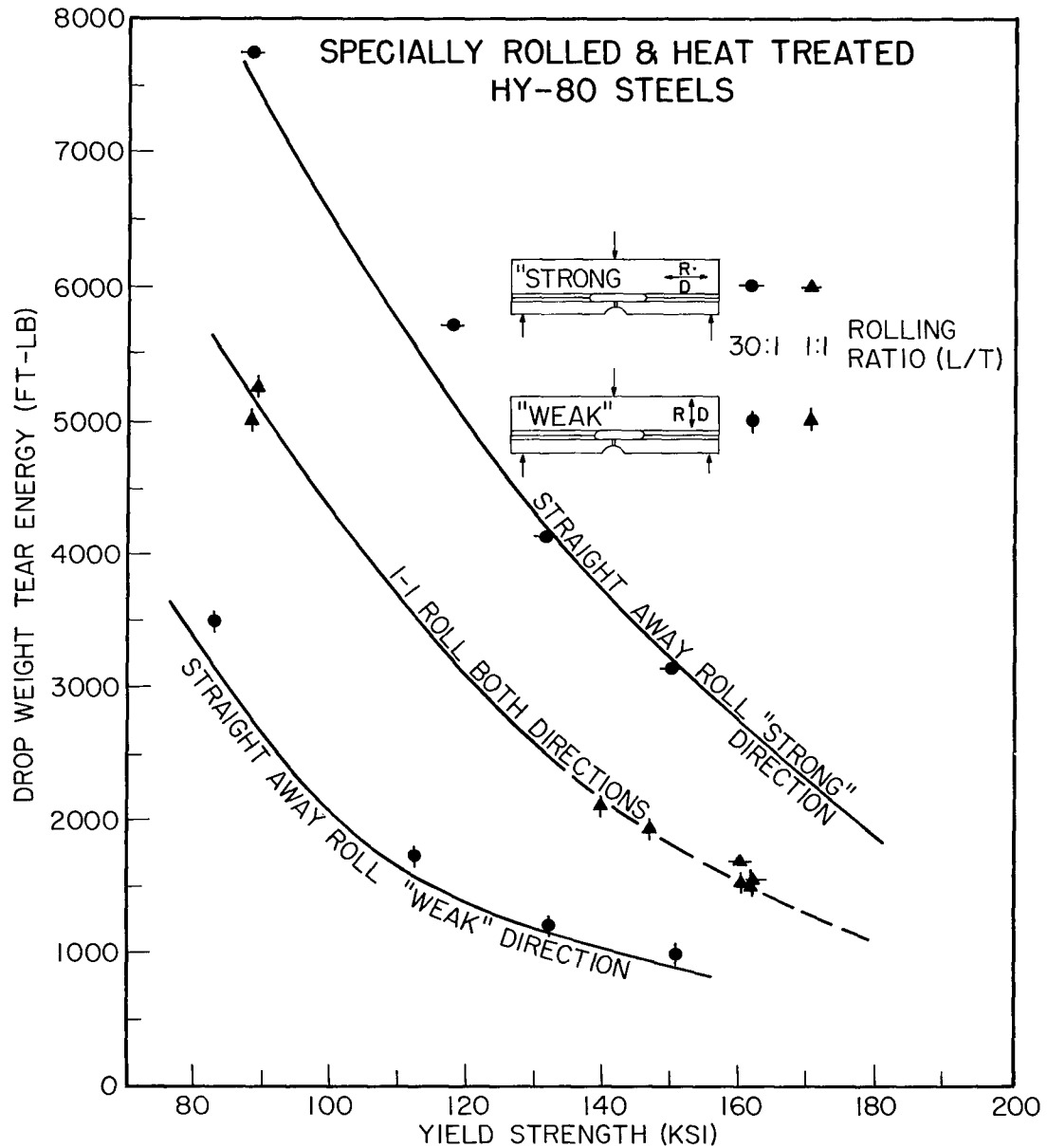


Fig. 17 - Relationships of DWT energy to yield strength involving various conditions of fracture orientation and cross-rolling practices for a conventional melt practice, HY-80 type steel

It should be emphasized that the data to be presented in summary data charts to follow always relate to the lowest level of fracture toughness in the plate, i.e., the "weak" direction of the rolled plate, providing such a direction exists. Plates of special 1 - 1 cross rolling presented in these charts reflect the benefit of such practices. The point to be made is that a fracture toughness value for a steel plate of a given YS cannot be considered as to its relative value compared to another steel of the same strength value without knowledge of both the test orientation and the degree of cross rolling. It would be very simple to show one steel as being "very glamorous" compared to another by using straight-away rolling and then testing in the transverse direction. This information was basic to the "sorting out" and frame-of-reference evaluation of steels on the comparable basis that is

presented in this report. This consideration of details eliminated what previously was a chaotic condition for inter-comparison of steels. Studies of orientation effects and the decision to compare on the weak direction basis represented was our first step in the evolution of summary data charts based on broad-scope evaluation of steels, as well as for the other metals covered in this report.

#### DWTT TESTS IN THE TRANSITION TEMPERATURE RANGE OF HIGH STRENGTH STEELS

As indicated by very low slope, essentially "flat"  $C_v$  energy transition curves, the best of the ultra-high strength steels do not exhibit the distinct transition temperature behavior which characterizes the best steels of less than 180 ksi YS. Low slope, low shelf, Q&T steels may be obtained at strength levels of 90-120 ksi YS, but these are steels of the commercially cost-competitive "low alloy" or lean analysis type. The DWTT fracture toughness properties of the best of the lower strength steels are highly temperature dependent in the transition range. It is such a sharp effect of temperature on fracture toughness that provides for the success of the standard drop-weight test in determining the NDT temperature.

It should be cautioned that the summary data to be presented in the diagrams to follow should not be extrapolated to structural applications which involve service temperatures lower than the maximum energy, ductile tear temperatures to which they are intended to apply. We have used the general designation of "shelf" temperatures to characterize this condition. Results of investigations of the effect of temperature on DWTT fracture toughness properties of high strength steels will now be presented to clarify this point. The effect is illustrated by DWTT results obtained for three specially melted and processed steels of HY-80 composition, heat treated to strength levels of approximately 110, 130, and 150 ksi yield strengths. The melt processing for these steels comprised vacuum ladle degassing and special control carbon deoxidation. A series of weak direction, DWTT specimens were prepared from each plate and DWT were also conducted in accordance with standard procedures (3) to determine the respective NDT temperatures. The DWTT were conducted at various temperatures from 30°F (on-the-shelf temperature for all of the samples) down to the NDT temperature of each respective steel.

The decrease in DWTT energy levels exhibited by these steels with decreasing test temperature is presented in Fig. 18. At test temperatures of approximately 40°F above their respective NDT temperature, the DWTT energy values for each steel increase slightly from the low value obtained at NDT temperatures. At approximately 50° to 60°F above their respective NDT temperature, a sharp increase in DWTT energy is obtained, approaching 50% to 75% of the maximum values developed by the steels at the 30°F (on-the-shelf) position. Because of the difficulty of fracture appearance definition for such steels, arrests could not be clearly defined; however, the rapid rise in the curve is in itself an indication of a sharp increase in the CAT curve. In all cases, at test temperatures of approximately 100 to 120°F above the NDT temperatures, these steels attain their maximum (shelf) fracture toughness. The relationships in the toe region of the curves are in general agreement with the concept of DWTT utilization as a CAT curve locator, as discussed in one of the previous sections.

Correlations of  $C_v$  upper shelf energy (to be described) with DWTT upper shelf values have been surprisingly good and documentation of the significance of  $C_v$  shelf energy values (100% shear fractures) have been established for steels by correlation with DWTT results and ETT tests. However, investigations of the effects of temperature on DWTT and  $C_v$  test energies in the transition temperature range indicate that the  $C_v$  test can be highly misleading for cases involving mixed fracture of the  $C_v$  specimens. Figure 19 summarizes

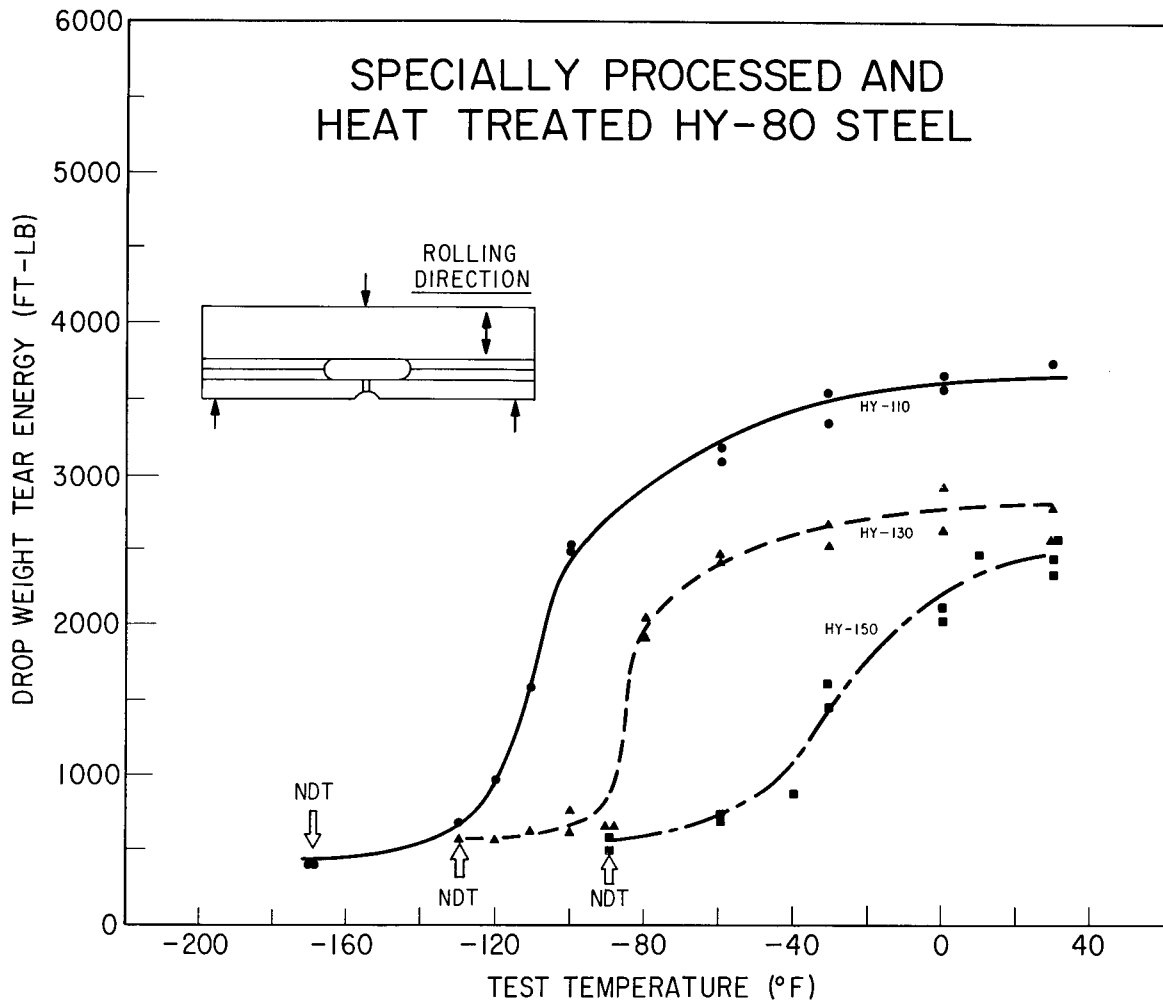


Fig. 18 - Illustrating the decrease in DWTT energy from the fully ductile to NDT temperatures for various strength levels of a special melt practice, HY-80 type steel

the  $C_v$  and DWTT data developed for the same 110 ksi YS steel shown in Fig. 18. The figure illustrates that the scatter range of  $C_v$  values at any test temperature is considerably larger for strong direction tests than is the case for weak direction tests. At the NDT temperature of  $-170^\circ\text{F}$ , the average  $C_v$  values are 46 and 84 ft-lb respectively for the two directions of testing. It should be recognized that these apparently "high"  $C_v$  numbers do not signify fracture tough performance of this steel at its NDT temperature as would be the case for similar  $C_v$  energy numbers when referenced as shelf-level temperature values. Of particular significance are the data for test temperatures ranging from  $-100^\circ$  to  $-140^\circ\text{F}$ . In this temperature range, the average weak-direction  $C_v$  value drops only 10 ft-lb (from 70 to 60 ft-lb) but the DWTT value is seen to drop drastically from 2500 to 600 ft-lb. Fracture appearance ratings of the  $C_v$  specimens tested in this temperature range disclosed 95% shear fracture at  $-100^\circ\text{F}$  and 65% shear fracture at  $-140^\circ\text{F}$ . From these data it should be cautioned that high  $C_v$  energy values for test specimens featuring the presence of cleavage (values in the transition range) are not necessarily indicative of high toughness. This is a "fine" but important point to be considered in interpreting  $C_v$  test values and adds to the complications of using the  $C_v$  test. In other words,

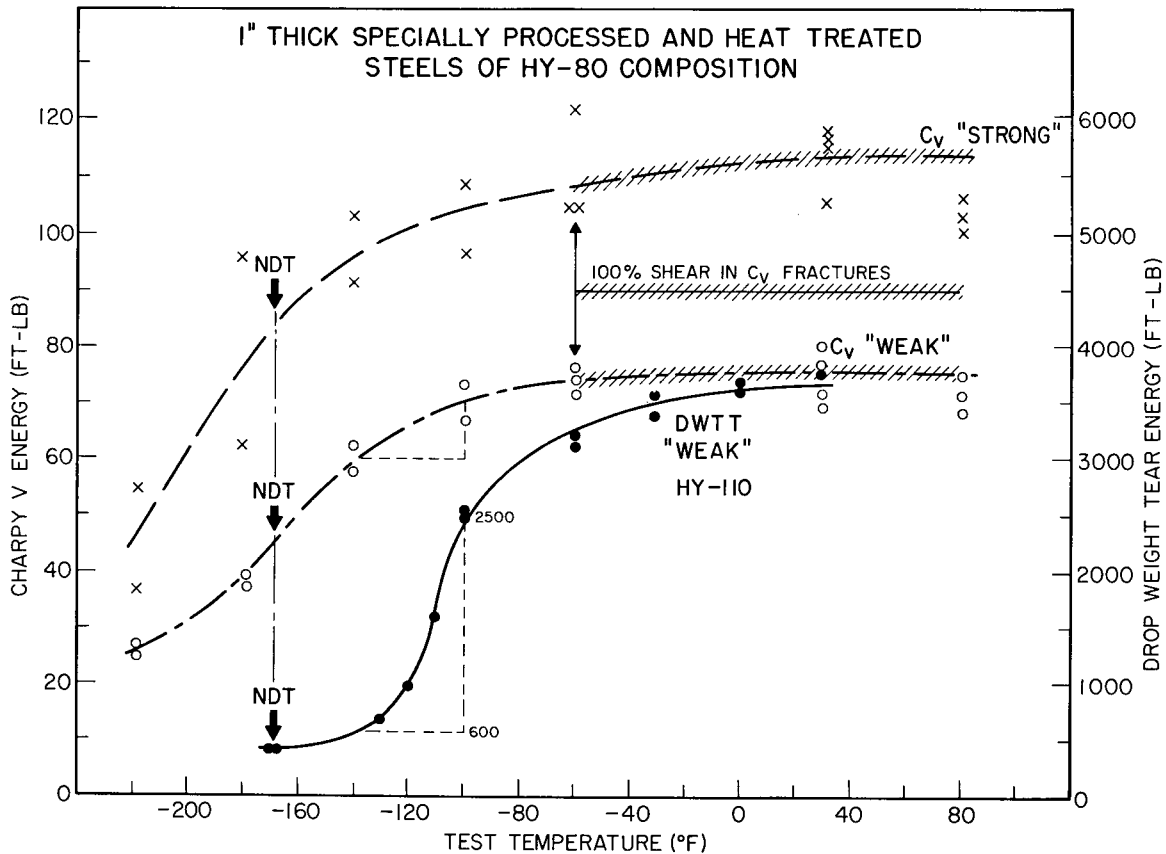


Fig. 19 - Comparison of DWTT and C<sub>v</sub> data for the steel of Fig. 18 that was heat treated to 110-ksi YS

do not use the C<sub>v</sub> -DWTT correlations to be presented in the following charts without due consideration that these must be C<sub>v</sub> shelf values, for all steels featuring definite temperature transition features. This caution does not apply to the essentially "flat" C<sub>v</sub> curves.

**FRACTURE TOUGHNESS INDEX DIAGRAM FOR HIGH STRENGTH STEELS**

Broad-scope DWTT studies of steels, coupled with ETT correlations have resulted in evolving DWTT energy vs YS Fracture Toughness Index Diagrams (FTID), relating to properties of the steel above the transition range. All tests were conducted at 30°F and met this criteria. Such a diagram relating specifically to 1-in.-thick steel plates is presented in Fig. 20. Correlations with ETT data served to index the strain levels for fracture propagation to specific DWTT energy levels, irrespective of yield strength. These charts are intended to serve as basic guidelines indicating the relative resistance to fracture propagation for steels of specific DWTT energy levels. The strain levels indicated on the charts relate to the ETT index of performance. The shaded region from 1000 to 1250 ft-lb is used to denote the range of DWTT energy level separating materials capable of ETT propagation of fractures at elastic stress levels from the materials that require small plastic strain overloads for ETT propagation of fracture.

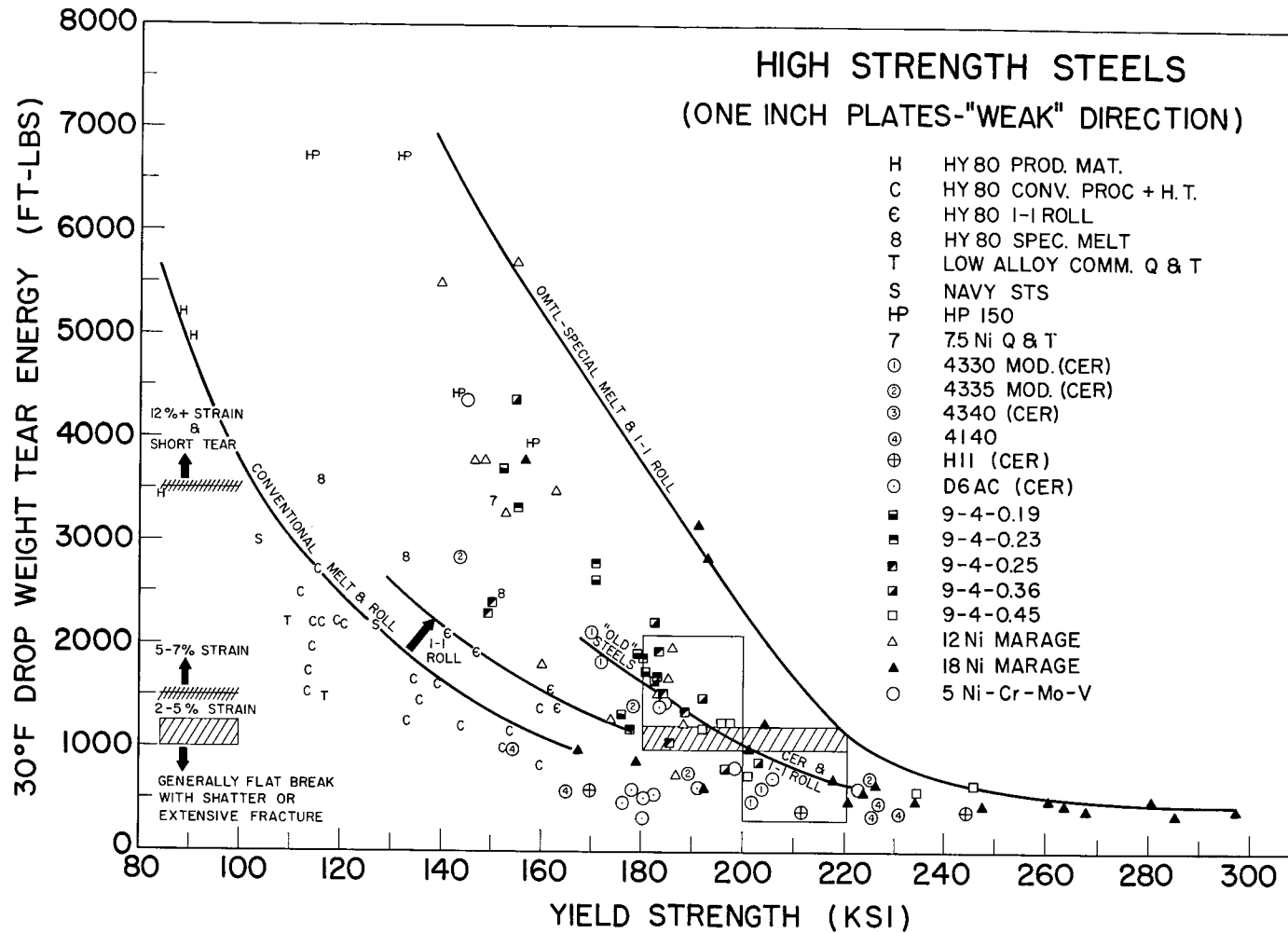


Fig. 20 - Spectrum of DWT data for high strength steels as a function of yield strength and of processing practices. By referencing the specific OMTL lines to the ETT performance index points (percent strain for fracture propagation), the chart evolves to a Fracture Toughness Index Diagram (FTID) for all steels represented.

The curves shown in Fig. 20 also separate the data points into characteristic groups relating to the processing variables (melting practice and/or cross-rolling). For each characteristic group of steels, a wide range of fracture toughness may be developed by different alloy steels of the same YS level. The maximum level for each grouping as depicted by the related curves, indicate that fracture toughness decreases with increasing strength level for all categories. The limiting ceiling curves for each group have been designated as the "optimum materials trend line" (OMTL) for the group. The individual OMTL may be recognized as the reference "yardstick" for evaluation of steels of the particular category with respect to the practicable upper limit of fracture toughness for any given strength level. Of particular interest is the fact that the highest or "ceiling" curve in Fig. 20 depicts the apparent presently attainable upper limits of fracture toughness for any strength level. The "ceiling" curve is attained by special melt practices and 1 - 1 cross-rolling of the new alloy steels developed within the past five to seven years. Note that all data relate to 1-in.-plate thickness.

One of the recent highlights of these studies has been the determination of the beneficial effects of special melting and rolling processes on the DWTT and  $C_v$  shelf fracture toughness properties of the "new" steels in the 150+ ksi YS when compared to the best practice for the "old" types. The "old" types are generally characterized as Ni-Cr-Mo composition of the HY-80 type, heat treated to a range of intermediate strength levels and the well-known 4330 - 4340, H-11, D-6, etc., types, heat treated in the range of 160 to 220 ksi YS. The "new" types (of matching strength) include the families of maraging and 9Ni-4Co varieties. The OMTL indicated in Fig. 20 for the "old" high strength steel alloys, that have long been in use for high strength applications, represent vacuum consumable-electrode-remelt (CER) practice and 1 - 1 cross-rolling. Thus, the illustrated OMTL for the "old" steels is the best attainable for the noted strength levels. The values developed for best practice of these steels are of significantly lower toughness levels than those of best practice for the recently developed "new" steels.

The data given in Fig. 20 are particularly significant to general conclusions that may be derived with respect to steels of 180+ ksi YS. Note the shaded region denoting the DWTT prediction of change from elastic to plastic loading requirements for fracture propagation, located in the 180/220-ksi YS range. Also, the "boxes" that have been drawn to encompass the population of steel data points above and below 200 ksi YS. Major implications are immediately apparent from consideration of these data: 1. - Above 200 ksi YS, the preponderance of steels reside in "box" regions of the FTID where propagation of fracture at elastic stress levels should be expected and are so confirmed by ETT results. It is thus considered that valid fracture mechanics toughness measurements should be obtainable for these steels. 2. - In the 180/220 ksi YS levels, many of the "old" steel types are also characterized by similar low resistance to fracture propagation so as to predict valid fracture mechanics determinations. 3. - The upper "box" of the diagram encompasses many of the "new" steels which are characterized by higher DWTT toughness. These steels, by FTID correlation have been shown to resist propagation of fracture unless subjected to at least 2-5% levels of plastic strain. The sharp change in population from the low fracture resistance "box" to that of the high fracture resistance "box" of the FTID is clearly in concurrence with the YS location of the "upswEEP" of the  $K_{Ic}$  upper bound (OMTL) curves shown in Fig. 1. This observation explains why it becomes impossible to obtain valid  $K_{Ic}$  values below the 200 to 180-ksi YS levels for the best quality steels of this thickness.

From these studies of high strength steel, it has become clear that the fracture toughness of steels at a particular strength level is critically related not only of the composition of the steel, but also the process history. Data for a particular analysis and thickness are relatively meaningless without simultaneous definition of the process practices. It is also necessary to specify the test direction with respect to the rolling direction. In general, the characterization of relative fracture toughness for specified directions and process conditions has evolved as a major contribution of this program which clarifies an otherwise

completely confusing picture of relative fracture toughness quality for particular compositions and strength levels. In the absence of this spectrum of data, it would not be possible to "index" the quality of a particular steel with respect to others.

#### APPLICABILITY OF $C_v$ TEST

The standard method for evaluating fracture toughness available generally to industry has been the  $C_v$  test. Correlations between the DWTT and the  $C_v$  tests have provided a means of calibrating the significance of the standard industry test within the described limitations. Figure 21 depicts the general relationship between DWTT and  $C_v$  data for the steels studied to date. It should be emphasized again that the surprisingly good correlation of DWTT energy values with  $C_v$  values applies to shelf level temperatures—i.e., the correlation relates to tests at temperatures of maximum energy for both the  $C_v$  and DWTT.

A summary of such 30° F  $C_v$  tests for steel is presented in Fig. 22, as a function of the yield strength of the test material. The curves in this figure separate the data into characteristic groups relating to the processing variables which are closely similar to those illustrated in Fig. 20. The DWTT and ETT index procedure was used to evolve this chart to FTID status. It is significant to note from repetition of the "two boxes" of population, that the  $C_v$  test also characterizes a high population density of steels in the 200/220 ksi YS range as materials capable of propagating fractures at elastic stress levels. Also, that many steels of 180/220-ksi YS range may be attainable with fracture resistance to above YS levels. These data provide for the useful application of  $C_v$  tests for high strength steels in fracture-safe design analysis by terms of simple FTID reference.

#### CONSIDERATION OF FATIGUE CRACK MODIFIED $C_v$ TESTS

Of the variety of steels surveyed in these studies, 34 high strength steels were selected for fatigue crack modified,  $C_v$  testing in order to determine whether an improved correlation definition would result. The steels were chosen to include both low and high toughness levels, covering the spectrum of yield strengths ranging from 80 to 280 ksi. All were tested using the standard  $C_v$  test specimen and two modifications - a fatigue crack induced at the root of the standard  $C_v$  notch and the same fatigue cracked specimen with the additional feature of notching the two sides of the test bar. Two types of loading, standard impact and slow-bending, were used for the modified  $C_v$  tests. The slow bend tests were conducted by courtesy of the Republic Steel Corp. Laboratory in a cooperative test program on this item (12).

The principal effects of fatigue cracking alone or fatigue cracking with the addition of side notches, are to lower the  $C_v$  test energy values. The effect was shown to be independent of the type or toughness level of the steels. When the steels were ranked in decreasing order of toughness, Fig. 23, on a basis of the conventional  $C_v$  test data and on the basis of data from the modified specimens, the relative orders were essentially the same, irrespective of the test specimen used. Minor exceptions occurred only in the results of slow bend tests. Generally, the results of the modified  $C_v$  testing program for the subject 34 high strength steels, indicated no particular value or necessity for use of fatigue crack modified  $C_v$  testing for evaluation of fracture toughness at temperatures of maximum energy. As a disadvantage, the use of notching procedures more severe than those of the conventional Charpy tests, causes a reduction of energy values such that discrimination between low energy value steels is seriously reduced, aggravating an already difficult problem of interpreting the  $C_v$  test.

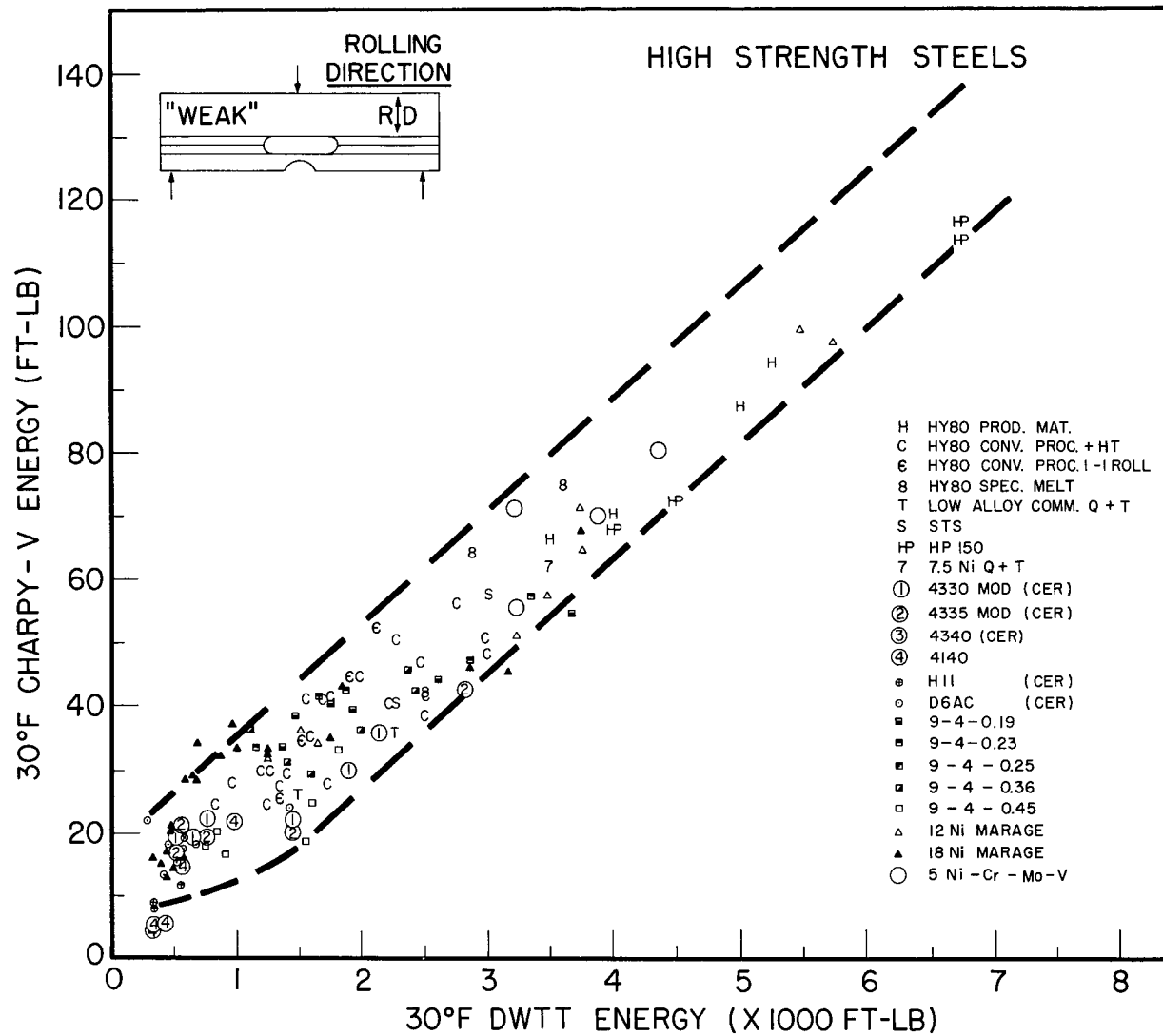


Fig. 21 - Correlation of  $C_v$  shelf energy with DWTT shelf energy. Shelf energies, for both tests, relate to test temperatures for which the fractures are of the fully ductile mode.

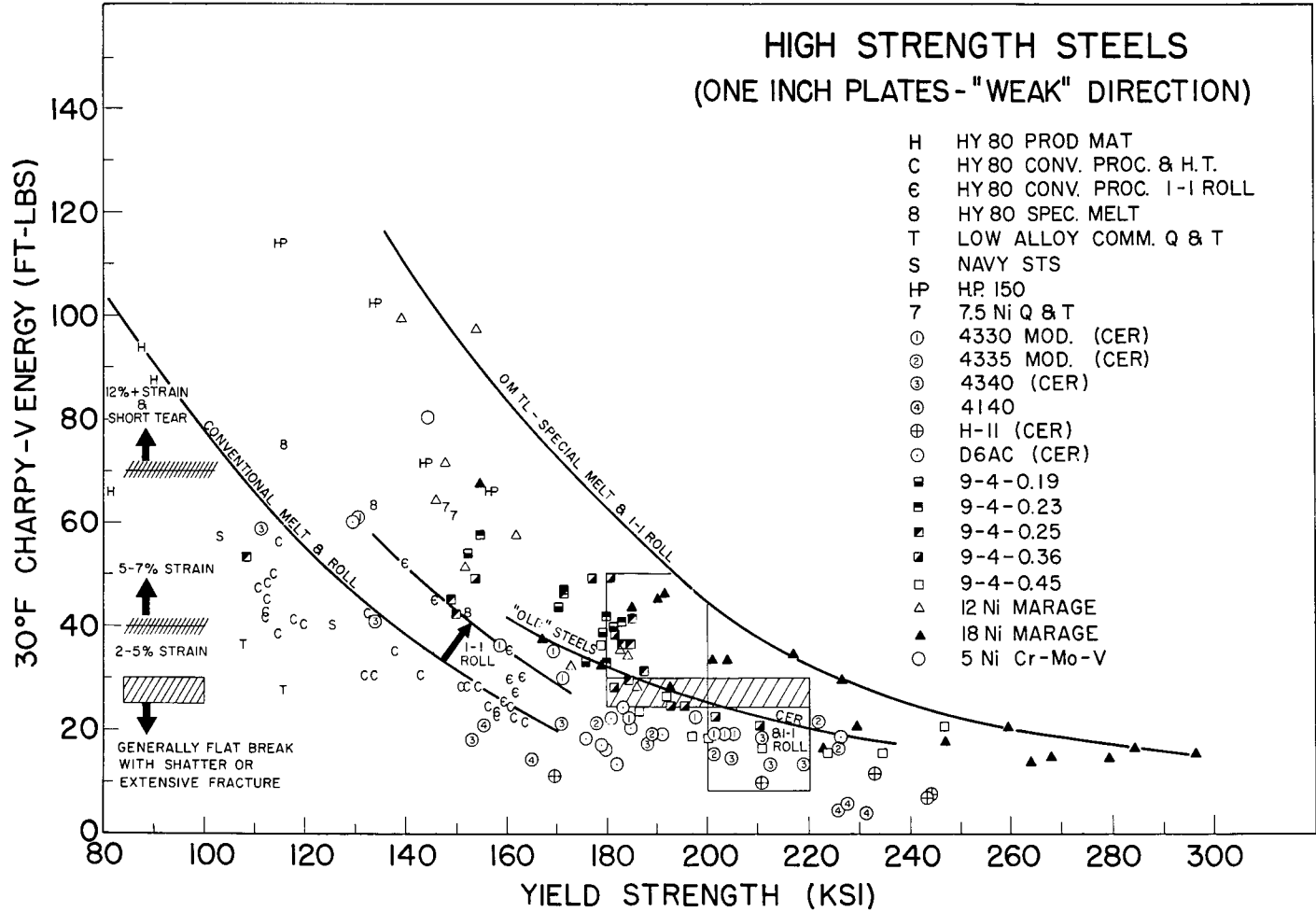


Fig. 22 - Spectrum of  $C_v$  test data for high strength steels as a function of yield strength and of processing practices. Note the various OMTL curves. By indexing to DWTT and ETT data, the Fracture Toughness Index Diagram (FTID) emerges. Compare with Fig. 20.

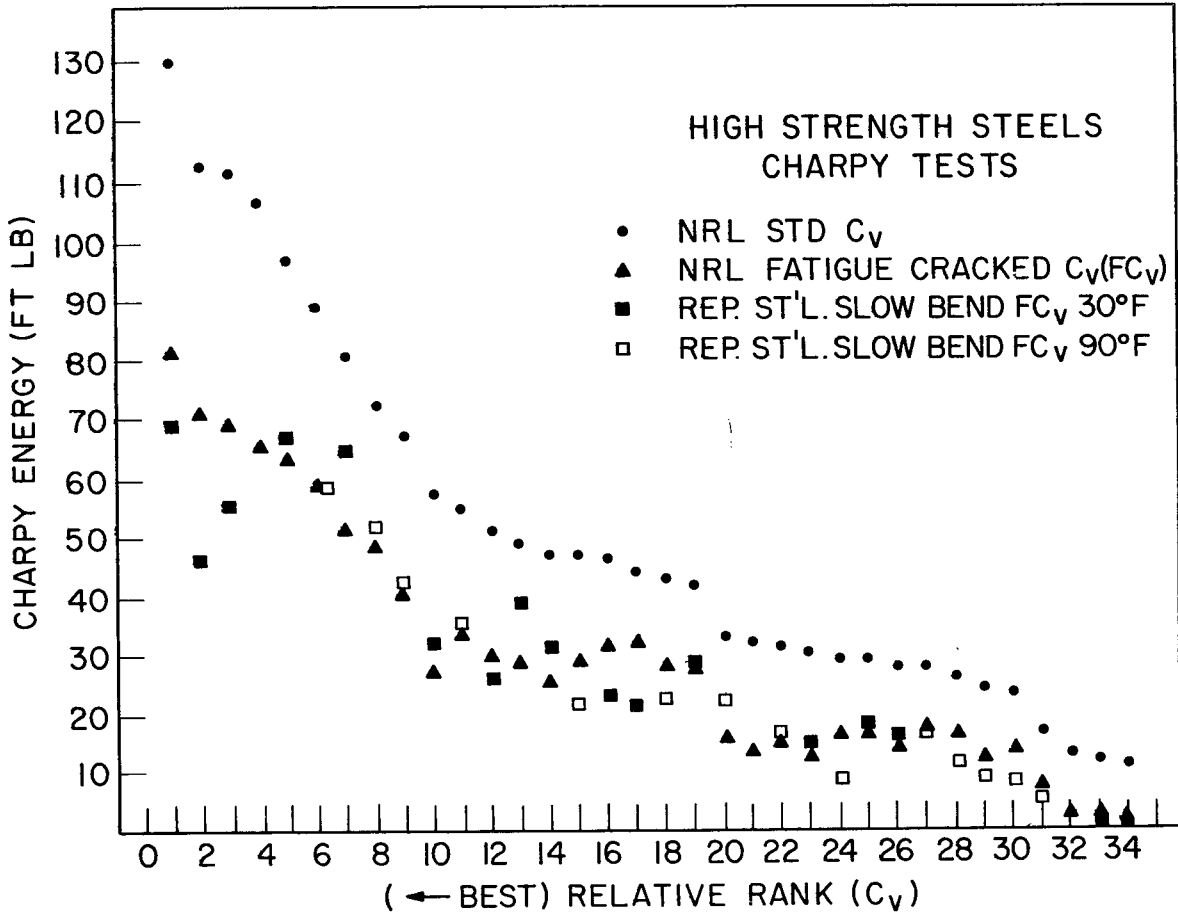


Fig. 23 - Results of conventional, fatigue cracked, and fatigue cracked plus side notched modified  $C_v$  tests of high strength steels, ranked in decreasing order of fracture toughness

## EVOLUTION OF FRACTURE TOUGHNESS INDEX DIAGRAM FOR TITANIUM ALLOYS

At the start of the NRL investigation of titanium alloys of plate thickness in 1962, a review of the literature was made to establish the extent of available fracture toughness information. Except for a few 1-in. thick plates that had been investigated by Charpy V ( $C_v$ ) tests, drop-weight tests (DWT), and explosion crack starter tests by Willner and Sullivan (13), there were very little additional data. Moreover, the first contacts with the industry disclosed that the effects of specimen orientation were generally ignored resulting in various alloys being reported to have surprisingly high  $C_v$  values in plate form. Further investigation revealed that the high values resulted from orienting the specimen so that the notch was parallel to the plate surface. From the total available information, the relative  $C_v$  values of various alloys of similar strength levels and the relation to processing practices could not be determined – this situation could be described as most confusing.

The literature review also indicated that fracture mechanics tests had been conducted primarily for alloys in the sheet thickness range and for materials of ultra-high strength. To this date, the available information on plane-strain fracture toughness for plates of 3/4 to 1-in. thickness is inadequate to prepare a chart of  $K_{Ic}$  vs yield strength (YS), as has been presented for steels in Fig. 1. Our present program includes obtaining data that would provide for the preparation of such a chart in terms of upper bound  $K_{Ic}$  values. It is also of interest to determine the range of YS at which questionable  $K_{Ic}$  values are obtained because of experimental difficulties deriving from plastic deformation of the crack tips, and below which plane strain fracture toughness cannot be measured because of high fracture toughness. It will be shown that the fracture toughness index diagram (FTID) for titanium alloys indicates that this range may be expected to be in the 125-130 ksi YS level for the majority of the better alloys of 1-in. plate thickness. Our initial work on  $K_{Ic}$  plane strain fracture measurement was aimed at 1-in. thick plates of 105-120 ksi YS. It was found that at room temperature valid  $K_{Ic}$  values could not be obtained because of the excessive fracture toughness of the alloys investigated. As a next step, attention is being directed to alloys of 130-150 ksi YS level.

A large body of  $C_v$  data developed by NRL tests during the past three years is summarized in Fig. 24 as a function of broad YS ranges. It is apparent from these data that the  $C_v$  transition occurs over a very wide range of temperatures ( $-200^\circ/-300^\circ$  F to  $+200^\circ/+300^\circ$  F). Accordingly, such transition features are considerably different from the rapidly falling  $C_v$  curves (sharp transition) developed by steels of low or intermediate strength level. Electron microscope fractographic studies of  $C_v$  fracture surfaces provide a partial explanation in that the fracture mode for all specimens involved in the bands of Fig. 24, at high or low temperatures, is "dimpled rupture," i.e., a ductile (non-cleavage) fracture mode. The size and fine features of the dimples may change with decreasing  $C_v$  energy, but the basic nature of the fracture mode is not changed. The comparative general features of  $C_v$  curves and fractographic appearance for steels, titanium, and aluminum are discussed in a subsequent section of this report. Contrasted to the low or intermediate strength level steels, the basic problem in using  $C_v$  energy as a measure of fracture toughness for titanium alloys is the lack of an abrupt  $C_v$  temperature transition in conjunction with the low  $C_v$  energy values for the moderately high strength materials.

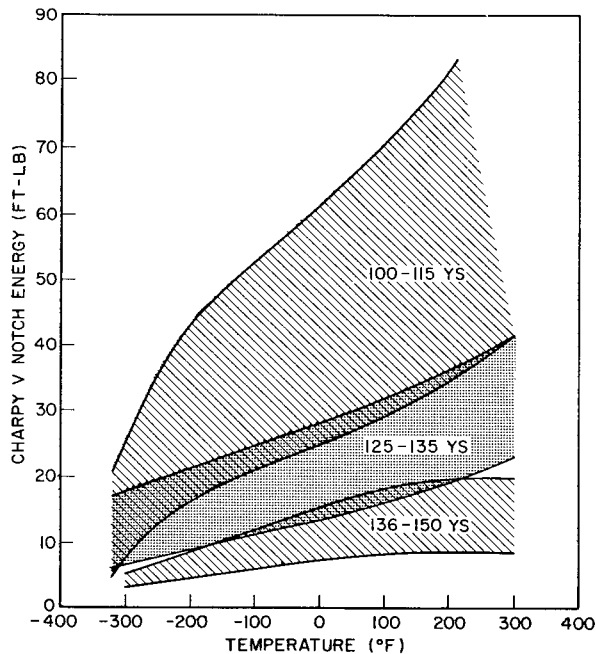


Fig. 24 - Generalized relationships of  $C_v$  energy decrease with decreased temperature, representing various broad ranges of yield strength for 1-in. thick titanium alloy plate

Charpy curves resulting from fatigue-precracked specimens have not provided a more discriminating interpretation of the  $C_v$  test for titanium alloys. The use of the precracked specimen shifts the  $C_v$  curve to generally lower energy values. The curves lie slightly below, but are essentially parallel to those of the standard specimen for the same material - no other features of the curves are accentuated. A typical example of this is seen in Fig. 25 which presents standard and precracked  $C_v$  curves for low interstitial Ti-6Al-2Mo and high interstitial Ti-13V-11Cr-3Al.

The relationship (at 30°F) between  $C_v$  energy and DWTT energy for a variety of 1-in. thick titanium alloy plate material is shown in Fig. 26. Although this relationship was developed for a single temperature of primary interest, it could also be developed for any other temperature. Because of the absence of a change in the fracture mode with temperature, the critical necessity of comparison of test specimen results at "shelf" positions described for steels does not enter the titanium alloy picture. For purposes of evaluating the rather gradual effects of temperature on the fine scale differences of the common ductile fracture mode, DWTT temperature effects studies will be conducted in the near future. The general low slope of the correlation band, Fig. 26, below 2500 ft-lb DWTT energy implies rather inaccurate prediction of DWTT (or ETT performance) from  $C_v$  data for high strength titanium alloys. We have concluded that  $C_v$  data for titanium are useful only for "broad brush" separation of brittle alloys from high toughness alloys and for establishing broad trends in heat-treatment studies of materials in the intermediate strength range. Similarly, the use of  $C_v$  tests should not be ruled out for specification purposes aimed at quality control on the basis of simple separation of fracture tough material from material that is accidentally contaminated so as to result in low fracture toughness.

The DWTT specimen size for titanium is 1 × 5 × 17 inches. The 1-1/2-in. deep, brittle weld, crack starting element is made by diffusing iron, nichrome, or stainless steel wire into the material, using an electron beam welding technique similar to that described in the steel section. This technique was first developed for preparation of titanium DWTT specimens and has been used exclusively since the beginning of the investigations of this metal.

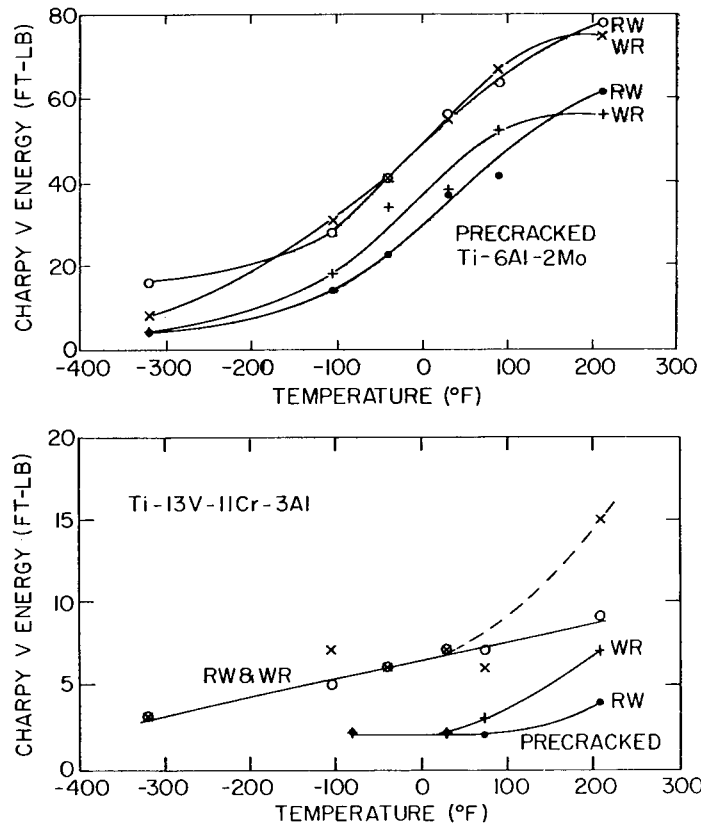


Fig. 25 - Standard and fatigue precracked  $C_v$  energy curves for a low interstitial Ti-6Al-2Mo alloy and a high interstitial Ti-13V-11Cr-3Al alloy

The ETT structural prototype correlation approach was used for titanium alloys, following the same procedures as described for steels, and with the same, previously described, interpretation of relative fracture propagability as a function of applied strain level. One difference has been found for titanium as compared to steels - no titanium alloy tested to date has been shown to be capable of withstanding as much as 10% plastic strain without complete tearing; however, low interstitial, unalloyed titanium can exceed 14% plastic strain without fracturing in the ETT. Thus, it appears that at the highest attainable toughness levels, titanium alloys do not possess the intrinsic, extremely high fracture propagation resistance of the best steels in the 80-150 ksi YS range. This fact may be of academic interest except for military applications involving the service attainment of extremely high plastic overload. Figure 27 illustrates an ETT example of "flat break" (elastic load propagation) and an example of material requiring 5-7% plastic strain level for fracture propagation. As for the steels, a large number of such tests were conducted to establish the "fix" relationships of DWTT energy with ETT fracture propagation resistance.

Figure 28 illustrates a spectrum of DWTT data, illustrating results for both weak (WR) and strong (RW) directions. The OMTL established from these data shows the same rapid decrease with increasing strength level as for the case of steels. Processing variables are known to be important; however, as of this date, we cannot "break out" the relationships relating to processing practice as has been done for steels - such definition should be obtained. Therefore, the presently available Fracture Toughness Index Diagram (FTID) chart for 1-in. thick titanium alloys should be considered as a preliminary edition. The

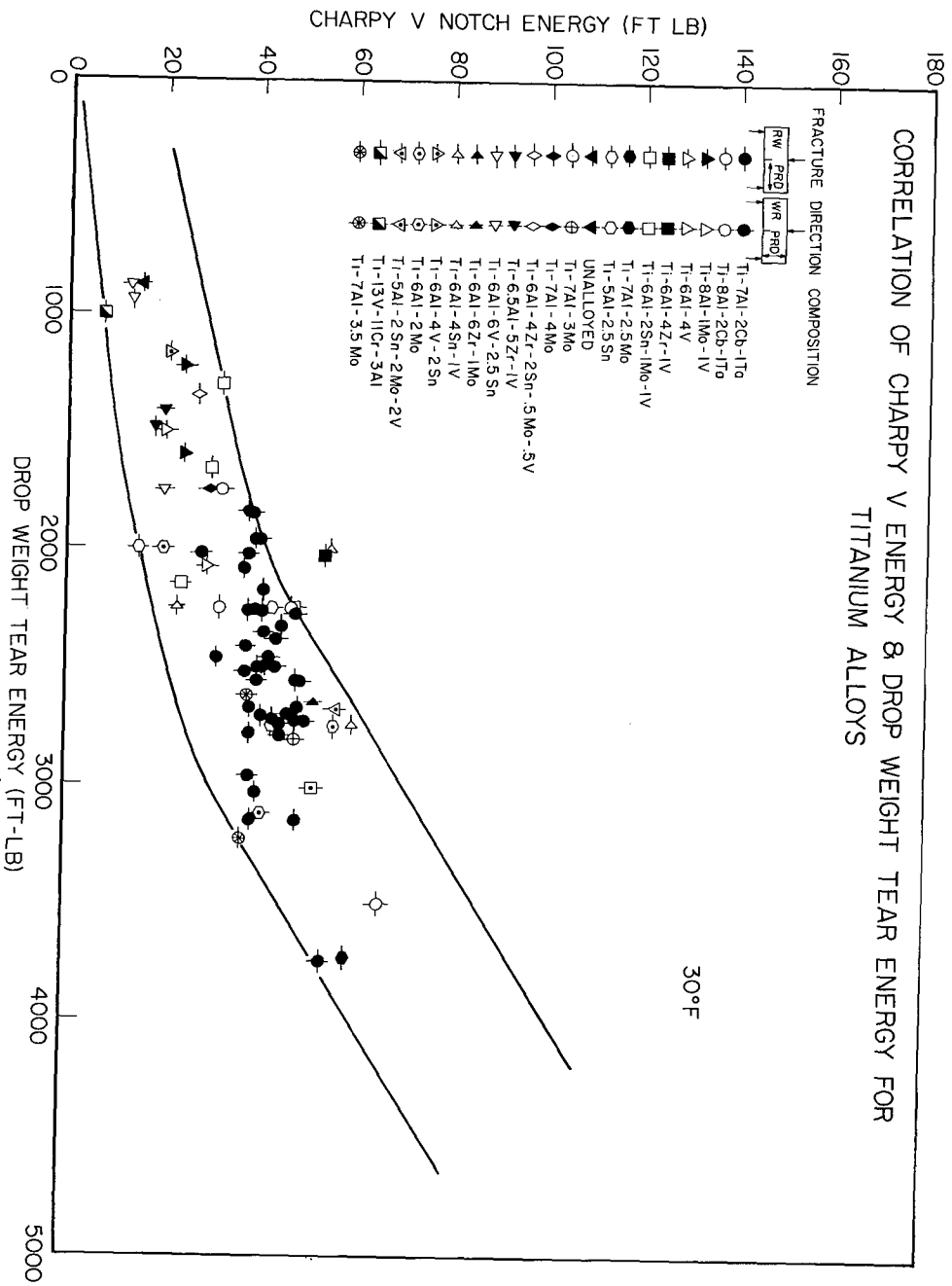


Fig. 26 - Correlation band between  $C_v$  and DWT fracture energy for 1-in. thick titanium alloy plates

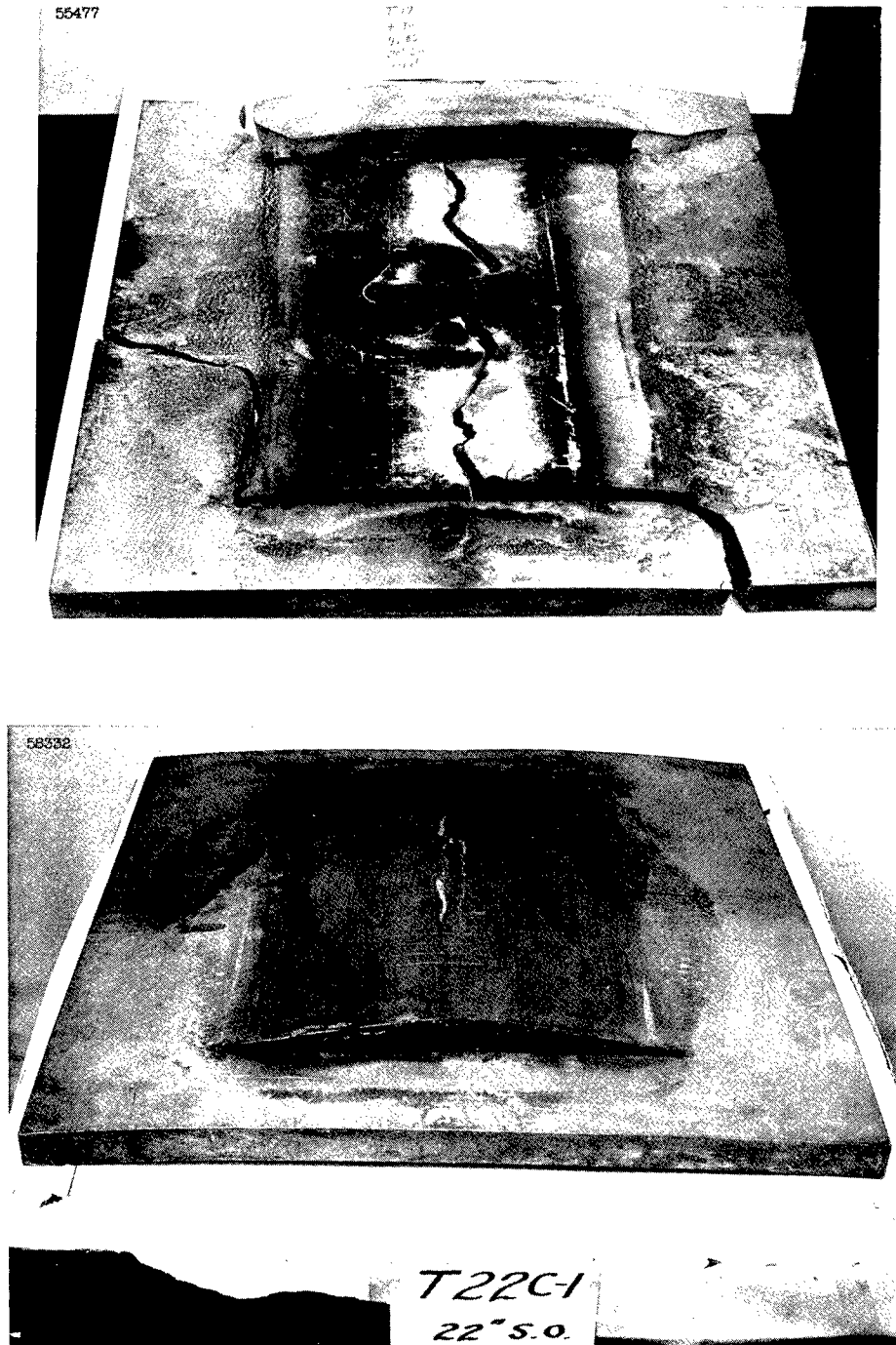


Fig. 27 - Examples of extremes in ETT performance of 1-in. thick titanium alloy plates

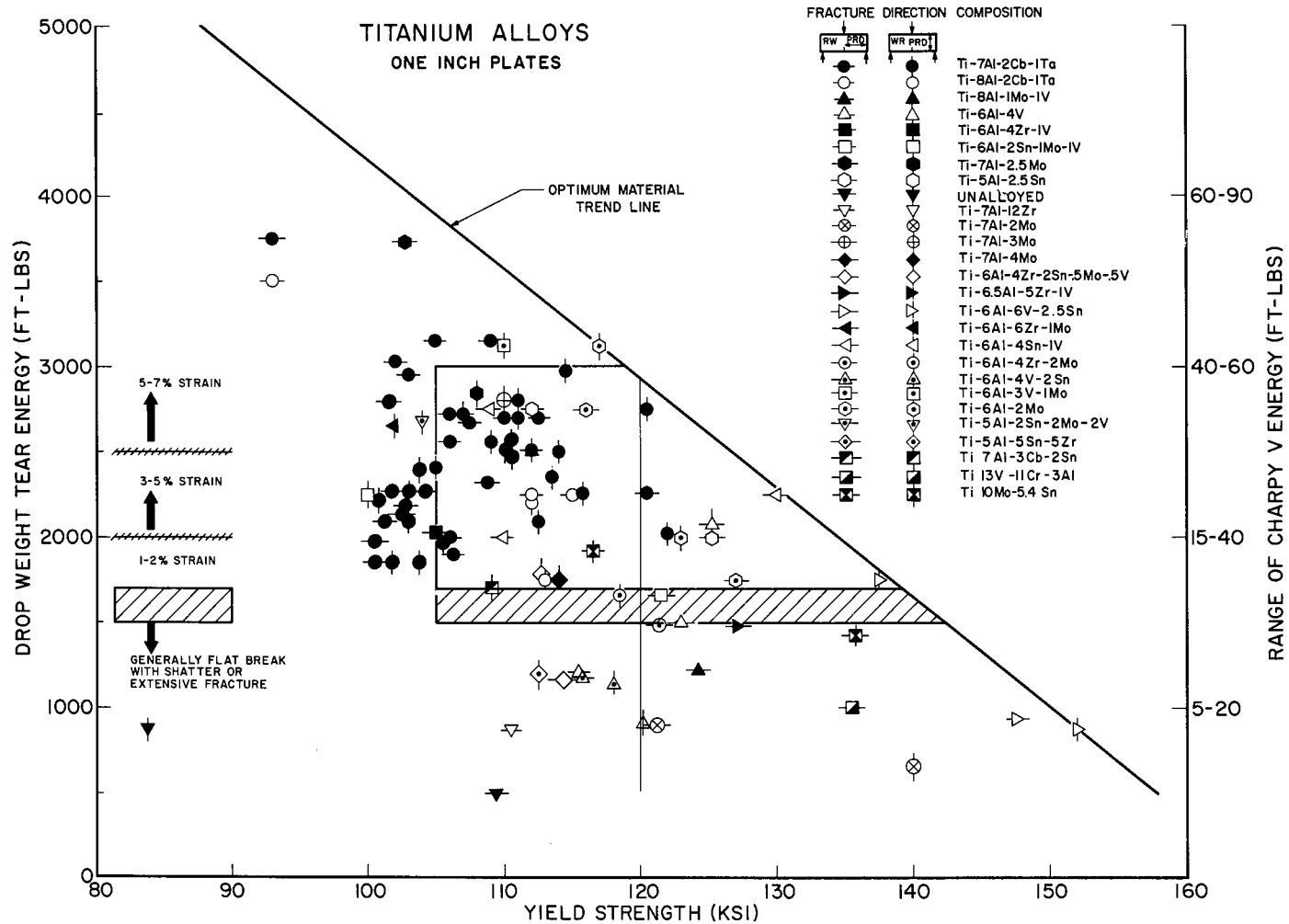


Fig. 28 - Fracture Toughness Index Diagram (FTID) for titanium alloys. DWTTE energy is correlated to ETT strain level requirement for propagation. The optimum materials trend line (OMTL) represents an estimate of the presently highest attainable levels of fracture propagation resistance for any given level of yield strength.

diagram shows that materials of below 1500-1700 ft-lb DWTT energy "break flat" in the ETT and thus should be expected to propagate fractures through elastic load regions. Above 1500-1700 ft-lb DWTT energy, plastic strain overload is required to propagate fractures, and the relative level of DWTT energy is indicative of the relative level of plastic strain required. For example, above 2000 ft-lb DWTT energy, 3-5% plastic strain would be required, while above 2500 ft-lb DWTT energy, 5-7% plastic strain would be required. This information was basic to the Navy decision to consider 2000 ft-lb DWTT energy as a minimum desirable requirement for titanium alloys used in structures that are not strictly stress analyzable - it guarantees (with a margin) the use of titanium alloys that will not propagate fractures through elastic load regions.

The cross-over point of the "flat break" limit, indexed at 1500-1700 ft-lb DWTT energy, with the OMTL indicates that all presently known alloys of above 140 ksi YS should be expected to propagate fractures through elastic load regions. Such materials should definitely be analyzed in fracture mechanics terms. On the basis of population density (the "two block" analysis described for steels), most materials between 120 and 140 ksi YS should also be expected to propagate fractures at elastic stress levels, unless the material has been metallurgically and process "optimized" to the highest attainable level of toughness. At strength levels below 120 ksi YS, a wide variety of alloys should be expected to require major plastic overload for fracture propagation and should not be analyzable by the present procedures of fracture mechanics. In fact, this has been our experience, as described previously. It should be cautioned that data described above relate to 1-in. thick plate material.

The DWTT provides a means of assessing the fracture toughness of weld metal deposits. Such tests have been conducted for titanium welds. The results are now used routinely as a guide in improving fracture toughness of welds by stress relief anneals and aging treatments. The "weld" DWTT specimen involves two halves of the DWTT specimen welded together across the 5-in. dimension, using a simple weld joint configuration - such as a single or double Vee. The 1-1/2-in. deep, brittle crack starter weld is located on the central axis of the test weld. Examples of weld metal fracture toughness determinations using the DWTT are presented for several alloys and treatments in the table below.

Weld Metal Fracture Toughness Properties (DWTT)

Alloy (%)	As Deposited (ft-lb)	Anneal		Age		
		Temp/Time	(ft-lb)	Temp/Time	(ft-lb)	
Ti-6Al-2Mo	1500	1800°F/1hrVac 1750°F/1hrVac 1800°F/1hrVac	1540-1600	1100°F/2hr 1200°F/2hr	1780 2800	1
Ti-7Al-2Cb-1Ta	2900 2780					2
Ti-7Al-2Mo	1400	1775°F/1hrAC	—————>	1200°F/2hr	1100	3

<sup>1</sup> MIG WELDS - Base plate properties with similar heat treatments exceed 2500 ft-lb.

<sup>2</sup> MIG WELDS - Base plate properties 2100-2200 ft-lb.

<sup>3</sup> EB WELDS - Base plate properties with similar heat treatment 2800 ft-lb. (Should be considered exploratory).

DWTT data for titanium welds are very limited at present but with the procedural technique now established, rapid collection of data is possible and it is planned to evolve FTID charts for titanium alloy weld metal. This will then provide a reference "yardstick" to evaluate the merits of various welding practices, which is required to further optimize weld procedures. The metallurgist and the research welding engineer may then assess new welding techniques and new weld metal alloys with the aim of satisfying the need for higher strength and higher toughness weld metal for use in complex structural applications. The same can be said for titanium alloy and processing optimization studies now underway for the base plate.

In the near future, these studies will include 2 to 3-in. thick titanium alloy plates and welds. Also, additional attention will be given to fracture mechanics studies of the high strength, relatively brittle alloys and welds of the 130-150 ksi YS range for 1 to 3-in. plates. Explosion bulge and drop-weight bulge tests are also planned for purposes of evaluating HAZ (heat-affected-zone) properties. The bulge test techniques are described in a section to follow.

## EVOLUTION OF FRACTURE TOUGHNESS INDEX DIAGRAM FOR ALUMINUM ALLOYS

Fracture toughness information for aluminum alloys in thick sections has been limited primarily to circular notch tests conducted over a wide range of strength levels and to fracture mechanics tests for the high strength, relatively brittle alloys. The Charpy V ( $C_v$ ) test has generally been disregarded for good reasons, as shown in Fig. 29. The  $C_v$  curves are "flat" and the values are very low, even for low strength alloys. In effect,  $C_v$  test data have been considered undecipherable even for purposes of relative fracture toughness discrimination and we would concur with this opinion at this date. It should be noted that NRL electron microscope fractographic studies have disclosed that "dimple rupture" is the basic fracture mode over the entire range of the  $C_v$  tests shown in Fig. 29.

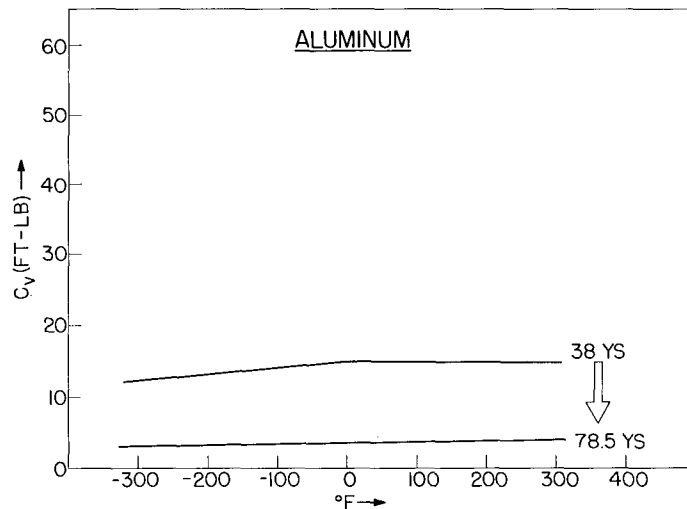


Fig. 29 - General features of  $C_v$  energy curves for aluminum alloy plate

The NRL approach to investigating aluminum alloys followed the already-described procedures for steels and titanium alloys. The drop-weight tear test (DWTT) energy relationship to  $C_v$  energy for aluminum alloys is shown in Fig. 30 in comparison to the previously described correlation bands for steels and titanium alloys. It is apparent from this figure that the very low  $C_v$  energy values that pose difficulties of discrimination between alloys are replaced by an expanded range of DWTT energy. Thus, the DWTT provides a means of fracture toughness discrimination that the  $C_v$  test does not. The same statement applies to the low  $C_v$  value range of steels and titanium alloys.

The ordinarily preferred method of evaluating fracture toughness of aluminum alloys, the notch-strength ratio determined for circular, sharp-notched tensile test specimens, has been correlated to DWTT results as a point of reference with the existing bulk of data in the literature. The correlation band is presented in Fig. 31. The notch-strength ratio

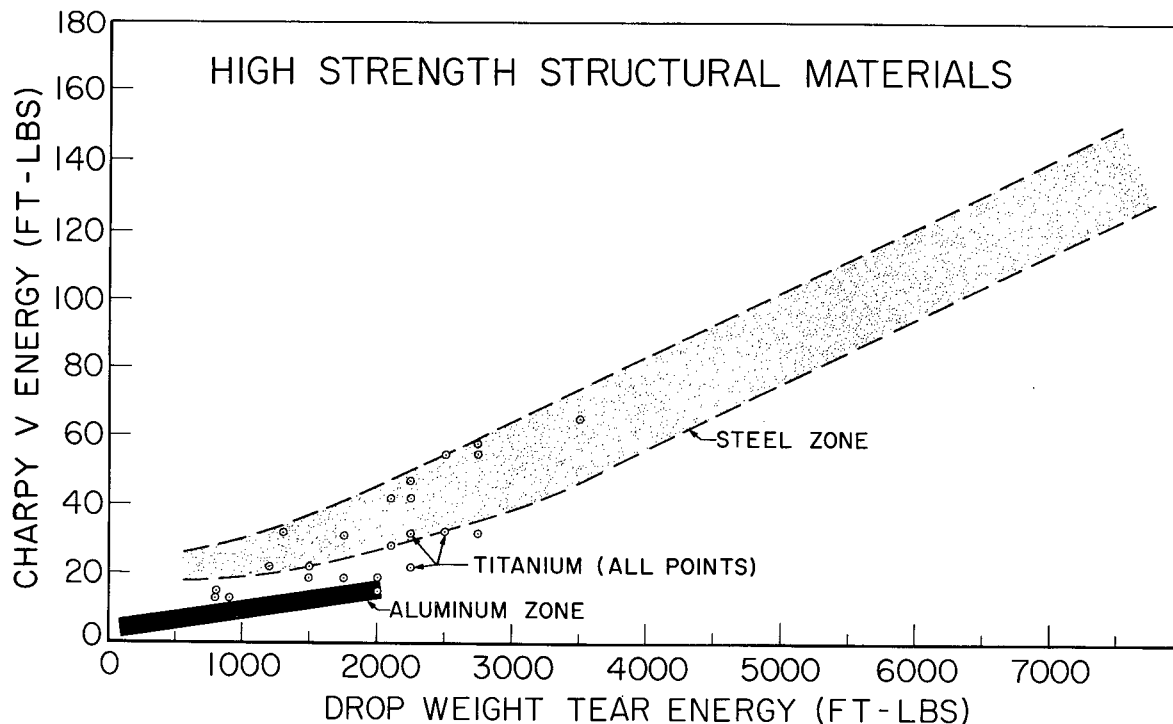


Fig. 30 - Correlations between  $C_v$  energy and DWTT energy for aluminum alloys as compared to other high strength structural materials

appears to have a slightly more definable relationship to the DWTT energy than the  $C_v$  test energy, as is evident from the slope of the  $C_v$  band at the top of the figure. Note that the data band includes tests of both simple machine-notched and fatigue cracked, circular notch specimens, as well as specimens of longitudinal and transverse orientation. In general, it appears that the circular sharp notch tensile test does not provide for a "fine" discrimination of fracture toughness such as is possible with the DWTT.

The aluminum alloy DWTT measures 1 × 5 × 17 inches. Phosphor bronze wire is diffused into the material using the previously-described electron beam welding technique to provide a 1-1/2-in. deep, through-thickness brittle weld for crack initiation purposes. As a matter of interest, less than 80 ft-lb energy is required to initiate fracture in the brittle weld.

A very preliminary Fracture Toughness Index Diagram (FTID) chart for 1-in. thick, commercially produced aluminum plates is presented in Fig. 32. As for the case of steels and titanium alloys, the diagram relates DWTT energy to ETT performance at 30° F. A relatively small number of alloys are represented in the DWTT energy - YS spectrum of data points. The alloy designations and temper conditions are listed beside the data points. An OMTL could be defined only for the strong (RW) fracture toughness direction because of the limited data available. The weak direction (WR) fracture toughness properties are considerably lower at all but the highest strength levels, indicating considerable anisotropy in the plate material. The ETT performance indicates that materials with less than 200-300 ft-lb DWTT energy will "break flat," i.e., propagate fractures, under elastic loading conditions. Figure 33 provides an example of such performance in the ETT compared to a condition of high resistance to fracture propagation. For materials of above 200-300 ft-lb DWTT energy, plastic overload is required for fracture propagation in the ETT. Materials having DWTT energies above 700-800 ft-lb require over 10% plastic strain for fracture propagation in the ETT.

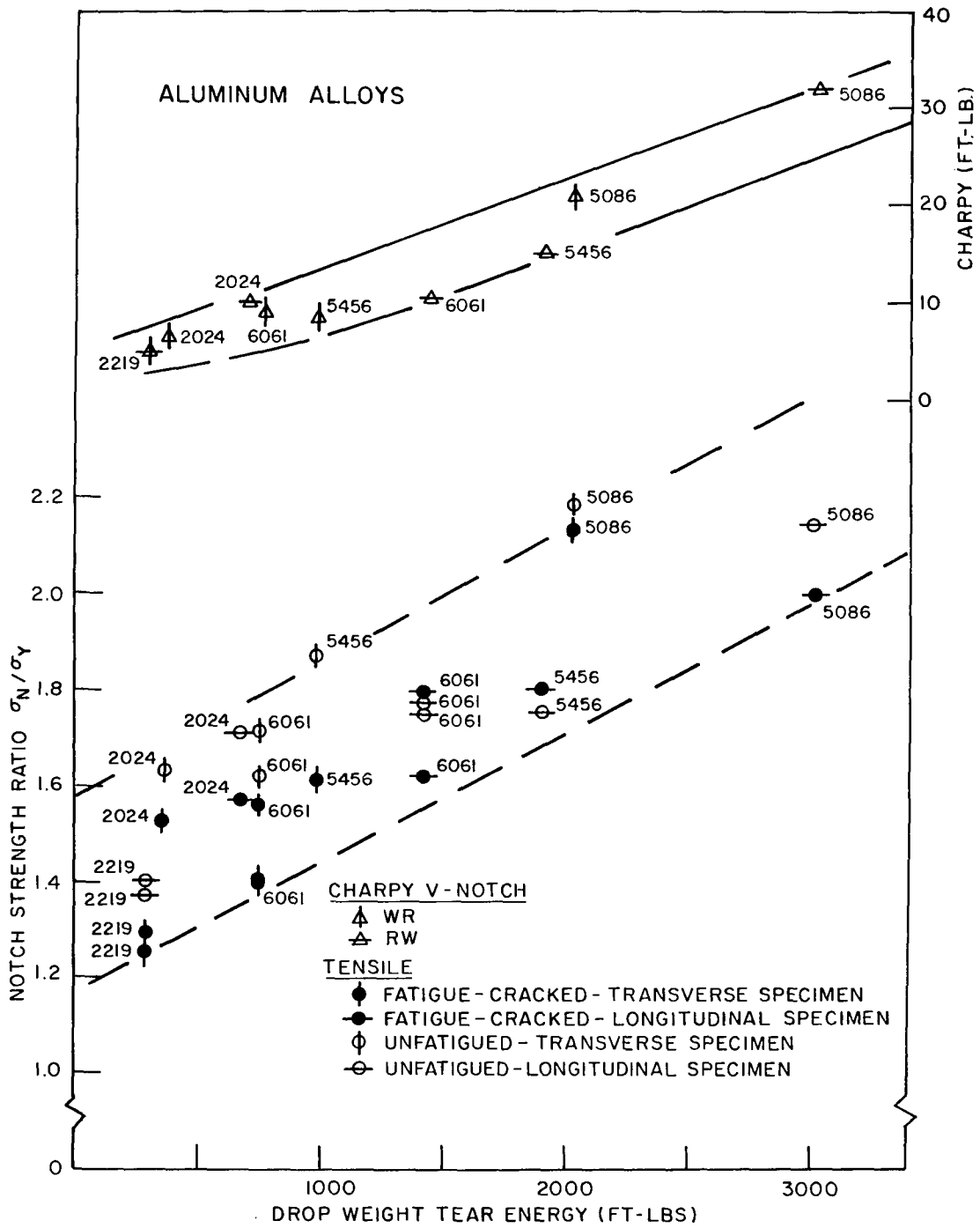


Fig. 31 - Circular, sharp notch tensile test, notch-strength ratio relationships to DWT energy for 1-in. thick aluminum alloy plate.  $C_v$  test relationships shown for comparison.

UNCLASSIFIED

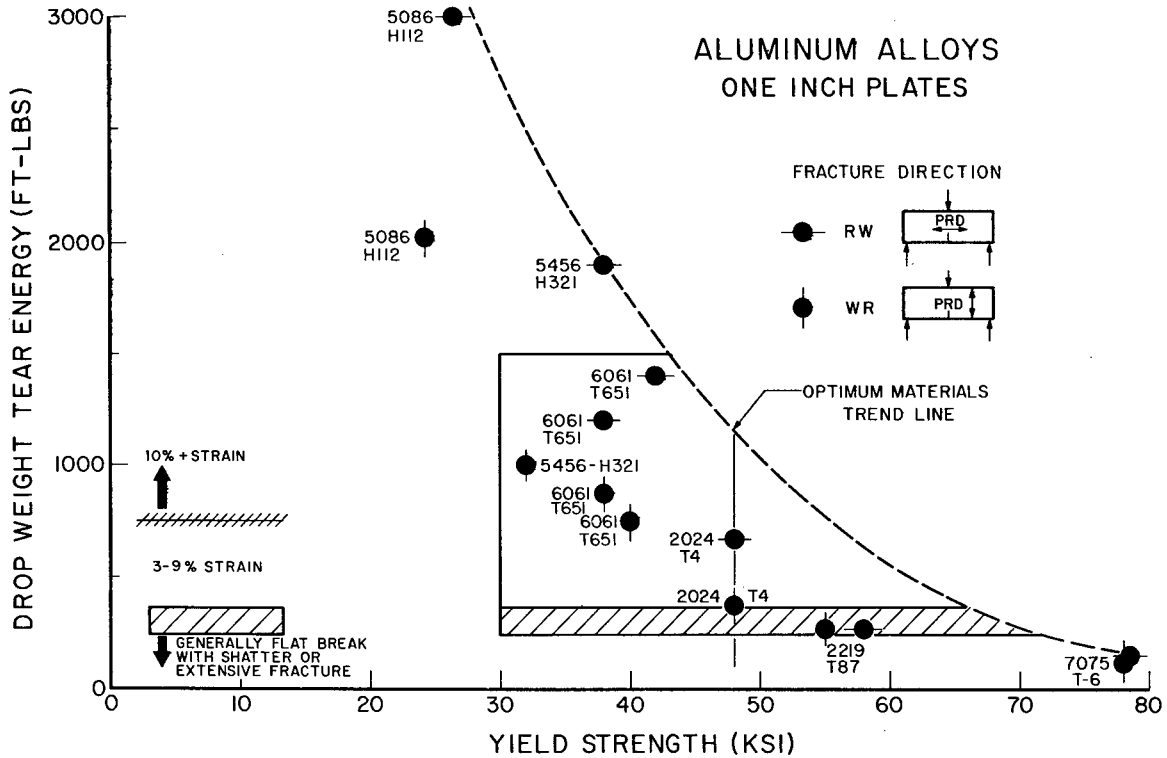
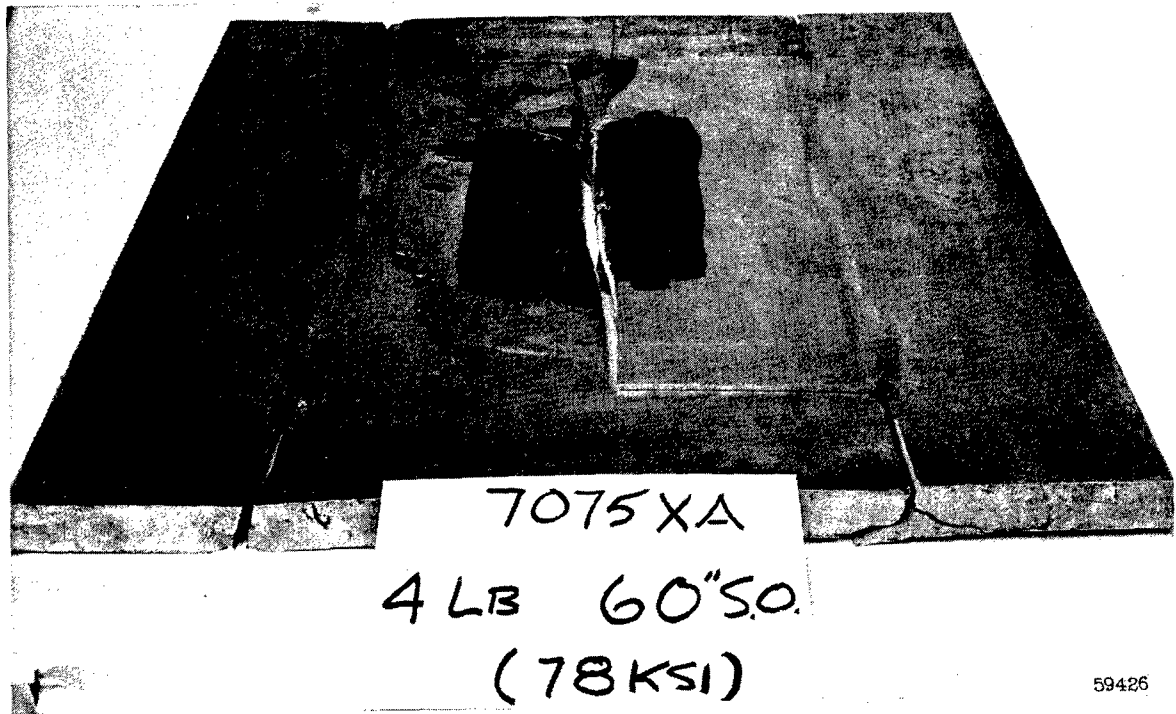


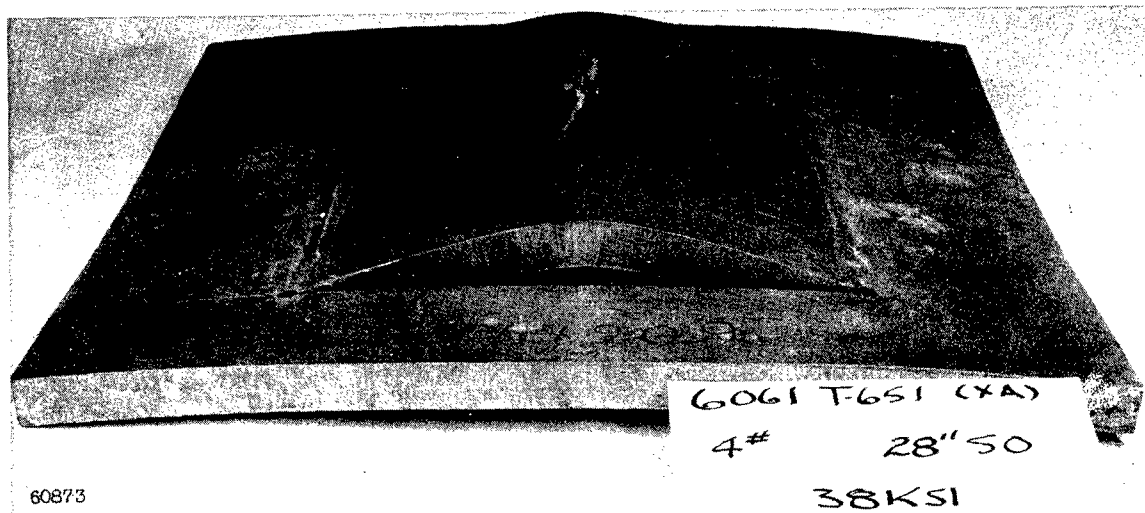
Fig. 32 - Preliminary Fracture Toughness Index Diagram (FTID) chart for 1-in. thick aluminum alloy plate. Alloy designations and tempers are indicated with data points. The OMTL relationship to yield strength is based on the strong direction of fracture propagation in this case because of limited data points.

The cross-over point of the lower limit band of the FTID chart (separating elastic level fracture propagation from plastic overload requirements for fracture propagation) with the strong direction OMTL indicates that in the range of 60-80 ksi YS most alloys should be expected to propagate fractures at elastic stress levels. In the 50-60 ksi YS range, there is a suggestion that optimized alloys - if well cross-rolled - may rise above this low level of fracture resistance. At strength levels below 50 ksi YS, it appears readily possible to develop a wide range of alloys which will require plastic deformation overload for fracture propagation.

At this point we should make a "fine" point of distinction - despite the fact that the described plastic overloads are required, the intrinsic energy absorption in fracture propagation is relatively low for aluminum as compared to that for steels and titanium alloys. Thus, engineering judgment may be required to assess if fracture safety is indeed attained for special cases where large regions of a structure may be subjected to plastic overload (say explosive attack). In such an event a large region of rupture may result, thus weakening the structure, such as a ship deck. Obviously, if the structure is not subjected to extensive regions of plastic overloads, this point is of academic importance. For the general engineering case, separation between fracture-safe and potentially fracture propagating alloys may be made on the usual basis. That is, if fractures do not propagate at elastic stress levels, the structure will be fracture-safe despite the development of plastic flow at geometric points that are stress indeterminate. The special case referred to above may be expected to apply to any material that features very low specific energy absorption - despite the fact that general plastic overload is required for fracture propagation. Another example of this case is the development of a very large crack in a structure (say a very long weld crack flaw) which automatically results in plastic overload at the crack ends regions (not only the crack tip) from a strictly P/A (load/section area -



(a)



(b)

Fig. 33 - Examples of extremes in ETT fracture propagation resistance of aluminum alloy plates

local nominal stress) point of view - as has been discussed for internally pressured and pneumatically loaded pressure vessels (1,2). Such a situation may occur if an extensive weld rupture should develop in a ship deck. The question then involves a change in general level of P/A and plastic overload, although not a subject of initial design, becomes a fact due to the accident. For such unusual situations, high specific energy absorption plays a part, as well as the plastic overload requirement for fracture propagation. This problem is of concern to designers of military ships and of pneumatically loaded pressure vessels.

It should be noted that the commercial alloys investigated to date have shown marked anisotropy with respect to fracture propagation resistance in the "weak" as compared to the "strong" direction. Again, these studies have not been carried to the same limits of fine distinction as made for the steels, and the present FTID chart is considered a crude first edition. We are proceeding to test thick section aluminum plates and welds, and bulge tests for evaluation of the performance of HAZ (heat-affected-zone), as is being done for steels and titanium alloys.

## CONSIDERATION OF THICKNESS EFFECTS

The drop weight tear test may be "scaled up" to evaluate the combined metallurgical and mechanical effects of increased thickness. By the use of large drop-weight test equipment and the "bracketing" technique for determining energy absorption, there is no practical limit of thickness that may be evaluated. Figure 34 illustrates a 2-in. thick titanium alloy DWTT specimen. Figure 35 is a photograph of the NRL 180,000 ft-lb energy drop-weight machine (6-ton weight with a 15-ft-drop height). Depending on the fracture energy absorption of the test material, it may be possible to test plate sections of 6-in. or greater thickness with relative ease, as compared to any other known test.

A program aimed at tests of thick steels, titanium, and aluminum alloys is now in its early stages of development, with material ranging from 2 to 4 inches in thickness. This program will include tests of "composite" materials comprised of high strength cores and lower strength (higher fracture toughness) roll-bonded surface layers. It will also include thick welds produced by various processes. Because of limited data obtained to date, we are not prepared to present thickness effects at this time. However, it is clear that the test procedures are practical and will be analyzable in the usual terms of: 1. - high fracture toughness sufficient to preclude fracture propagation at elastic stress levels, and 2. - low fracture toughness that permits fracture propagation at elastic stress levels.

A plate specimen similar to the explosion tear test (ETT) with a central crack flaw, loaded by the drop of the large weight impacting on an aluminum striker pad, schematic

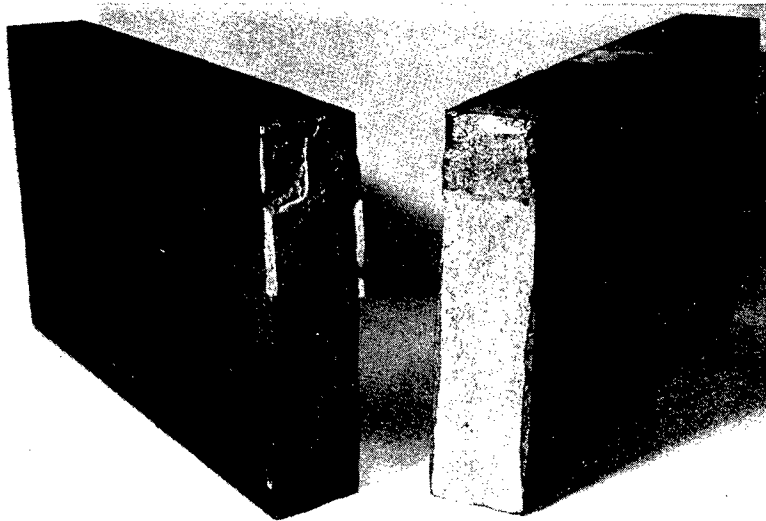


Fig. 34 - Electron beam embrittled weld DWTT specimen scaled for test of 2-in. thick titanium alloy

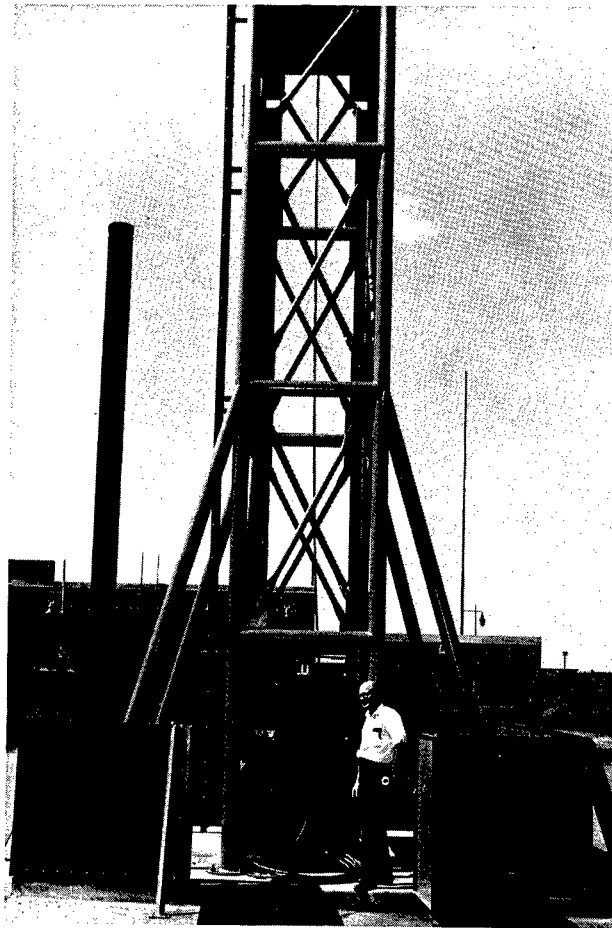


Fig. 35 - NRL 180,000 ft-lb drop-weight test machine designed for thick section DWT and for drop-weight bulge tests

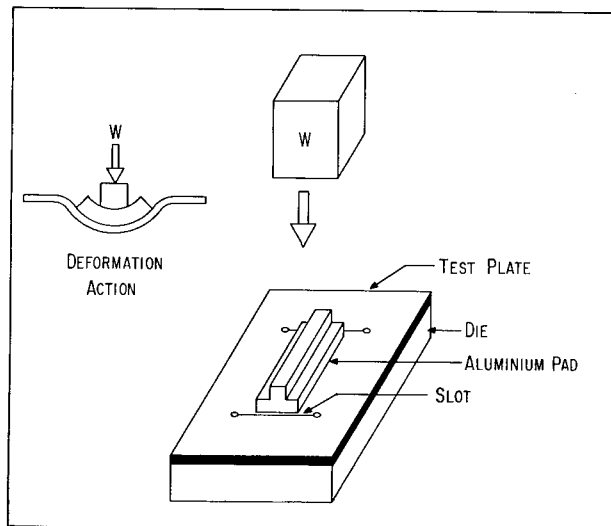


Fig. 36 - Schematic illustration of drop-weight-loaded version of ETT

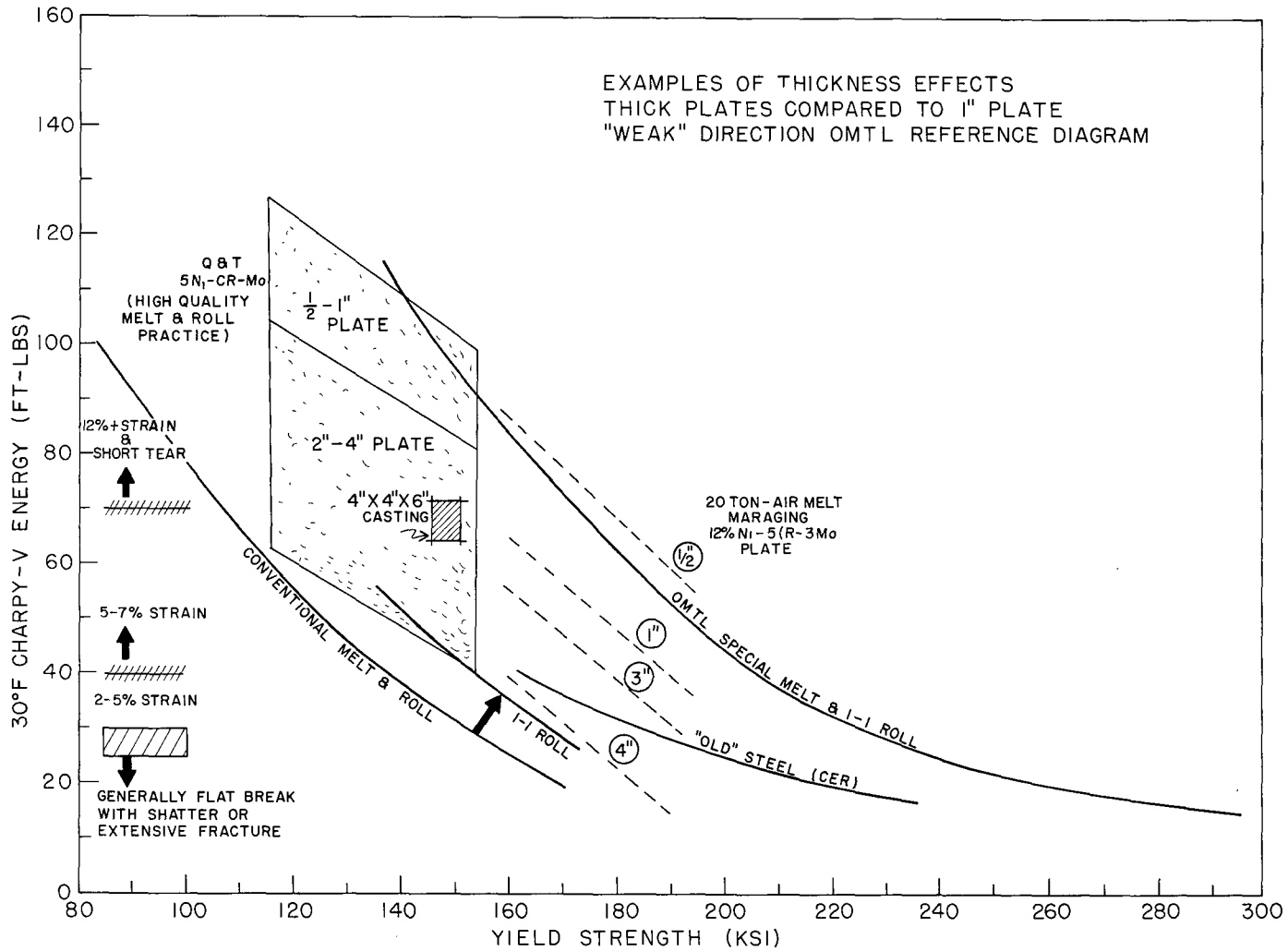


Fig. 37 - Illustrating data of possible effects of increased steelplate thickness on decrease in fracture toughness by comparison with the OMTL chart presented in Fig. 22 for 1-in. thick steel plates. The  $C_v$  values for the thick sections are not necessarily representative of materials that are process optimized for thick sections.

drawing shown in Fig. 36, is in initial trial stages for use in providing correlations of fracture propagability for thick sections under conditions of elastic and plastic loads. The metallurgical effects to be expected for increased thickness may be substantial in many cases. A "rough" index of thickness effects may be deduced from comparison of  $C_v$  data with the previously presented OMTL base line data for 1-in. steel plates (Fig. 37). The thickness effects data for the two steels illustrated were obtained by the U.S. Steel Research Laboratory under the BUSHIPS-U.S. Steel research contracts. These results are intended only to illustrate possible thickness effects - the specific values for the materials are not necessarily representative of the best that are attainable for thick steels and should be considered in such terms. Metallurgical, compositional, processing, and heat-treatment variables may be adjusted to minimize the decrease in fracture toughness with increased thickness. The main point to be made is that all of these effects require exhaustive evaluation and definition. The improvements attained should be based on evaluations of full thickness DWTT performance to provide a more exact intercomparison than that developed by  $C_v$  data taken at some arbitrary position in the thick plate section, as discussed previously.

This phase of the studies is expected to be time consuming from all points of view; however, the existence of practical test techniques should provide impetus for such studies which heretofore have been avoided because of test inadequacies.

## EVALUATION AND CONTROL OF WELD METAL PROPERTIES

We are entering an era in which a multiplicity of weld techniques may be used to produce welds in thick sections of high strength steels, titanium, and aluminum. It is already known, from limited weld DWTT data of 1-in. thickness specimens and from  $C_v$  determinations of thick section welds, that the weld technique as well as the weld analysis (as deposited), are mutually interacting and critical in establishing the level of fracture toughness – small amounts of  $O_2$ ,  $N_2$ ,  $H_2$ , etc., may be highly detrimental for high strength metals. For explorations of evolutionary development possibilities and “direction seeking” in optimizing weld fracture toughness, relatively simple test procedures are required. Test finesse that requires research laboratory techniques must be relegated to metals that approach low fracture toughness levels (at the optimum) and therefore require such measurement precision. Again, if DWTT can demonstrate consistent attainability of high fracture toughness for specific welding procedures and alloys, it may not be necessary to conduct specially precise fracture toughness tests; in fact, it may not be possible to obtain valid numbers of fracture mechanics type. The point of view is – that for the welds, as for the base metal, the role of the metallurgist is to evolve metallurgical and processing methods which in fact provide high fracture toughness to the highest attainable strength levels. Above these strength levels, it becomes necessary to exercise the usual change-over to precise measurement and to build “precise” structures to prevent fractures that may follow weld paths. Figure 38 illustrates examples of  $C_v$  energy values attainable for welds in 1/2 to 1-in. thick steel plates, as referenced to the FTID-OMTL charts for 1-in. thick steel plates presented in Fig. 22. There is a suggestion in these data that weld toughness (in multi-pass welding) for high strength steels, may attain higher values than the base metal toughness as section sizes are increased. The full thickness DWTT should allow for discriminating comparisons over a wide range of weld thickness for all structural materials of interest. The importance of integrated evaluations of metallurgical and mechanical effects of increased thickness for welds cannot be overemphasized. Any laboratory equipment (or crane yard) that permits the dropping of a large weight from a variable height provides the required capabilities for such exploratory evaluation and process developments of welds.

It should be recognized that a great deal of exacting metallurgical and process control in the shop must be exercised in controlling weld metal properties to retain optimized properties that are achieved by laboratory investigations. The higher the strength level, the more rigorous must be the control over the procedures – this applies to steels, titanium, and aluminum alloys. Such requirements unavoidably lead to the directions of automatic, down-hand welding for the high and ultra-high strength ranges of the subject metals. A more exact definition would be that for any characteristic family of alloys within a generic metal group, the need for exact control is accentuated as the strength level range of change from the above-yield to the below-yield fracture propagation characteristics is passed. The change point varies with family; for example, in Fig. 38 the Ni-Cr-Mo composition MIG weld family “as deposited” shows a sharp change in fracture toughness in the range of 130-150 ksi YS. The 12% Ni, maraging steel MIG-TIG weld family “as aged” apparently enters the critical range of change in the 160-190 ksi YS level. As an additional example, the Ni-Cr-Mo composition of the stick electrode family “as deposited” does not match the MIG process capabilities of the same compositions. Now, all of the properties presented in the chart relate to “down-hand,” essentially “laboratory” produced welds. These data should not be taken as necessarily representative of vertical or shop welded properties. The importance of a reference diagram to serve as a “yardstick” for evaluation of specific processes and welding procedures becomes evident from these discussions.

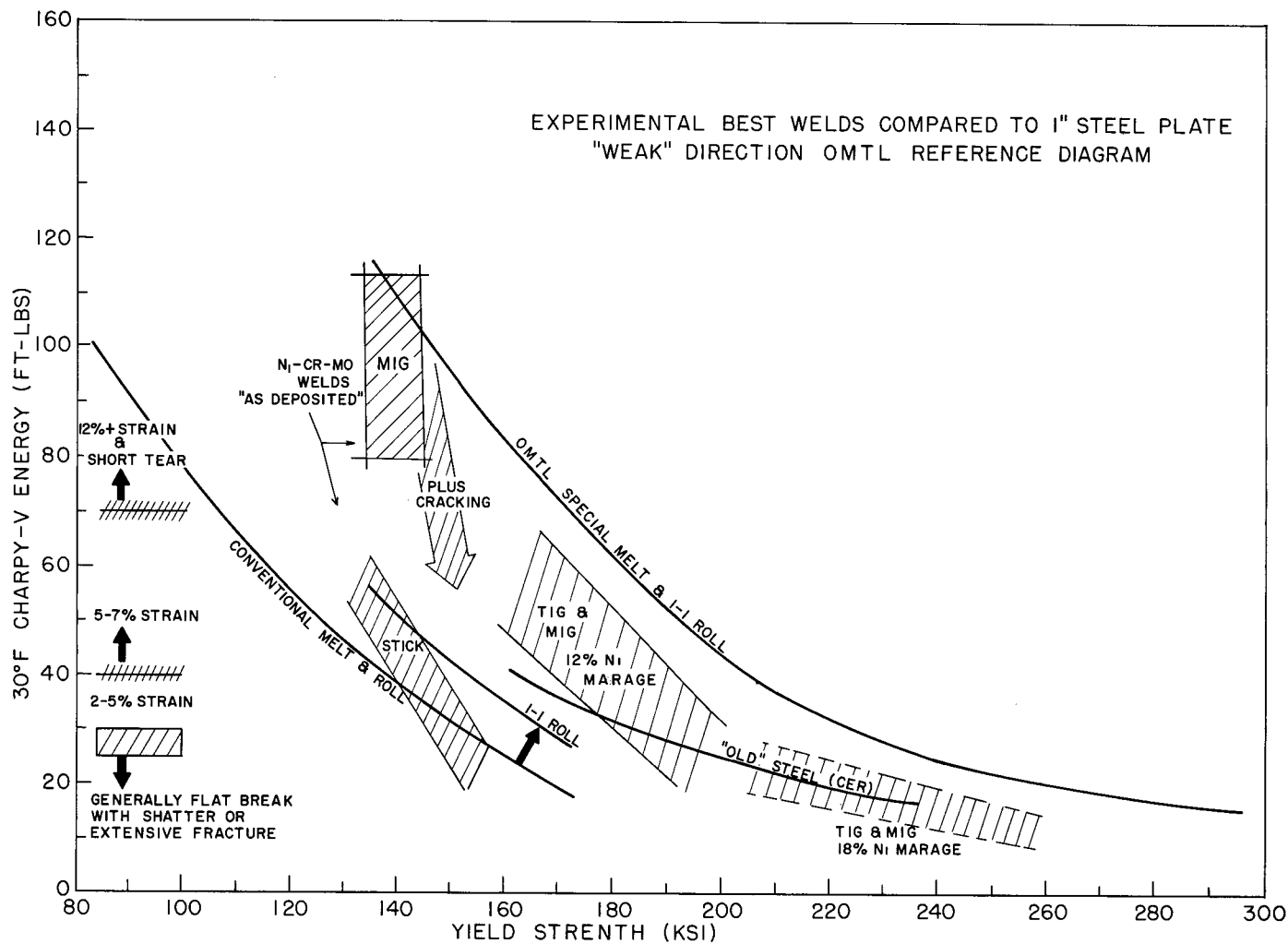


Fig. 38 - Illustrating preliminary weld metal Fracture Toughness Index Diagram (FTID) projections, based on  $C_v$  tests referenced to 1-in. thick plate steel data presented in Fig. 22

However, weld properties are determined during the "act of welding" and retention of optimum characteristics may require exact shop control. The degree of control that is required is determined by the "margin" between the desired design value based on laboratory optimized procedures and values that may be obtained in the shop. This statement is particularly important for the case of strength levels which fall in the 50-150 ksi  $\sqrt{\text{in.}}$  plane strain  $K_{Ic}$  territory. A slight deviation in procedures and an expected 100+  $K_{Ic}$  value can slip to 40 or less, thus decreasing the critical flaw size from the inspectable to the uninspectable range. Such a case is a considerably different order of production control problem as compared to the case of a 30-40 ksi lower strength weld of the same generic family which could be laboratory optimized to have high DWTT values and, therefore, a considerable "margin" for statistical variance in production. Each situation must be analyzed on its own merits; however, it becomes clear that complex structures cannot be built using weld metal that has minimal "margin" features - the fracture toughness margin for such structures must be substantial if shop welding is to be practical. The "old time" supervisory welding metallurgist merely had to assure himself that the welder used the proper electrode and was occasionally "qualified." The high strength materials welding supervision control is orders of magnitude more involved and demanding of exactness. "Old line" shops that attempt to enter this field must drop preconceived notions of welding know-how. Past experience with low strength steel becomes of no consequence; education in the new field of high strength materials must "start from scratch" - the results of reliance on old experience may be catastrophic in both a structural and financial sense.

## EVALUATION AND CONTROL OF HEAT-AFFECTED-ZONE PROPERTIES

This is the most debatable, least understood, and most difficult area of weldment performance evaluation. The heat-affected-zone (HAZ) is a composite of "zones" - it is not one zone or one intrinsic material. The interaction of the material in these "zones" with the surrounding weld and plate elements provide mechanical conditions of involving plastic flow and fracture that defy mathematical analysis. We do not, at this time, propose the use of the DWTT for HAZ evaluation, or the  $C_v$  test, or for that matter any other single test of small size. We may eventually reach such a stage of development, but for the immediate future the possibilities of such attainment are not very promising, to say the least.

It is believed that HAZ fracture toughness evaluations require test specimens in the order of a Robertson crack arrest type or its equivalent - in other words, a large specimen which allows the metallurgical-mechanical "weakest" zone to be self-selected in the compendium of zones in the heat-affected region. Such selection is self-determined in an explosion bulge test utilizing a crack starting (flaw) element. The fracture resistance may be assessed by noting the characteristics of the fracture path - limited or extensive. This process may not be mathematically sophisticated, but it is most persuasive to visual examination of results. In order to bring the bulge test practices within the capabilities of laboratories not having access to explosion sites, the large drop-weight test machine has been developed additionally as a bulge test device. The technique is based upon using an aluminum striker-pad of the general features shown in Fig. 39. On impact, the soft aluminum pad assumes the contours of a spherical surface, and the test plate likewise is forced into this configuration. Again, it must be emphasized that such tests discriminate between HAZ regions of intrinsically high resistance to fracture propagation from those of low resistance. Figure 40 illustrates an example of low energy HAZ fracture path for a weldment of plate and weld of high fracture toughness. For HAZ regions that show high

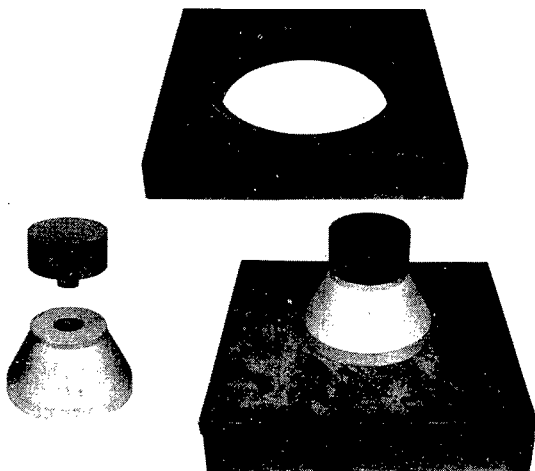


Fig. 39 - Feature of NRL drop-weight bulge test. The cast, soft aluminum alloy pad deforms to a perfectly spherical configuration, causing a spherical bulge to develop in the test weldment. A flat-surface steel pin is inserted at the top of the pad to conform to the striking surface of the weight.

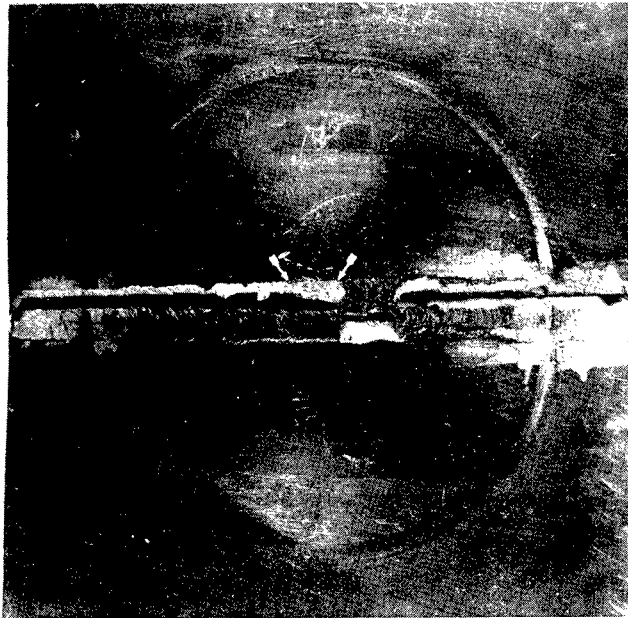


Fig. 40 - Illustrating the case of low fracture energy propagation by HAZ path in a weldment of high strength steel featuring high fracture toughness plate and weld metal

fracture propagation resistance, there is no need to attempt obtaining exact numerical evaluation of fracture toughness, if such could be done. Mathematical evaluation procedures, as may be evolved, can best be saved for HAZ conditions that intrinsically cannot be made reasonably fracture resistant by metallurgical procedural control. Again, the argument is not against using sophisticated mathematical techniques but to reserve these for the HAZ with properties that require such treatment.

Drop-weight bulge test screening can readily establish if high HAZ fracture toughness is attainable by any of the many options of metallurgical and weld processing methodology. When attained with sufficient margin to allow for manufacturing variables, it becomes possible to exercise practical control over the welding operation to ensure reproducing weldments of reliable HAZ properties. With the move to automatic (more reproducible) welding techniques, the promise of this simple approach becomes possible with narrower limits on the "margins" required. The discussions of procedural controls presented in the section on weld metal properties may properly be repeated at this point, for the case of the HAZ of weldments.

## MICROMECHANISMS OF FRACTURE PROCESSES

U.S. GOVERNMENT PRINTING OFFICE: 1965 O 345-160

Electron microscope fractography has become a standard tool for understanding the nature of the micromechanisms of fracture that are associated with the fracture toughness properties measured for the high strength materials described in this report. We do not propose to extensively document these studies in this report. Excellent references as to procedural techniques and interpretive procedures have been issued by Beachem (14,15, 16), based on NRL studies.

It should be understood that the classical concept of fracture propagation, in the sense of physical separation of the metal at the exact point of the crack tip, is not a factual representation of the micromechanism of fracture except for materials of extreme brittleness, such as glass and ceramics. In fact, the energy absorption process in fracture propagation is involved with the genesis and growth of defects, cleavage fissures, voids, grain boundary separations, etc. in advance of the crack tip. All such processes involve a certain degree of plastic flow, even for metals of high relative brittleness. It is the degree of plastic flow in advance of the crack tip that determines the energy absorption of the fracturing process. In fracture mechanics terminology, the plastic flow zone at the crack tip is termed "the process zone" and the mathematical idealization that is made involves considering the "effective" length of the crack as including the "process zone" to its calculated center-point position. The plastic zone in advance of the crack tip is idealized as being of circular cross section. With increasing fracture toughness, the plastic zone size increases and presents difficulties of mathematical analysis and thereby difficulties of experimental definition of the plane strain fracture toughness.

The extent of growth of the plastic zone with increasing stress intensity is determined by micro-processes of fracture at the sub-optical microscopic level of resolution. Because of its inherently high resolution capabilities and high depth of focus, the electron microscope is eminently suited to examination of film replicas of the fracture surfaces. Such examinations provide post-fact analyses of the fine details of the genesis and growth of micro-fractures in the plastic zone during its growth and to the point of macroscopic rupture in advance of the crack tip. Such knowledge provides a guide for establishing the basic nature of the processes which control the plastic zone size and thereby the energy absorption of the material. These guides also provide information to the physical metallurgist that is useful in optimizing the toughness level of the metal.

In a brief introductory form, we shall compare  $C_v$  curve energy data to the basic micro-fracture modes for various metals. Figure 41 illustrates the sharp temperature transition (HY-80 steel) which is associated with a change from dimple rupture fracture of high energy absorption (involving the genesis and growth of spherical voids in the plastic zone) to low energy absorption cleavage fracture (involving microscopic flat fracture regions with "river patterns"). This figure also illustrates that as the  $C_v$  curve "rotates" downward to a low shelf energy and to a low slope appearance, the basic cause for this effect could be due to various basic microfracture mechanisms. For example it may be due to development of dimple rupture of "rudimentary" form - that is, the spherical voids in the plastic zone begin to form but do not progress very far before the connecting "bridges" are broken. Or it may be due to grain boundary separation, basically involving weakening of grain boundaries by preferential precipitates or other microstructural embrittling agents. It may also be due to the development of "quasi-cleavage" - not

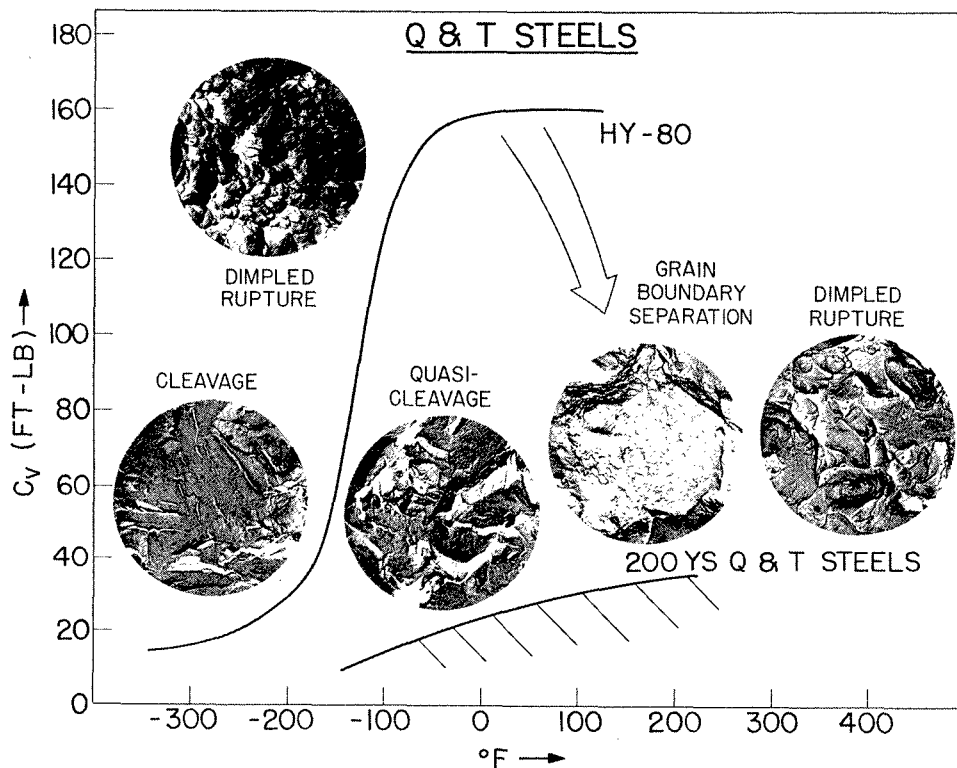


Fig. 41 - Electron microscope fractographs illustrating various micromechanisms of fracture of steels in relation to  $C_v$  curves—approx. 4000X

true cleavage on specific crystal planes but “flattish” break regions, perhaps the ultimate form of rudimentary evolution of dimples that do not enlarge significantly before rupture occurs.

Figure 42 illustrates the result of studies on maraging steels. At intermediate levels of yield strength, a sharp transition temperature effect is noted, consequent to a change from dimple rupture fracture to quasi-cleavage fracture. At high levels of yield strength, characteristically flat, low energy  $C_v$  curves are obtained. The dimple rupture mode of fracture is retained over the entire temperature range shown but with change to the rudimentary form with decreasing temperature.

Figure 43 illustrates the case for titanium alloys taken from an earlier version of the  $C_v$  summary bands shown in the titanium section. In all cases, the fracture mode is noted to be dimple rupture; however, for specimens of high  $C_v$  energy the dimples are large and quite distinct, while those of low  $C_v$  energy show dimples of rudimentary form.

Figure 44 illustrates the case for aluminum alloys. The aluminum matrix grains always show fracture of dimple rupture type, but with the fine details and size of the dimples changing with decreasing  $C_v$  energy. The high strength alloys also show cleavage fracture of second phase particles which may serve as crack initiation agents at a microscopic level.

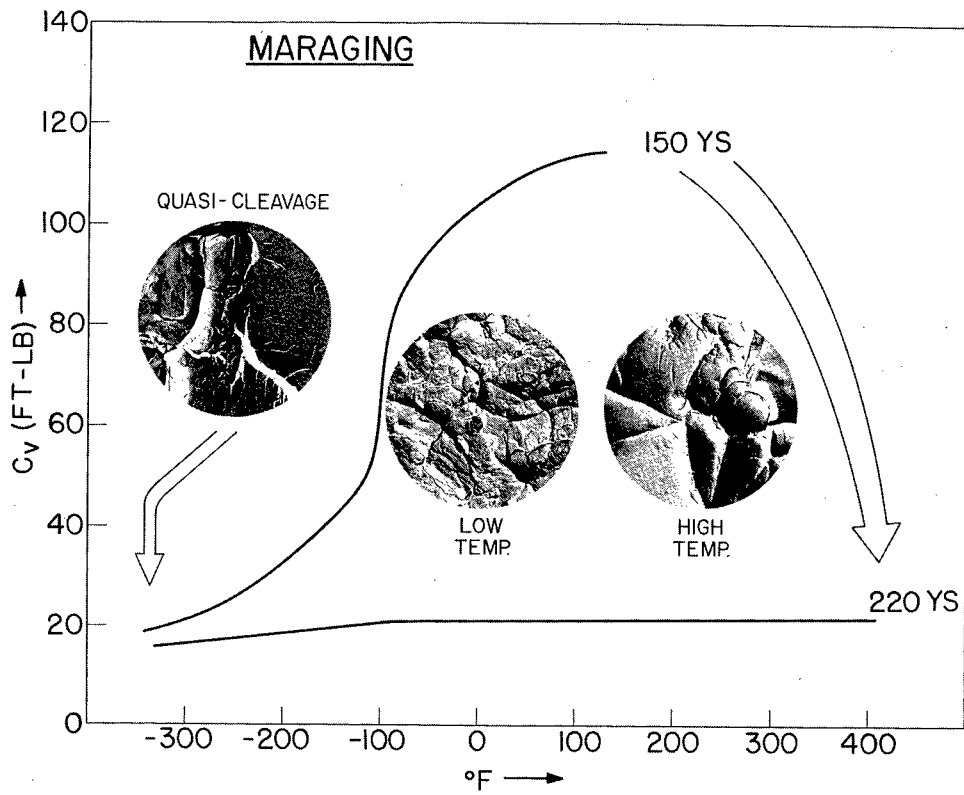


Fig. 42 - Micromechanisms of fracture for maraging steels in relation to  $C_v$  curves—approx. 4000X

## NAVAL RESEARCH LABORATORY

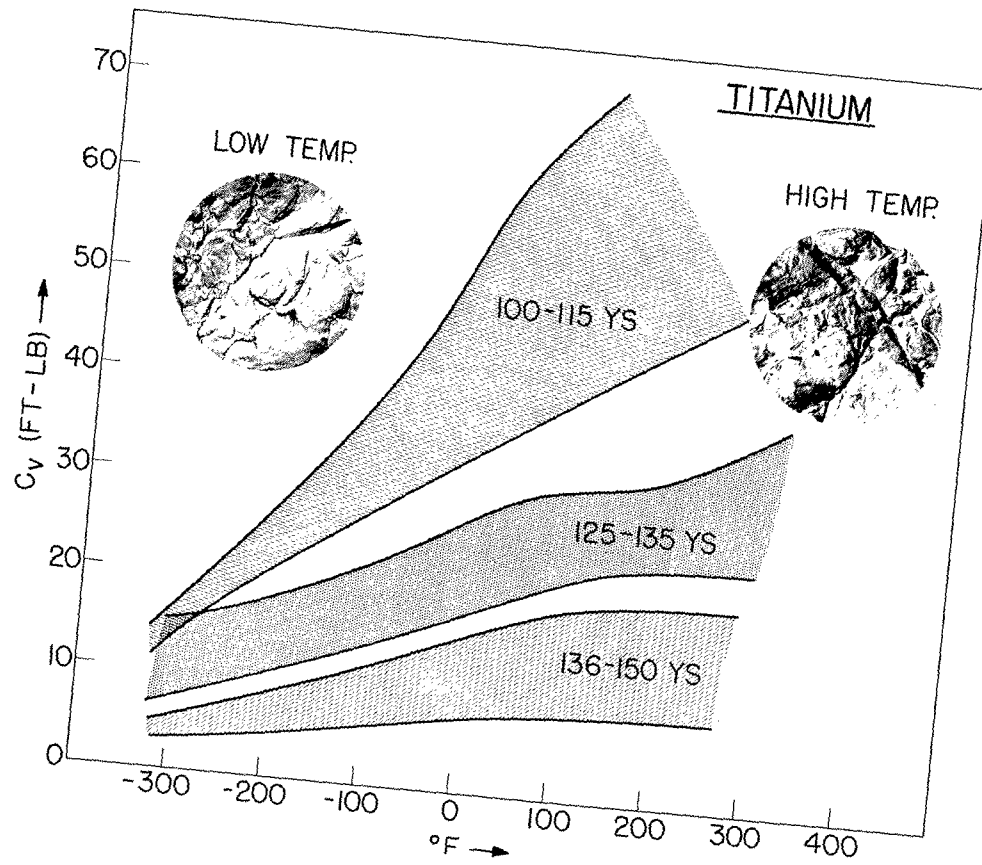


Fig. 43 - Micromechanisms of fracture for titanium alloys in relation to  $C_v$  curves—approx. 4000X

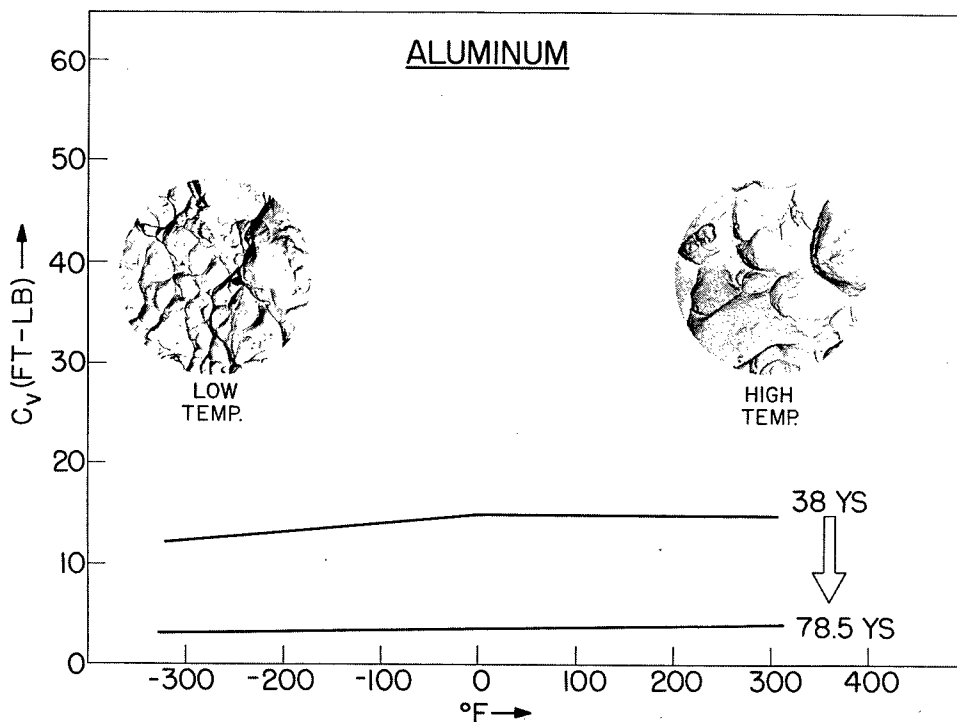


Fig. 44 - Micromechanisms of fracture for aluminum alloys in relation to  $C_v$  curves—approx. 4000X

Now, there are some surprises - in the presence of water and for tests involving "slow" growth propagation of fracture, such as stress corrosion cracking tests (SCC) or low cycle fatigue tests, the basic microscopic mode of fracture may be changed from that observed in  $C_v$ , DWTT or "dry" fracture mechanics tests, all of which may be represented as relating to the general "fast" mode of fracture propagation. An outstanding example is that of titanium-7Al-2Cb-1Ta alloys, which under the conditions of water environment, involving both static SCC tests and low cycle fatigue tests (17), showed a dramatic decrease in resistance to fracture propagation of the "slow mode" compared to tests conducted in air. Examination of the fracture surfaces for the "wet" tests indicated a change in fracture mode to quasi-cleavage fracture. The point to be emphasized is that quasi-cleavage fractures have not been observed for titanium alloys in the absence of a water (or moist air) environment. The environmental effects are both time and stress intensity dependent.

Thus, environmental effects may change the nature of the microscopic fracture modes and promote instability (that is, growth) of flaws that otherwise would not propagate. High strength steels and aluminum alloys are similarly susceptible to such environmental effects involving slow crack growth. The slow growth fracture propagation processes and the nature of environmental effects will be discussed in the two sections to follow. These processes are not to be confused with the "fast" fracture propagation discussed in the previous sections of this report, but nevertheless they present serious problems of analysis of fracture safety, as will be discussed.

Electron microscope fractographic techniques provide a tool for metallurgical understanding of causative effects for low energy fracture and thereby suggest procedures for evolving metallurgical improvements.

## IMPLICATIONS OF STRESS-CORROSION-CRACKING ASPECTS

A specific flaw in a given metal and at a specified sub-critical stress level may be considerable "stable," i.e., nonpropagating if the material is used in a "dry air" environment. For materials that are not sensitive to change in environment from dry air, to water or moist air, the fracture toughness measured under normal laboratory atmospheric conditions provides adequate information of flaw stability (no extension or increase in flaw size expected) at the specified sub-critical stress intensity conditions. For illustration of the potentially dramatic effects of stress corrosion cracking (SCC), let us now consider a 1-in. thick plate of 7-2-1 titanium alloy (7Al, 2Cb, 1Ta) of 107 ksi yield strength (YS) that, as measured by the drop-weight tear test and as evaluated by the explosion tear test, shows resistance to fracture propagation to stresses considerably above YS levels. Thus, even for relatively large flaws such material would have "stable" nonpropagating fracture properties at all levels of elastic stress. As described, fracture mechanics tests of the 7-2-1 titanium alloy resulted in inability to define a plane strain fracture toughness because of high fracture toughness. As the  $K_I$  (stress intensity) level is increased for a fatigue crack (notched) specimen, a point will be reached where the crack tip "dimples," indicating plastic flow in advance of the crack tip and rounding of the notch tip. Thus, the determination of a valid  $K_{Ic}$  (critical) plane strain fracture toughness cannot be made. Now, the 7-2-1 alloy (at least in certain heat treatment and process conditions) happens to be highly sensitive to SCC. The same notched specimen, if loaded in sea water will propagate SCC fracture from the fatigue crack tip at stress intensity levels that may be relatively low. The SCC propagation is "slow" in the sense that it does not involve a fast running (spontaneous) fracture across the test section or through a structural member. Nevertheless, it can occur at rates of "inches per minute or hour" which becomes "fast" in a structural engineering sense. Such crack propagation processes in fracture mechanics terminology are termed "sub-critical crack growth" which translates to growth (movement) of the crack at stress intensities that would not provide "pop-in" or fast extension of the fracture in the usual sense. Thus, we can be involved in situations where the material is fracture-safe in an "inert" environment but not in an environment that catalytically promotes "slow" growth extension of the crack. For some high strength steels, ordinary tap water or "moist" air may be sufficiently active agents for promoting sub-critical SCC crack growth. Aluminum alloys may be similarly affected.

The SCC characteristics of the 7-2-1 titanium alloy were first discovered by B. F. Brown of NRL late in 1964 in the course of extensive investigation of SCC, sub-critical crack growth characteristics of a wide range of materials, including steels, titanium and aluminum alloys (18). This discovery was surprising because titanium alloys had previously been considered immune to SCC.

Brown's experiments were conducted using a simple cantilever loading equipment, shown in Fig. 45 (19). The cantilever specimen, shown in Fig. 46 (left) features a fatigue crack notch and is located at the position of the plastic "cell" container for "flowing" synthetic sea water, actual sea water, or any other liquid of choice, as illustrated in Fig. 46. The stress intensity applied to specimen is defined by equation "1" of Fig. 46 (20). The load level is adjusted by shot placed in the bucket at the end of the lever arm. The thickness "B" is adjusted to the fracture mechanics requirements of retaining a sharp crack front (elimination of dimpling at the crack tip). Such adjustments are possible within limits determined by the level of  $K_{Ic}$  fracture toughness. Materials of very low  $K_{Ic}$  values may require a "B" of only 1/4-in. while materials of higher  $K_{Ic}$  value

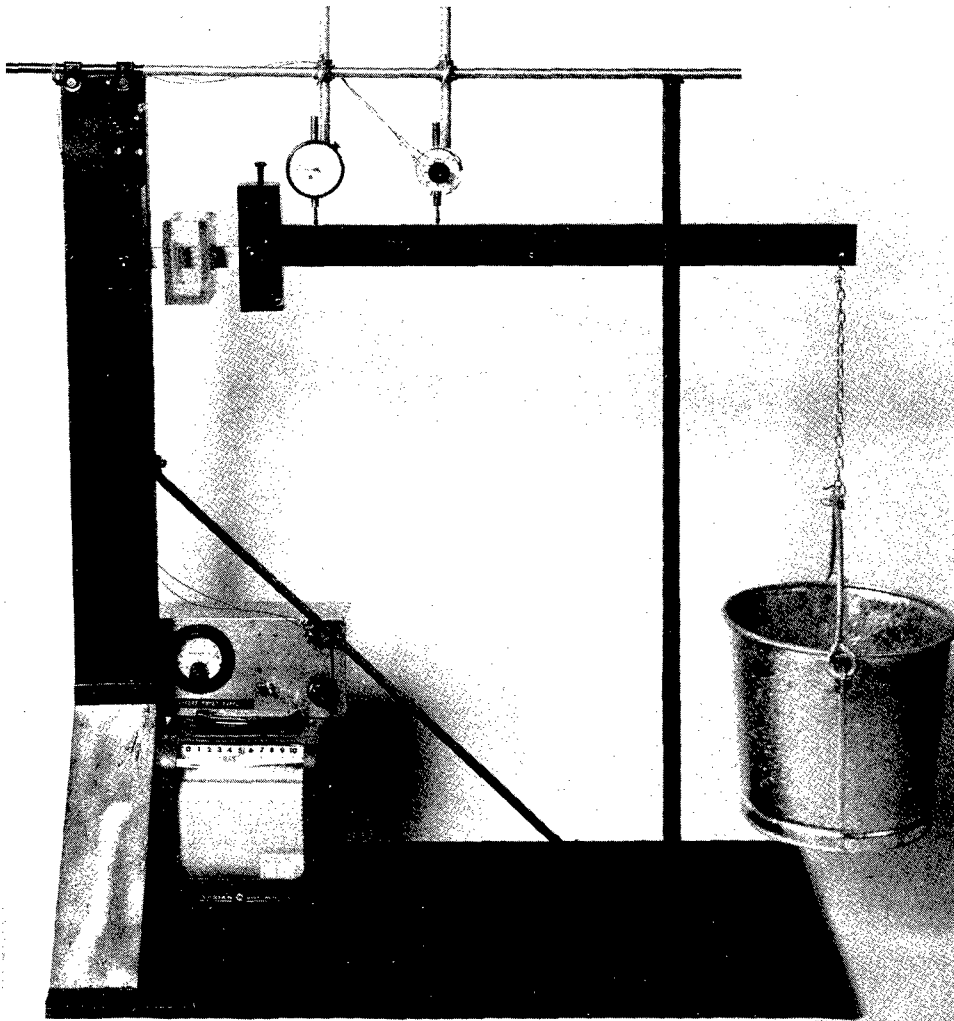


Fig. 45 - NRL cantilever test rack designed by B. F. Brown for evaluating SCC susceptibilities of metals at known levels of plane strain stress intensity. The fatigue-cracked test specimen is located at the point of connection to the vertical frame member.

may require "B" of 1 to 1-1/2-in. to retain plane strain conditions. At some point the dry test  $K_{Ic}$  value may become sufficiently high that a valid  $K_{Ic}$  number cannot be obtained and side growing is then used as an equivalent of increased thickness, again within limits defined by fracture mechanics principles.

The importance of Brown's approach is that it does not rely on obtaining an exact "dry"  $K_{Ic}$  value but in determining the "wet" value for long term, sustained load. Thus, materials which do not allow for obtaining usual accurate  $K_{Ic}$  values may, if SCC results, be measured accurately for the "wet" value. In such a case the dry test values are simply reported as a fracture strength of "lower bound," undefinable fracture mechanics significance. The important aspect is whether or not the wet environment causes a decrease in the resistance of the metal to propagation of the sharp fatigue crack. Brown's experimental approach involves first obtaining the "dry" value of  $K_{Ic}$ , or the breaking strength if an accurate "dry" number is not obtainable. This is then followed by "wet" tests at various levels of stress intensity to determine the time required to obtain definite movement of the crack by SCC if the material is so susceptible. The movement of the crack is

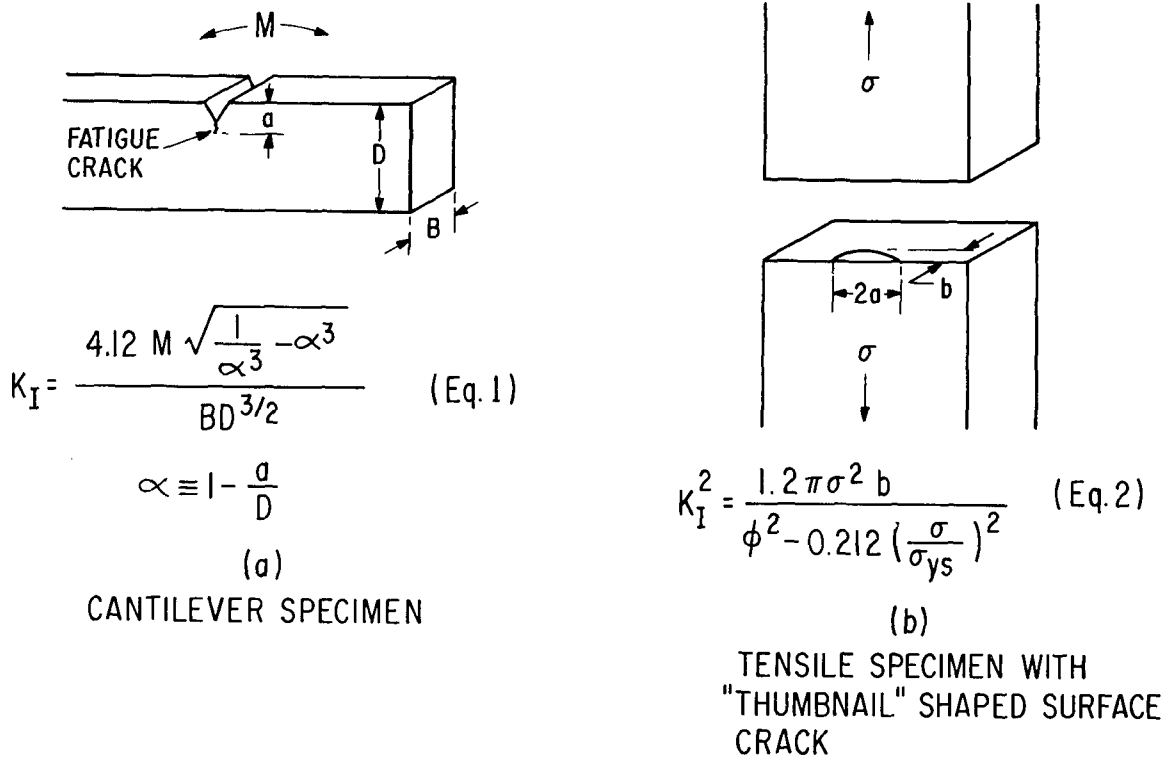


Fig. 46 - Details of the fatigue-cracked specimen devised by B. F. Brown for use in the cantilever test rack. The "thumbnail" crack, tensile test specimen has been used for SCC studies by other investigators, but is less desirable for screening purposes. Respective equations for calculations of stress intensity are indicated.

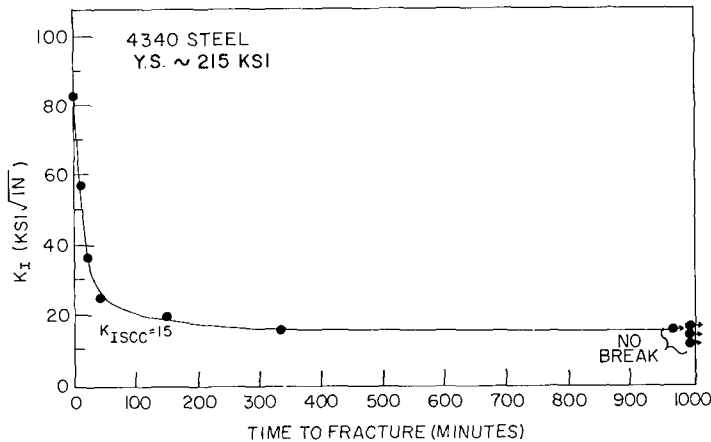


Fig. 47 - Illustrating the general nature of relationships of ( $K_I$ ) stress intensity to time for SCC propagation; data relate to 4340 steel of approximately 215-ksi YS

indicated by dial gages placed on the lever arm. Figure 47 illustrates data for a SAE 4340 steel of approximately 215 ksi YS; Fig. 48 presents similar data for a highly SCC susceptible type of 7-2-1 titanium alloy. It should be noted that the SCC susceptibilities of the 7-2-1 and other titanium alloys varies widely with composition and processing practices; this, essentially is a "worst" case example.

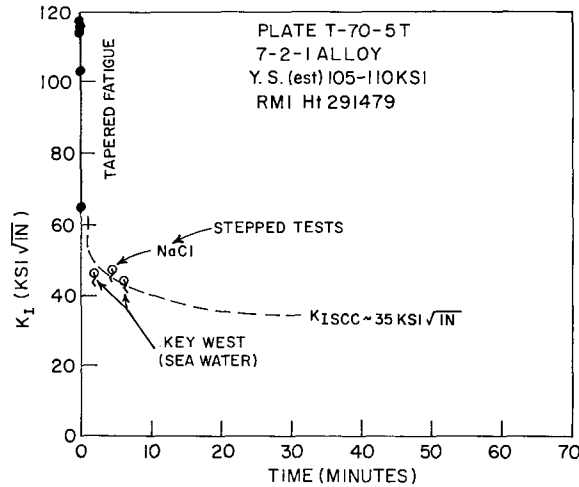


Fig. 48 - Relationship of stress intensity to time for SCC propagation, involving an exceptionally SCC sensitive 7-2-1 titanium alloy.

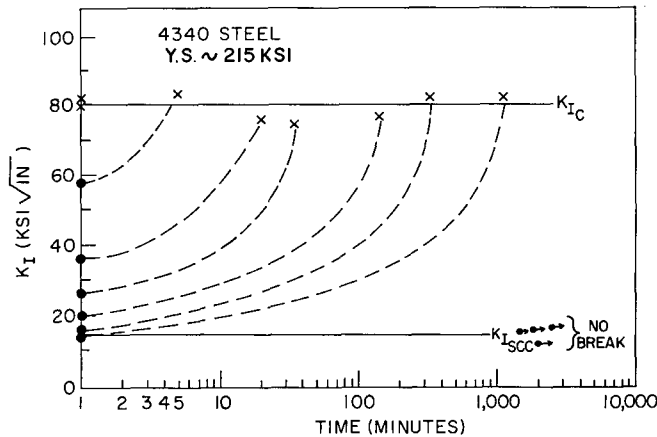


Fig. 49 - Generalized interpretations of the effects of ( $K_I$ ) stress intensity level on the rate of SCC propagation to the point of fast fracture of the cantilever type test bar; as deduced by Brown and Beachem (20)

The fixed load test conditions of the cantilever machine result in increasing of stress intensity with increasing depth of the propagating crack; the breaking times of the specimens have been analyzed by Brown and Beachem (20) in terms of the family of curves shown in Fig. 49. The process is obviously both stress intensity and time dependent - low plane strain stress intensities result in slow sub-critical crack growth rates and higher stress intensities result in fast sub-critical crack growth rates. It is obvious from these data that an asymptotic level is attained by decreasing stress intensity, below which SCC instability is not noted. Brown denotes this as the  $K_{Ic}$  for SCC or simply  $K_{I SCC}$ . Depending on the relative sensitivity to SCC, a material may be characterized by a low value of  $K_{I SCC}$ , a value slightly less than the "dry" value or it may indicate no degradation due to the environment by the fact that "dry" and "wet" stress intensity values for fracture of the specimen are at same.

For the case of the cited, highly SCC sensitive type of 7-2-1 titanium alloy of 107 ksi YS, the  $K_{I\text{ SCC}}$  is 35 ksi  $\sqrt{\text{in}}$ . By application of the standard fracture mechanics calculations applicable to the case of a long flaw (depth to length ratio of 1 to 10), commonly known as the "worst case," the following relationships of stress level and flaw size for SCC propagation may be calculated:

$$a = 0.2 \left( \frac{K_{I\text{ SCC}}}{\sigma} \right)^2$$

a = critical crack  
depth  
 $\sigma$  = applied nominal  
stress

<u>Nominal Stress Level</u>	<u>SCC Critical Flaw Depth for 10-1 Ratio Flaw</u>
1/4 yield stress	0.45-in.
1/2 yield stress	0.11-in.
3/4 yield stress	0.05-in.
at yield stress	0.02-in.

Discussions with experts in the field of fracture mechanics indicate that the  $K_{I\text{ SCC}}$  value may be used as equivalent to a valid  $K_{Ic}$  value obtained by usual test procedures. However, it is granted that verification of the exactness of the calculations may require more precise definition by the tensile test, thumbnail surface crack method, as illustrated in Fig. 46 (right). If these values are essentially correct, as believed by fracture mechanics experts, the fracture safety of such a material becomes critically dependent on the environment.

These facts point to the importance of considering possible SCC sensitivity of materials in fracture-safe design. Returning to Fig. 1, it may be noted that the best steels indicated by the bands are SCC sensitive. In particular, for steels featuring the highest yield strengths and concurrently  $K_{Ic}$  values of less than say 160 ksi  $\sqrt{\text{in}}$ , SCC degradation effects are known to be quite severe, requiring fracture mechanics calculations based on the low value  $K_{I\text{ SCC}}$  numbers rather than on the conventionally determined  $K_{Ic}$  numbers noted in Fig. 1. This fact is emphasized by the bold arrows pointing down and to the left in the subject figure. It should be noted additionally that "wet" environments may relate to "moist" air and not necessarily to immersion in water.

From preliminary screening, the best quality steels appear to be SCC insensitive below approximately 175 ksi YS and generally increase in SCC sensitivity with increased YS above this level. Brown's dramatic finding that titanium alloys of 105-120 ksi YS may, under certain conditions, be highly SCC sensitive effectively moves the fracture propagation resistance of such materials from above YS levels to very low elastic stress levels. The difference being that while fast, "unstable" fracture propagation is not possible as defined by the FTID, relatively "slow" (inches per minute or hour) fracture propagation by SCC in water or possibly even in moist air may become possible. For such conditions the structure may be expected to fail by SCC due to elastic load stresses or even due to residual fabrication stresses.

Because of the critical importance of information on the SCC susceptibilities of high strength structural materials (including base metal, welds, and HAZ) a broadscope program of screening and categorization of the materials described in this report will be conducted by Brown and coworkers. It should be noted that an alloy such as 7-2-1 which may be highly susceptible, can be modified by composition and process history adjustments to greatly alleviate, if not possibly entirely eliminate SCC susceptibilities. This is an area of particular emphasis in the present research program for titanium alloys. It represents another aspect of the optimization process in the evolution of fracture-safe materials.

## IMPLICATIONS OF LOW CYCLE FATIGUE CRACK PROPAGATION ASPECTS

There are two basic aspects of the low cycle fatigue crack growth problem for structures subjected to nominal elastic loads. One aspect relates to the enlargement of small flaws initially present in the structure and the other to the development of such flaws in initially flaw-free regions. In the presence of flaws the "incubation" period for initiation of a fatigue crack is eliminated. Metals which feature high rates of fatigue crack growth are greatly dependent on the incubation period for retention of reasonable low cycle life. If this period is eliminated by flaws, the effect on total cycles to failure can be drastic. Our point of view is that the incubation period cannot be "relied upon" for all types of structures and metals - particularly, it cannot be relied upon for complex structures. In general, whether or not it can be relied upon is a matter of engineering judgment; however, the data to be presented may cause considerable "qualms" to those who would like to utilize the incubation period "across the board" for all types of metals and structures. We shall now discuss this subject in the same general manner of concept plus data used in the previous sections.

For brittle materials, low cycle fatigue crack growth provides for the attainment of the critical instability flaw size for the existing level of nominal stress; the result may then be the initiation of a "fast" fracture which propagates through the structure. Accordingly, for such metals the low cycle fatigue life of structures, which initially contain barely-subcritical flaws, may be a few cycles! For materials of high fracture toughness, low cycle fatigue crack growth at points of stress concentration may result in a gradual slowing down of the fatigue crack as regions of low stress are entered or in the loss of net section which results in increasing the nominal stress and thereby may introduce plastic overload stress conditions. Plastic overload fracture propagation for pneumatically loaded pressure vessels provides a special case if the fatigue crack is long compared to the thickness of the section. In such a case (see discussions in references (1,2)), the plastic overload occurs at the crack tip regions due to local "bulging" of the pressure vessel in the flaw-weakened region, and rupture may occur even though the design nominal hoop stress level is low.

The philosophy that the flaw growth rate is the crucial factor in determining the low cycle life to the point of structural failure was inherent to the NRL selection of a crack propagation test for low cycle fatigue studies. Such studies are being conducted "across the board" for the various materials of interest. For simplicity, a strain range index of mechanical conditions was chosen because it is the only index that can always be measured by strain gaging after "shake-down" of a complex structure. At positions of geometric complexity, the stress conditions existing after fabrication are changed by the applications of proof tests or after several cycles of service loading, i.e., "shake-down." Thus, strain measurements at critical points in a structure can provide meaningful information even though the specific stress level may be indeterminate.

At the present stage of development of these studies, the information obtained relates to fatigue crack growth rates (FCGR) for a specific condition of loading. The crack growth rates provide a screening index of metals that may be expected to have very low, intermediate, or high orders, of "low cycle" fatigue crack growth characteristics. The translation of this information to exact predictions of cycle life is highly dependent on the specific features of the structure and the environment. Considerable accumulation of data for tests conducted under a wide range of loading conditions would be required to

CONFIDENTIAL

evolve more exact definition of structural life, providing the structure is in fact strain range analyzable at critical locations. Considering the ordinary accuracy of determination of levels of strain concentration for specific points of design complexity, it is not necessary to develop test criteria that are more rigorous than the capability to analyze the structure. For example, in pressure vessels the best possible theoretical attainment of nozzle design configuration represents a strain intensification in the order of two times (2X) the nominal hoop stress level. Ordinary nozzle design may easily approach strain intensification levels in the order of 4X, and higher "X" values may be attained for more complex structural configurations. These are the general guidelines used by the design trade involved with ordinary structures for which exact strain gage analyses of the finished product are not made. Such analyses, combined with data to be presented, are adequate for placing the cycle life of such structures in "decade" steps - such as 100, 1000, 10,000 or 100,000 cycles to failure. These "rough cuts" are all that is required, or could be obtained, for most engineering structural applications.

The question to be answered by the compilation of fatigue test data is - for a given metal, in a given environment, what is the expected cycle life considering the general features of the structure at points of stress intensification? The NRL strain range procedure for determining FCGR is designed to provide for broad range screening of metals with sufficient information to answer such questions in the stated manner. The problem of refining the answer lies more in the area of accuracy of indexing the structural design features than in the area of laboratory test refinement.

Tests of structural configurations are an essential part of the refinement studies. The PVRC pressure vessel test series (9,10,11) represent such an approach to the problem involving configuration studies as well as studies of low cycle life based on laboratory tests. The configuration studies separated cycles to propagate a crack through the pressure vessel wall, as well as cycles to fatigue crack initiation. These procedures have served very well for use with low strength steels at temperatures above the NDT for which there is considerable remaining life after the crack incubation period. As we consider metals of higher strength levels, laboratory test data based solely on life-to-fatigue-crack-initiation become inadequate. The reason for this is that in the fracture tough temperature range, low strength materials feature rather long initiation periods plus rather slow FCGR. The metals of high strength discussed in this report have greatly reduced life remaining after fatigue crack initiation, even at temperatures of maximum fracture toughness. The FCGR may become rapid, particularly if environmental effects enter - accordingly, the FCGR becomes a crucial matter of investigation.

Recognizing these aspects of the problem, the NRL approach was specifically tailored to providing definition of FCGR in preference to the usual laboratory studies of "cycles-to-first-cracking." The test development was initiated in 1963, and is now considered sufficiently evolved to proceed on a broad base "across the board" screening of materials of interest.

Plate specimens are cyclically loaded by machines, such as shown in Fig. 50, using a fully-reversed (balanced  $\pm$ ) cycle, with a mean strain of 0. The "starting" fatigue crack is developed by a machined notch in the center of the test section as illustrated in the close-up photograph, Fig. 51. Following the initiation of the crack, measurements of crack growth rates are established for specific strain ranges. The strain range is monitored with a film-type strain gage at the surface of the specimen. The surface length of the crack is precisely measured with an optical micrometer to 0.0001-in. Constant strain range conditions are maintained by adjusting (decreasing) deflection as the crack grows.

It has been determined from these studies that for a specific environment and strain ratio, the growth rate of low cycle fatigue cracks is critically dependent upon the applied total (elastic plus plastic) strain range, as expressed by the relationship:

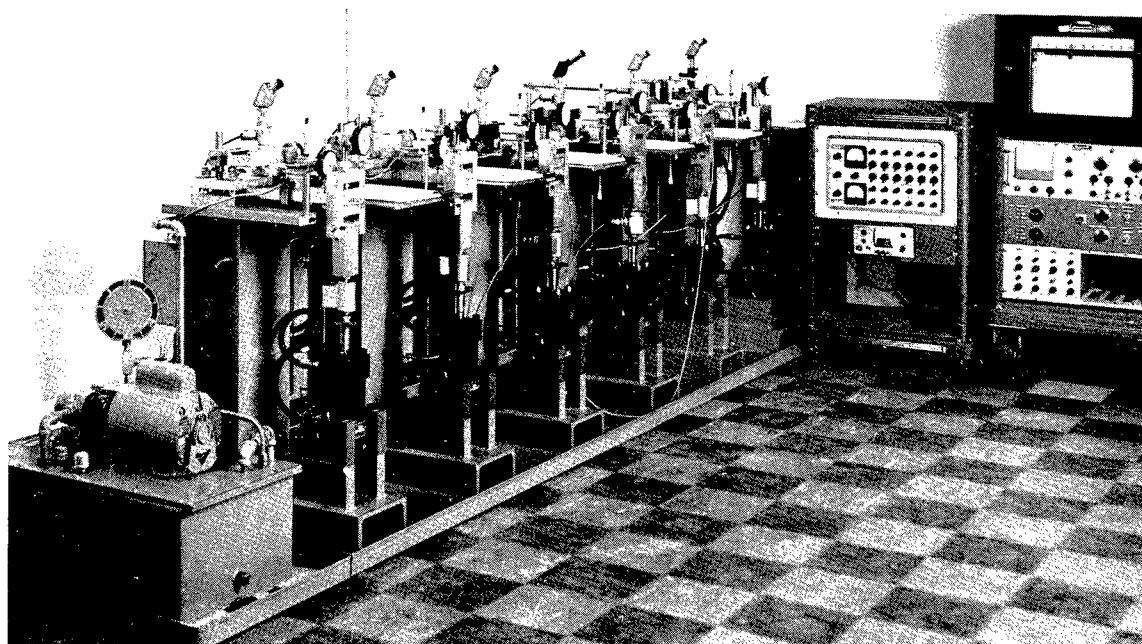


Fig. 50 - General features of low-cycle fatigue test equipment

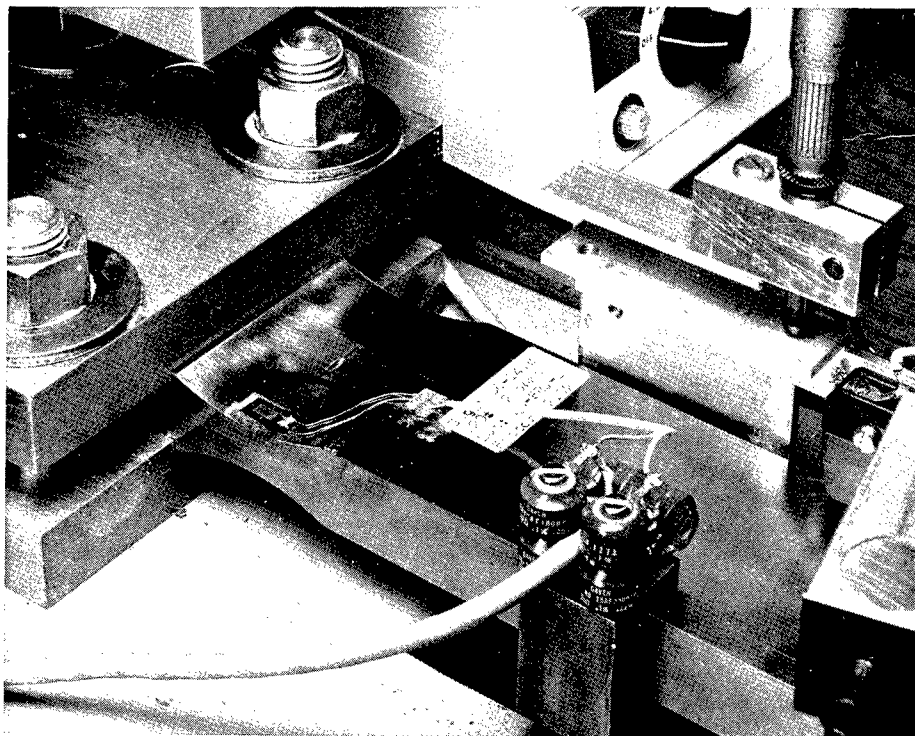


Fig. 51 - Low-cycle fatigue test specimen. Note central-machined notch to facilitate crack initiation and foil-type strain gage for monitoring strain range.

$$dL/dN = C(\epsilon_T)^m$$

where

- L = total crack length
- N = cycles of loading
- $\epsilon_T$  = total strain range
- m = exponent
- C = constant.

By establishing the validity of this relationship, the NRL studies simplified the evaluation of factors such as mean strain and environment by reducing the data to straight lines on a log-log graph. For a specific type of metal, such as Q&T steel of HY-80 composition, FCGR data on a total strain range basis are apparently independent of yield strength (YS) and fracture toughness. This is illustrated in Fig. 52 by the FCGR data for the subject steel heat treated to 80, 130, and 150 ksi YS which fall upon a common curve.

This basic interrelationship establishes the fact that low cycle fatigue rapidly enters the picture of the useful life of structures with the use of steels of high YS. As the YS of materials increases, the value of attainable  $\epsilon_e$  (elastic strain) increases to a point that smaller amounts of  $\epsilon_p$  (plastic strain) can be tolerated for a given life, and finally to a point that no  $\epsilon_p$  can be tolerated. This is illustrated by the FCGR relationships for steels ranging 48 ksi YS (A201B) to 212 ksi YS (D6AC). For easier interpretation of low cycle life data, the FCGR is presented as a function of the ratio of total strain range to the proportional limit strain range. Since the proportional limit strain corresponds to the strain at yield in a conventional tension test, comparisons in Fig. 53 are essentially on a YS basis, and the ratio value of 1.0 corresponds to YS loading for all materials and test conditions cited. Plotting in this form provides for evolving the charts to the status of reference diagrams to be noted as Index of Structural Fatigue Life (ISFL). This is attained by the addition of index estimates of cycle life based on the cycles to growth of very large flaw sizes. From these index points of reference, shown on the right scale of Fig. 53, it may be interpreted that limited fatigue lives (less than 1000 cycles) can be expected for structures of 200 ksi YS steels if a small flaw and plastic strains are present.

In comparing the FCGR curves for various materials, we may take the HY-80 (air) curve as a point of reference; this material requires cycling in the plastic range to develop high FCGR of 100/200 microinches per cycle. In synthetic seawater, the same FCGR may be attained at stresses slightly below yield, Fig. 54. It is noted that the effect of maximum strain level (maximum stress for  $\pm$  loading of zero mean strain) is quite large since the FCGR is related to the 4th power of the strain range ( $m = 4$  in the equation cited). The high strength nonferrous alloys generally feature 6 to 8 power relationships, which account for the steepness of the titanium alloy (air and saltwater) curves. The subject titanium alloy tested in air shows the same 100/200 microinches/inch FCGR at high elastic stress levels as the HY-80 shows in salt water; however, it should be noted that this is the crossing point of the two curves, the slopes are different.

The titanium alloy shows not only increased FCGR in saltwater as compared to air, but also a "break-away" point. At maximum stress levels of approximately 0.6 of yield, the fatigue crack stops propagating in the ordinary, gradual stepwise fashion and begins to "sprint" erratically, indicating a SCC (stress corrosion cracking) rupturing mechanism, resulting effectively in unmeasurably fast FCGR. In fact, the fractures under these conditions are not propagating by the classic fatigue process and are more aptly described as SCC fractures. Electron microscope fractographs are presented in Fig. 55 showing the fracture surfaces produced by classical fatigue crack propagation (left and quasi-cleavage (right) characterizing the SCC fractures above the subject "break-away" point.

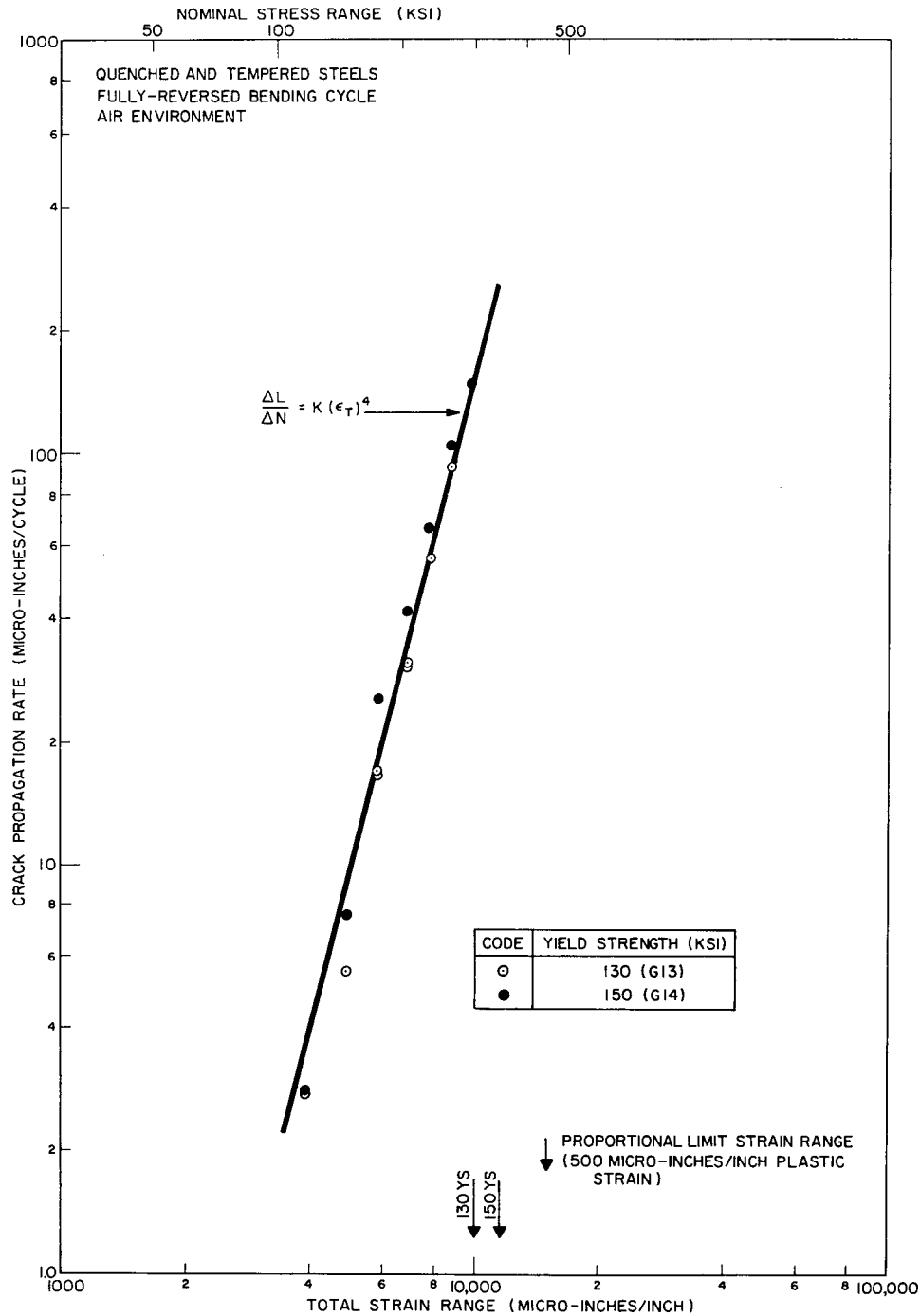


Fig. 52 - Illustrating the common relationship of total strain range (elastic plus plastic) on the fatigue crack growth rates (FCGR) of HY-80 type steel heat treated to 80- 130- and 150-ksi YS levels. The curve relates to previously established data for 80 ksi YS; the indicated data points relate to the 130- and 150-ksi YS levels.

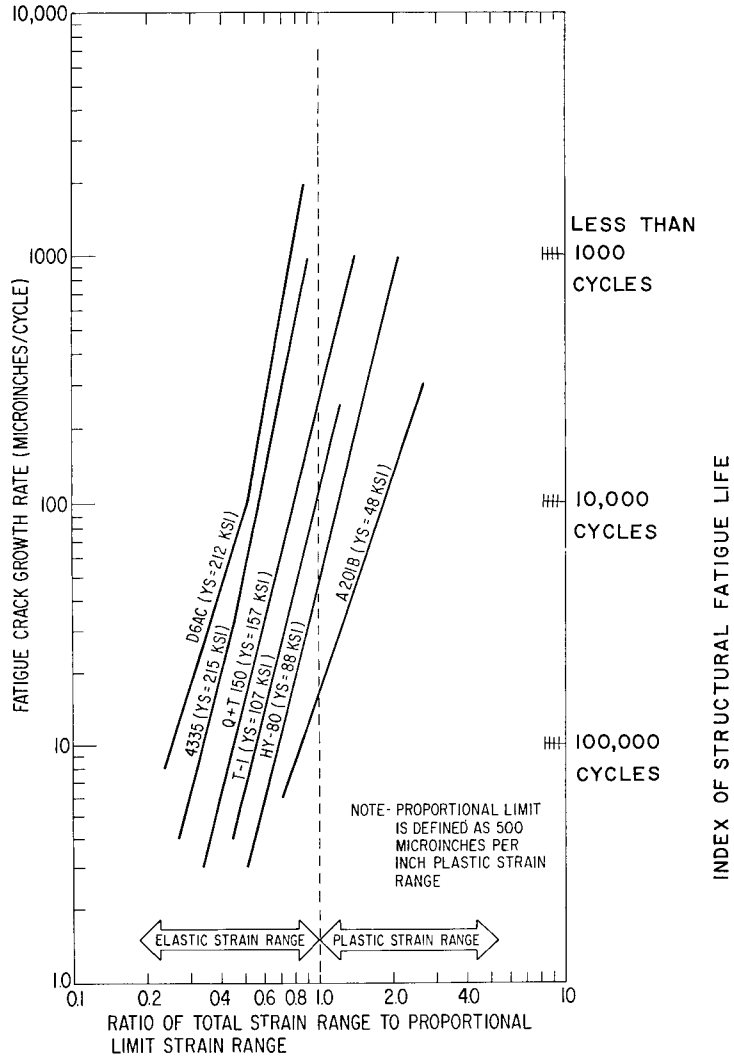


Fig. 53 - Effect of increasing yield strength on the low-cycle fatigue crack growth rates of steels covering a wide range of strength levels. By cross-referencing the relative levels of elastic and plastic stress (plotted on the strain range axis) to the approximate number of cycles required for the growth of a 1-in. crack (plotted on the crack growth rate axis), a simple chart Index of Structural Fatigue Life may be deduced in decade steps for each material. Note that rapidly increasing FCGR may be expected in a structure after the flaw size has attained growth to 1-in. size.

In Fig. 56, the low cycle fatigue characteristics of two high strength aluminum alloys are compared to those of HY-80 steel. The FCGR curves for the aluminum alloys have a much steeper slope and thereby indicate greater sensitivity to strain range than the HY-80 steel. The effects of such high sensitivity are most apparent when one considers that the ISFL drops from 10,000 cycles to less than 1,000 cycles if the loads peak at 70% of the YS rather than approximately 50% of the YS. It may be noted by comparison at the FCGR

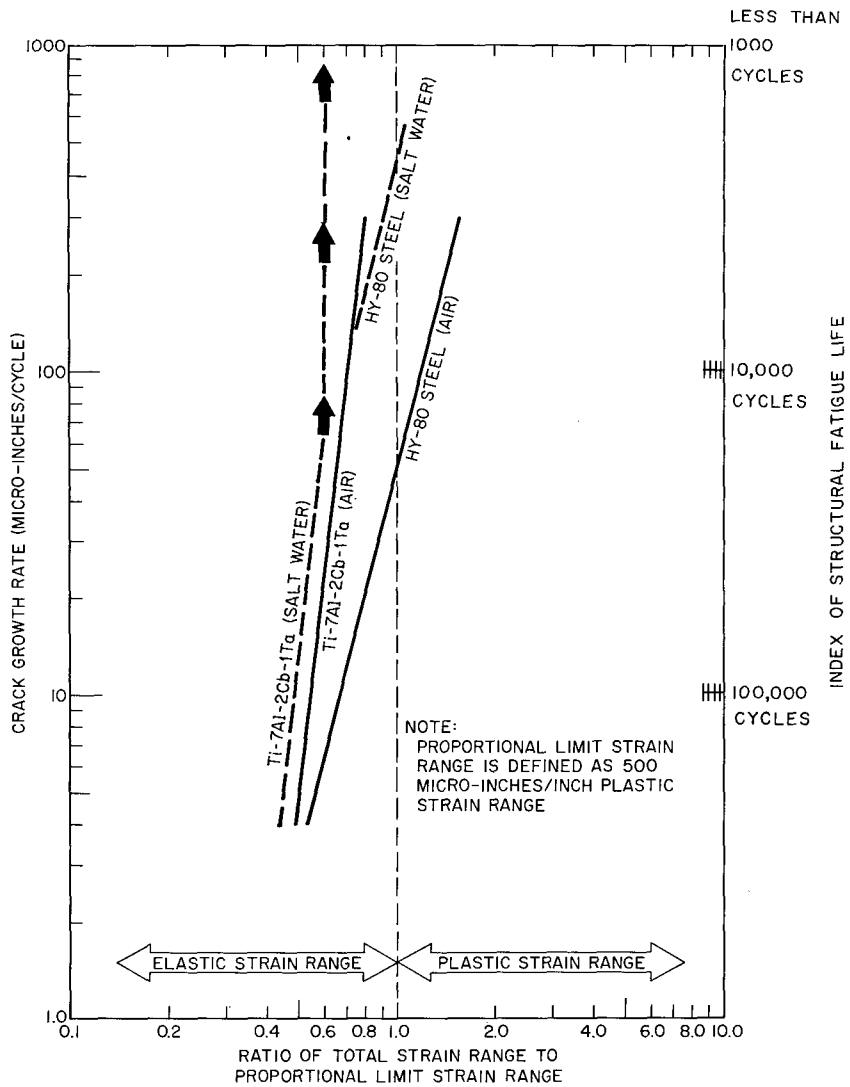


Fig. 54 - Comparison of the low-cycle fatigue crack growth rates of 7-2-1 titanium alloy to those of HY-80 steel in air and in salt water environments. Arrows indicate rapid fracture propagation by SCC (break-away point) for 7-2-1 titanium alloy in salt water.

curves for 7079 aluminum alloy in air and saltwater, that this alloy is also sensitive to aqueous environments; however, a "break-away" point, such as observed for the 7-2-1 titanium alloy, was not observed. The high exponents for FCGR relationships of aluminum alloys indicate that this metal is highly sensitive to design stress, and life in the low cycle fatigue range may drop to low values for high stresses.

There are other practical engineering generalizations that may be made from the data shown in Figs. 53, 54, and 56. The HY-80 steel may be expected to condone regions of plastic strain concentration with retention of relatively long, low cycle life (say 10,000 to 20,000 cycles at points of high (X) strain concentration). Moreover, extensive fracture extension by fatigue will be allowed without collapse of the structure due to fast fracture propagation because of the high fracture toughness of HY-80 steel. Such test predictions have been proven out in large scale model tests. Metals having 6 to 8 power strain range

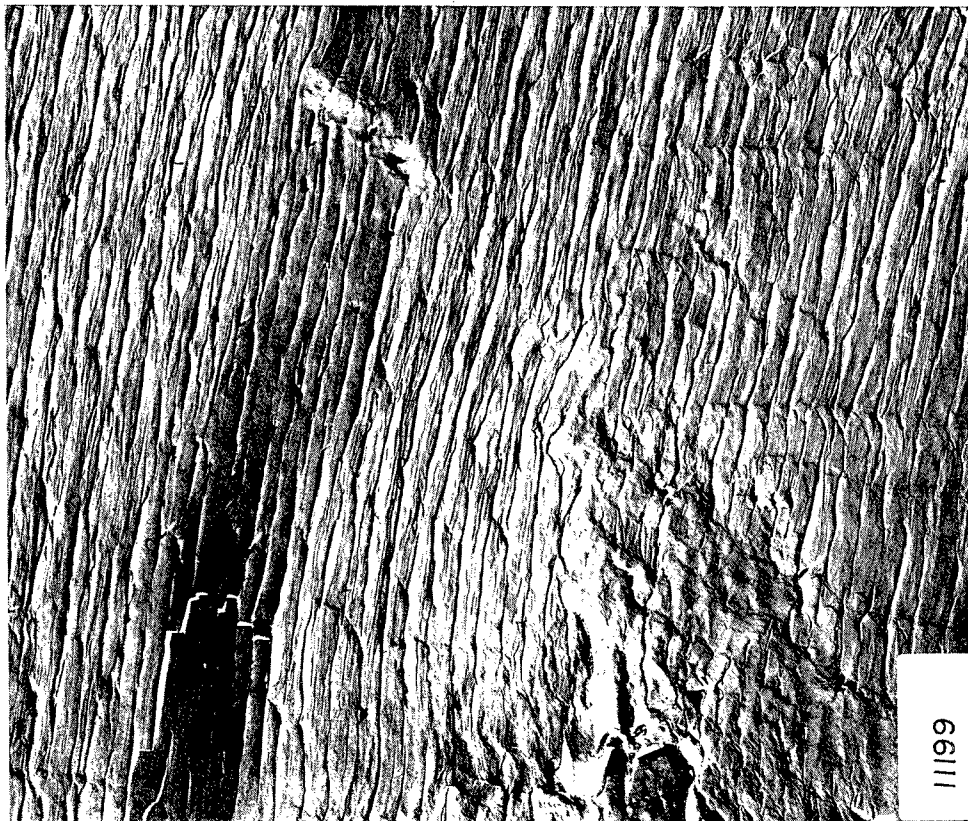


Fig. 55 - Electron microscope fractograph of classical, stepwise fatigue crack propagation observed for Ti-6Al-4V and 7-2-1 titanium alloys in air, 3000X (left). Quasi-cleavage fracture mode developed in fatigue test sample at the "break-away" point of Fig. 54 for the 7-2-1 titanium alloy in salt water, 3000X (right).

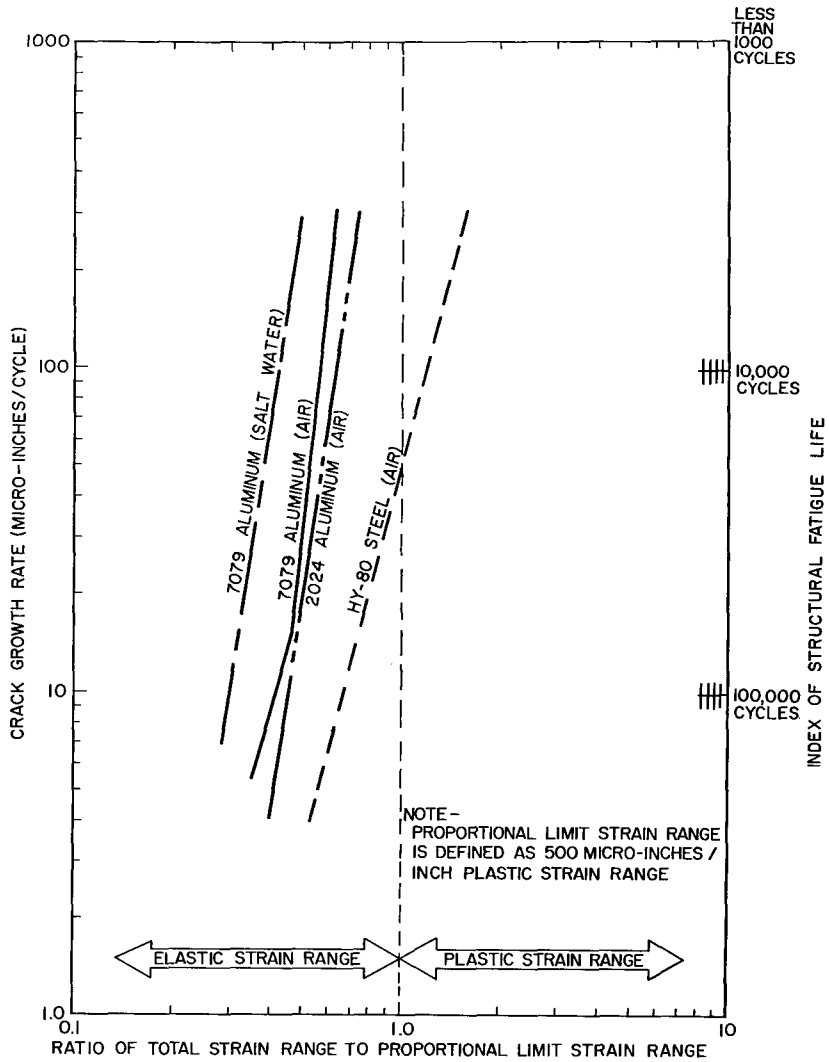


Fig. 56 - Low-cycle fatigue crack growth rates of 2024 and 7079 aluminum alloys compared to HY-80 steel; note increased slopes

sensitivity to FCGR, should be expected under the same conditions to have very limited, low cycle life - say, in the few hundred cycle range. Thus, structures of such metals must be designed with considerable attention to strain concentration "X" factors, and the "X" factors should be reduced as low as possible, even for fracture tough metals. For brittle metals of 6 to 8 power sensitivity, the potentials for fatigue cracks to initiate catastrophic failure becomes very high - prohibitively high for complex structures of high "X" factors.

These data may be summarized to signify that low cycle fatigue action, particularly if coupled with environmental sensitivity, provides potential dangers in the use of relatively brittle metals having high elastic range fatigue fracture propagation characteristics for applications in complex structures. The problem of retaining safety under low cycle fatigue conditions in complex structures is much less severe for the use of fracture tough metals which are not environmentally sensitive. In fact, fracture toughness is the first "premium" item that must be considered - all other aspects then "fall in line" as being

crucial or merely bothersome. These other aspects additionally emphasize that it is most difficult to conceive practical use of high strength brittle metals, except with structural perfection as the sole safeguard. For such metals, the attainment of reasonable guarantee of structural perfection presents vexing and difficult problems of design and quality control carried to the ultimate possible limits.

**STATISTICAL PROBLEMS IN APPLICATIONS OF  
LOW FRACTURE TOUGHNESS METALS**

If we return to the upper bound curve of Fig. 1, it is apparent that there are definite relationships between critical flaw sizes and yield strength levels for steels in the range of 200 to 250 ksi yield strength (YS). These data apply to 1/2 to 1-in. thick steels - for thicker steels the relationships may be expected to move in the direction shown in Fig. 57. The shift to lower  $K_{Ic}$  values and thereby to smaller critical flaw sizes may be expected to be relatively minor for the steels in 180 to 200 ksi YS range but relatively major for steels of progressively higher strength levels, as indicated by the bold arrows.

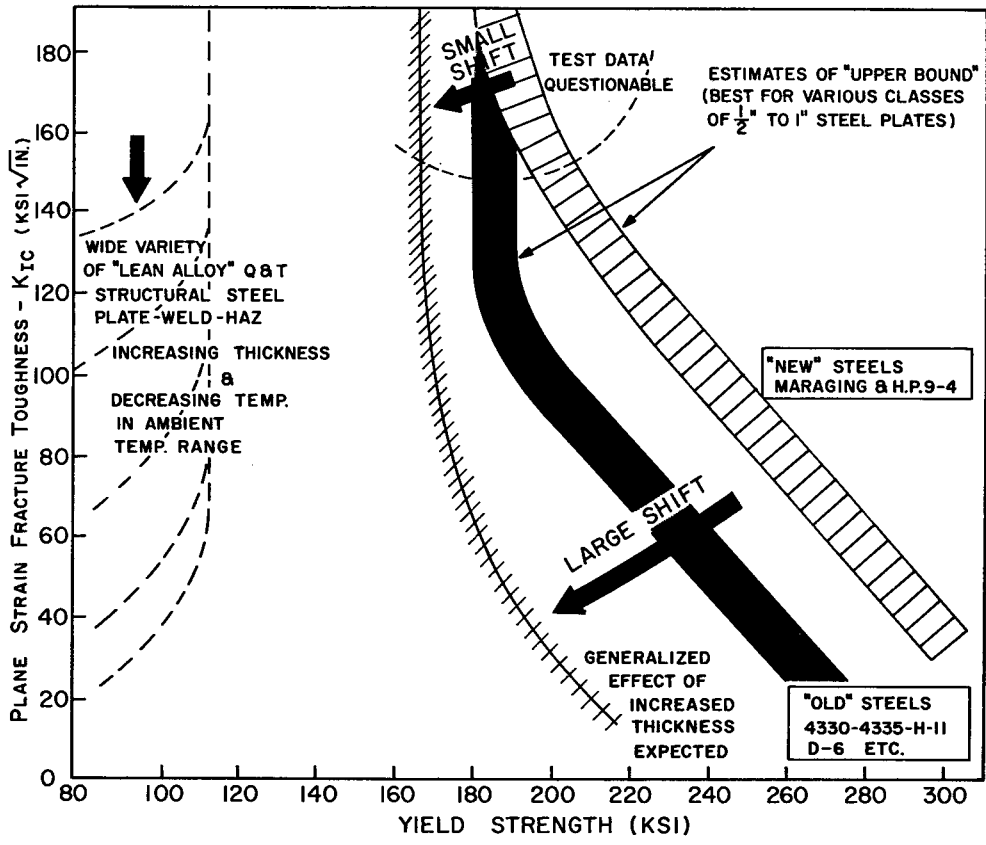


Fig. 57 - Illustrating the expected degrees of decrease of plane strain fracture toughness ( $K_{Ic}$ ) of high strength steels with increased thickness. Also, the potentially low values that may be obtained in plate, weld, and HAZ of various commercial "lean" alloy Q&T steels of relatively low strength level. Major reductions of alloy content, compared to optimized Ni-Cr-Mo compositions, result in marked reduction of "shelf level" fracture toughness, particularly for HAZ regions of weldments.

Now, let us consider the fabrication of a large structure – say a large motor case composed of a large number of high strength steel plates, insert forgings, and welds. Considering only the plates, it is well known that melt, process and heat treatment response variables will unavoidably result in a Gaussian distribution of YS values and a similar distribution of  $K_{Ic}$  fracture toughness values. The insertion in the subject rocket case of members of different thickness – say at heads as compared to the cylinder, at “Y” rings, at ports and openings, etc., implies that the gaussian distributions will be expanded, not only with respect to YS but also with respect to the  $K_{Ic}$  fracture toughness, Fig. 57. From these considerations a very real engineering question arise as “how to cope” with such a multiplicity of analytical problems presented by the range of strength and fracture toughness characteristics involved in a single structure. This problem is quite different from that of a single component item for which it may be assumed that a unique YS and a unique plane strain fracture toughness may be determined. Actually, this is not quite so even for such a single item because of producibility variables – in any event we shall emphasize the multicomponent case for purposes of discussion.

The question is – do we design based on the low end of the frequency distribution curve, the median or the high end? Or – do we specify different criteria for different locations as a function of thickness and potential flaw orientation? Such questions present severe and difficult problems of analysis. For example, if the high end of the distribution range is taken as a conservative approach for a steel of nominal (median value) of say 240 ksi YS, it will result in lack of flaw size inspectability capability because the frequency distribution range will involve the potential presence of higher strength levels of very low  $K_{Ic}$  values. Also, the thicker members may likewise have low  $K_{Ic}$  values as compared to the Fig. 1, 240 ksi steel chart index value of  $K_{Ic}$ . If any other point (median or low end) is taken it will result in unrealistically optimistic analyses of critical flaw sizes. It appears that such “composite” construction at the stated “nominal” high yield stress levels is unrealistic and fracture safety may be assured only by hydrotest procedures; perhaps including repeat tests which involve accepting the possibility of fatigue failure of the “few cycle” life range, if slightly sub-critical flaws are present. This problem is further compounded in hydrotest because both low cycle fatigue crack growth rates and the short time maintaining of static proof loading are environmentally sensitive to stress corrosion cracking flaw growth. It would appear more practical and certainly more astute engineering, to “back-off” to a lower nominal strength level for which there is a much higher inherent fracture toughness and to recover structural efficiency by “working” the metal to slightly higher levels of elastic stress. Each case must be analyzed separately and with a fund of statistical knowledge of the YS and  $K_{Ic}$  fracture toughness frequency distribution ranges involved. It becomes clear that the required sophistication for multicomponent construction based on very high strength low fracture toughness metals is considerably beyond any that has been candidly described in the literature – but it is a fact of life that must be faced.

The statistical type problems are not restricted to the ultra-high strength range – they are inherent to any strength range for which the particular metal has plane strain fracture toughness in the 40 to 160  $K_{Ic}$  (approximate) range and for which there is a sensitivity to compositional and process variables. The lean alloy Q&T steels that have emerged as articles of commerce may have fracture toughness falling in this range (see Fig. 57 – left side plots), depending on specific thickness, temperature variations from summer to winter, weld quality, and HAZ characteristics. The HAZ regions of such steels may involve low energy fracture propagation characteristics that essentially eliminate temperature effects – i.e., low slope, very low shelf value Charpy V curves. Because of the very “lean” levels of alloy content of certain of these steels and marginal or even inadequate metallurgical weldability of specific types, the best that can be obtained for HAZ toughness is difficult to retain in the shop without rigorous technical supervision of the welding processes. We must leave the problem of analyzing the potential statistical, fracture toughness variations in complex structures composed of such “lean alloy” Q&T steels to those who have pertinent, valid data on the subject. Again, we would prefer to

identify and then use metals that do not involve statistical base metal and HAZ variations which may "dip" into the low fracture toughness regime, if it can be avoided economically. Again, the analysis that such approach is, in fact, to the best interest of the particular structure must be made from an engineering basis - do we need to avoid such possibilities or it is possible to accept them? This is not our decision, but we wish to call attention to this problem area. For low alloy Q&T steels in present commercial use the question often arises for a structure "in being" as to the "estimated" level of HAZ fracture toughness. The answer to this question is - that it depends on the welding technique, not the welding techniques supposedly specified, but those that were actually used in the shop by the welder. The nature of the control problem is all too evident to those that are acquainted with the varieties of such steels on the market and with the variety of welding shops that utilize such steels in complex structures.

CONFIDENTIAL

## SUMMARIZATION OF TECHNOLOGICAL IMPLICATIONS

It may be noted that this report emphasizes philosophy as well as the presentation of specific data and test procedures. The problem of practical, fracture-safe design of a broad spectrum of structures, involving a broad spectrum of materials is fortunately definable into various "compartments" that require somewhat different, but fortunately, basically straight-forward solutions. The specific information required for each compartment and the specifics of the use of the resulting information are intimately intertwined. Engineering evaluation difficulties based on present limitations of even existing knowledge may have the appearance of chaos in the high strength metals field to the frustrated designer requiring exact information, or may simply appear as the evident need for more time to evolve additional information to the metallurgist, the welding engineer and to the specialist in structural mechanics. In great part, the "apparencies" of chaos result from basically similar technological situations in other fields, generalized as "chaos in the brickyard"—each investigator is busy in his compartment producing the most polished and perfect "brick," i.e., papers on specific technical subjects. However, these single "bricks" which provide the basic substance required to evolve the total technological structure are simply placed randomly in the literature "brick pile."

This report attempts to select out compartments, identify the individual elements of technical knowledge within the compartments and systematically evolve an integration of the product of the various compartments. It is only by this means that the full picture can emerge of the evolution of fracture-safe design processes, of the promise and limitations of existing materials, and of the road to improvements. It is important that such integrations be made by those who are fortunate by being broadly involved with the multifaceted aspects of the total problem. The socially stimulated "publish or perish" desire to publish in terms of discourse with one's peers in the field leads to a situation such as described by Shaw for the washerwomen of Cardiff, "who earned a precarious living taking in eachother's washing." In our collective field there has been too much attention to debate and discourse on details between experts and too little to candid explanation of the status in any given compartment. Isolation in compartments can lead to "tube vision" and to ignoring of what is going on in other compartments. It is utterly unreasonable to expect that the ultimate engineering user of the information can afford the time to read, integrate and assess the conflicting ideologies of the separate compartments, representing literally hundreds of papers. Library archives or computerized literature searches are not the answer—there is too much "tube vision" bias in the product of the individual compartments. Such integrations of philosophy and of the product of interrelated compartments, as is attempted in this paper, are ordinarily unpublishable in the usual literature outlets because the generally available publications are reserved for "bricks" of effort. There is a real need to counter this situation and the initiative must be taken by collective action of groups active in various broad areas of technical effort.

We have taken such initiative as a matter of basic duty and because it is more satisfying to discuss the total picture—while not initially intended, the integration that has evolved leads to the delivery of specific summary messages of various types to several audiences. These are as follows:

1. To Designers – Moving to the use of high strength metals demands an entirely new perspective of the properties of the materials and a new respect for the critical

nature of the integration of knowledge of structural mechanics and of metals properties. Despite the fact that this paper may have to be read several times to grasp the extent of the necessary integration; such minimal comprehension is critically necessary. Experience with low strength metals cannot be relied upon and in fact, can be highly misleading for this new field.

2. To Investigators and Users of Fracture Mechanics – The case for fracture mechanics in its present state is perfectly valid for the best of metals of the highest strength range or for poor quality metals in lower strength ranges. However, the resourcefulness of the metallurgist and welding engineer in developing best materials to some limit of high strength that do not require such elegant treatment should not be discounted. Also, it should be recognized that mathematical treatment requires a corollary of stress analyzability for the structures. It is not to be expected that all structures will be designed and fabricated to provide for such treatment. The purpose of fracture mechanics is fulfilled for situations involving metallurgical failure to produce materials of high fracture toughness. Do not expect to impose or use rigorous mathematical procedures for materials that do not require it. Lastly, do not attempt to report or use “lower bound,” plane strain fracture toughness numbers for materials of high fracture toughness. Recognize that “no” numbers are obtained and thereby avoid confusion. The usual rationalization that, at least, these represent conservative lower bound levels of higher values that actually cannot be measured is unworthy of any method that is based on calculations using exact numbers. There are too many amateurs entering the scene who conduct invalid fracture mechanics tests—these should either be “educated” or their product excised from the literature, lest they hopelessly muddle what is a promising future for fracture mechanics.

3. To Investigators of Engineering Test Approaches for Fracture-Safe Design – The designer and fabricator of complex structures has a critical need for such information. This report amply documents what can be done in the simplest possible manner if fracture tough materials are used. This area of effort should be expanded to develop such procedures to greater finesse, to evolve an understanding of the significance of classical engineering test methods and to add to the investigation of newly developed test methods. The ultimate promises of such approaches are just as exciting and valuable as those of the mathematical calculation techniques; moreover, the latter have real limitations for the present and the foreseeable future. It is time to recognize that activity in this field is a scientifically defensible course of action.

4. To Metallurgists and Welding Engineers – The comprehensive summarizations of fracture toughness indices for high strength base metal, welds, and HAZ that are evolving will provide “yardstick” comparison of specific capabilities. As chaos of inter-comparison is replaced by “frames of reference,” the course of action will become clearer, individual attainment of success more documentable and individual failures more glaring. Unless, an adequate comprehension of the scope of the problem is attained, out-of-dateness for work in the high strength metals field will be inevitable.

5. To Fabricators – As middlemen between the designers, the metals producers, the welding engineers and the users, you are in a difficult situation. Not all fabrication of high strength materials must move in the direction of precise aerospace practices. This report summarizes strength levels and fracture toughness “transition” points below which continuance of high quality, “ordinary” fabrication is acceptable as compared to levels that require shifting to more exotic types of construction. Be certain not to attempt to use ordinary fabrication for materials that do not allow for such. Similarly, do not be pushed to exotic, expensive construction practices for materials that do not require it. Again, it is essential that the contents of this document be understood before decisions are made affecting costs or reputation. Mistakes in either direction can be financially ruinous.

In closing, we shall repeat that this report must be studied carefully and assimilated in an integrated fashion. The various separate sections should then merge into a coherent whole. It is this "whole" that must be understood before collective progress can be made from a basis of engineering realities.

Any one intending to cope with, or compete in, the production and utilization of high strength metal structures cannot afford to understand less, even if the understanding in some cases represents awareness of limitations rather than exact knowledge. The report represents a first edition on the subject, a subsequent edition is planned for a later date with more philosophy, more information and hopefully more refined procedures than is possible at this date. We have a serious concern—the pace towards widespread use of high strength metals with limited and/or misleading knowledge is much too rapid for comfort. Because of this it is to be expected that there will be lively activity in "failure analyses" and most likely, the usual assessment of cause as being due to accidental or unforeseen errors! However, it is hoped that some of this unproductive activity will be eliminated by the expositions of this text.

## REFERENCES

1. Pellini, W.S., and Puzak, P.P., "Fracture Analysis Diagram Procedures for the Fracture-Safe Engineering Design of Steel Structures," NRL Report 5920, March 15, 1963, and Welding Research Council Bulletin Series No. 88, May 1963
2. Pellini, W.S., and Puzak, P.P., "Practical Considerations in Applying Laboratory Fracture Test Criteria to the Fracture-Safe Design of Pressure Vessels," NRL Report 6030, November 5, 1963; also, Trans. of the ASME, Series A, Journal of Engineering for Power, October 1964, pp. 429-443
3. NavShips 250-634-3, "Method for Conducting Drop-Weight Test to Determine Nil-Ductility Transition Temperature of Ferritic Steels," August 21, 1962; also ASTM E208-63T, "Tentative Method for Conducting Drop-Weight Test to Determine Nil-Ductility Transition Temperature of Ferritic Steels," 1963
4. Pellini, W.S., and Puzak, P.P., "Factors that Determine the Applicability of High Strength Quenched and Tempered Steels to Submarine Hull Construction," NRL Report 5892, December 5, 1962
5. Pellini, W.S., Steele, L.E., and Hawthorne, J.R., "Analysis of Engineering and Basic Research Aspects of Neutron Embrittlement of Steels," NRL Report 5780, April 17, 1962; also, The Welding Journal 41 (No. 10) 455s, October 1962
6. Puzak, P.P., "Advances in Fracture-Safe Design for Structural Steels - 1943-1963," Oral presentation at Special Conference of AISI Subcommittee on Line Pipe Research, Pittsburgh, Pa., April 29, 1963; no manuscript available
7. Eiber, R.J., and McClure, G.M., "Laboratory Fracture Tests - Their Relation to Full-Scale Properties," Oil and Gas Journal, September 23, 1963
8. Brubaker, E.H., and Dennison, J.D., "Use of the Battelle Drop-Weight Tear Test for Determining the Notch Toughness of Line Pipe Steel," Presented at the Seventh Mechanical Working Conference of the Metallurgical Society of AIME, Pittsburgh, Pa., January 19, 1965
9. Lange, E.A., and Klier, E.P., "A Study of Fracture Development and Materials Properties in PVRC Vessels 1 and 2," The Welding Journal 41 (No. 2) 53s to 61s, February 1962
10. Kooistra, L.F., Lange, E.A., and Pickett, A.G., "Full-Size, Pressure-Vessel Testing and Its Application to Design," Trans. of ASME, Journal of Engineering for Power, Vol. 86, Series A, No. 4, October 1964
11. Lange, E.A., Pickett, A.G., and Wiley, R.D., "Failure Analysis of PVRC Vessel No. 5. Part I - Study of Materials, Properties and Fracture Development," Welding Research Council Bulletin No. 98 August 1964

12. Pellini, W.S., Goode, R.J., Huber, R.W., Howe, D.G., Judy, R.W., Puzak, P.P., Lloyd, K.B., Lange, E.A., DeFelice, E.A., Crooker, T.W., Morey, R.E., Chapin, E.J., and McGeady, L.J., "Metallurgical Characteristics of High Strength Structural Materials (Sixth Quarterly Report)," NRL Report 6258, December 1964
13. Willner, A.R., and Sullivan, V.E., "Metallurgical Investigation of Titanium Alloys for Application to Deep-Diving Submarines," DTMB Progress Report 1482, December 1960
14. Beachem, C.D., "Electron Fractographic Studies of Mechanical Fracture Processes in Metals," TRANS of the ASME, Journal of Basic Engineering, 1964
15. Beachem, C.D., and Meyn, D.A., "Illustrated Glossary of Fractographic Terms," NRL Memorandum Report 1547, June 1964
16. Beachem, C.D., Brown, B.F., and Edwards, A.J., "Characterizing Fractures by Electron Fractography, Part XII. Illustrated Glossary, Section 1, Quasi Cleavage," NRL Memorandum Report 1432, June 1963
17. Judy, R.W., Jr., Crooker, T.W., Morey, R.W., Lange, E.A., Beachem, C.D., and Goode, R.J., "Fractography Analysis of Ti-7Al-2Cb-1Ta and Ti-6Al-4V Fractures Developed in 'Wet Fatigue'," (pending publication as an NRL report)
18. Brown, B.F., et al, "Marine Corrosion Studies, Third Interim Report of Progress," (pending publication as an NRL report)
19. Brown, B.F., "A New Stress-Corrosion-Cracking Test Procedure for High-Strength Alloys," to be presented at 68th Annual Meeting of ASTM, June 13-18, 1965, Lafayette, Indiana (pending ASTM publication)
20. Brown, B.F., and Beachem, C.D., "A Study of the Stress Factor in Corrosion Cracking by Use of the Pre-Cracked Cantilever Beam Specimen," to be presented by G.R. Irwin at Joint "SEMAINE de la CORROSION" (held by International Committee on Thermodynamics and Electrochemistry and The European Federation on Corrosion), June 7-11, 1965, Brussels, Belgium

## DOCUMENT CONTROL DATA - R&amp;D

(Security classification of title, body of abstract and indexing annotation must be entered when the overall report is classified)

1. ORIGINATING ACTIVITY (Corporate author) U.S. Naval Research Laboratory Washington, D.C. 20390		2a. REPORT SECURITY CLASSIFICATION UNCLASSIFIED	
		2b. GROUP	
3. REPORT TITLE REVIEW OF CONCEPTS AND STATUS OF PROCEDURES FOR FRACTURE-SAFE DESIGN OF COMPLEX WELDED STRUCTURES INVOLVING METALS OF LOW TO ULTRA-HIGH STRENGTH LEVELS			
4. DESCRIPTIVE NOTES (Type of report and inclusive dates) Special Summary Progress Report			
5. AUTHOR(S) (Last name, first name, initial) Pellini, W.S.            Lange, E.A. Goode, R.J.            Huber, R.W. Puzak, P.P.			
6. REPORT DATE June 1965		7a. TOTAL NO. OF PAGES 90	7b. NO. OF REFS 20
8a. CONTRACT OR GRANT NO. M01-05, M01-18, M03-01, 63R05-24A & 63R05-24B, F01-17, & MIPR Eng-Nav-65- 12 b. PROJECT NO. SF 020-01-01-0724, -0731, -0850, & -0854; RR 007-01-46-5405 & -5420; WW 041; & SP-00405 c. d.		9a. ORIGINATOR'S REPORT NUMBER(S) NRL Report 6300	
		9b. OTHER REPORT NO(S) (Any other numbers that may be assigned this report)	
10. AVAILABILITY/LIMITATION NOTICES Unlimited availability. Available at Clearinghouse for Federal Scientific and Technical Information (CFSTI), Sills Building, 5285 Port Royal Road, Springfield, Virginia 22151			
11. SUPPLEMENTARY NOTES		12. SPONSORING MILITARY ACTIVITY Department of the Navy (Bureau of Ships, Office of Naval Research, NRL Special Projects), & Army Corps of Engineers	
13. ABSTRACT This report presents integrated analyses and substantiating data on problems of metallurgical optimization and solutions to fracture-safe design and fabrication of large welded structures, utilizing high strength metals. The apparent complexities of attaining practical engineering use of high strength metals derive primarily from lack of appreciation of the close interrelationships that exist between the intrinsic susceptibilities of these metals to various failure modes and the intrinsic structural mechanics features of the structures. Metals of high intrinsic resistance to failure may be matched to structures of high intrinsic design complexity and ordinary fabrication techniques, with assurance of structural safety. Metals of low intrinsic resistance to failure must be matched only to structures that are exactly stress analyzable and thereby are restricted to designs of the utmost attainable simplicity and to fabrication by techniques of utmost precision. Such separations are basic to the theme of this report and provide the "starting point" for analyses of the potentials of utilizing various metals, within the range of metallurgically attainable strength levels. The metallurgical problems of optimizing the base metals, welds and heat-affected zones have been complicated by the absence of parametric "frames of reference" required as bases of comparison. The absence of such broad-base guide lines arises from the failure to evolve an adequate understanding of the significance of conventional engineering tests and from the previous absence of definitive tests that provide assessment of failure mode sensitivities across the full spectrum of materials and attainable strength levels. The development of such test procedures has been one of the principal aims of the investigations conducted by the authors and their associates. The spectrum view that has emerged clearly defines metals and specific strength ranges that provide for matching to applications involving conventional fabrication of complex structures as compared to those that require exact design and fabrication. Thus, applications that may provide fracture-safe design based on the use of simple engineering test methods may be separated from applications that require the exact mathematical analyses of fracture mechanics.			

14. KEY WORDS	LINK A		LINK B		LINK C	
	ROLE	WT	ROLE	WT	ROLE	WT
Engineering Principles Fracture-Safe Design Structures Fracture Analysis Diagram Fracture Toughness Index Diagrams Fracture Mechanics Thickness Effects Weld Metal Properties Processing Effects Low Cycle Fatigue Fatigue Crack Growth Rates Index of Structural Fatigue Life Heat-Affected Zone Properties Fractography Micromechanisms of Fracture Stress Corrosion Cracking Drop-Weight Test Drop-Weight Tear Test Explosion Tear Test						
Crack Arrest Temperature Nil-Ductility Transition Q&T Steels High Strength Steels High Strength Titanium & Aluminum Alloys						

INSTRUCTIONS

1. **ORIGINATING ACTIVITY:** Enter the name and address of the contractor, subcontractor, grantee, Department of Defense activity or other organization (*corporate author*) issuing the report.
- 2a. **REPORT SECURITY CLASSIFICATION:** Enter the overall security classification of the report. Indicate whether "Restricted Data" is included. Marking is to be in accordance with appropriate security regulations.
- 2b. **GROUP:** Automatic downgrading is specified in DoD Directive 5200.10 and Armed Forces Industrial Manual. Enter the group number. Also, when applicable, show that optional markings have been used for Group 3 and Group 4 as authorized.
3. **REPORT TITLE:** Enter the complete report title in all capital letters. Titles in all cases should be unclassified. If a meaningful title cannot be selected without classification, show title classification in all capitals in parenthesis immediately following the title.
4. **DESCRIPTIVE NOTES:** If appropriate, enter the type of report, e.g., interim, progress, summary, annual, or final. Give the inclusive dates when a specific reporting period is covered.
5. **AUTHOR(S):** Enter the name(s) of author(s) as shown on or in the report. Enter last name, first name, middle initial. If military, show rank and branch of service. The name of the principal author is an absolute minimum requirement.
6. **REPORT DATE:** Enter the date of the report as day, month, year; or month, year. If more than one date appears on the report, use date of publication.
- 7a. **TOTAL NUMBER OF PAGES:** The total page count should follow normal pagination procedures, i.e., enter the number of pages containing information.
- 7b. **NUMBER OF REFERENCES:** Enter the total number of references cited in the report.
- 8a. **CONTRACT OR GRANT NUMBER:** If appropriate, enter the applicable number of the contract or grant under which the report was written.
- 8b, 8c, & 8d. **PROJECT NUMBER:** Enter the appropriate military department identification, such as project number, subproject number, system numbers, task number, etc.
- 9a. **ORIGINATOR'S REPORT NUMBER(S):** Enter the official report number by which the document will be identified and controlled by the originating activity. This number must be unique to this report.
- 9b. **OTHER REPORT NUMBER(S):** If the report has been assigned any other report numbers (*either by the originator or by the sponsor*), also enter this number(s).
10. **AVAILABILITY/LIMITATION NOTICES:** Enter any limitations on further dissemination of the report, other than those

imposed by security classification, using standard statements such as:

- (1) "Qualified requesters may obtain copies of this report from DDC."
- (2) "Foreign announcement and dissemination of this report by DDC is not authorized."
- (3) "U. S. Government agencies may obtain copies of this report directly from DDC. Other qualified DDC users shall request through \_\_\_\_\_."
- (4) "U. S. military agencies may obtain copies of this report directly from DDC. Other qualified users shall request through \_\_\_\_\_."
- (5) "All distribution of this report is controlled. Qualified DDC users shall request through \_\_\_\_\_."

If the report has been furnished to the Office of Technical Services, Department of Commerce, for sale to the public, indicate this fact and enter the price, if known.

11. **SUPPLEMENTARY NOTES:** Use for additional explanatory notes.
12. **SPONSORING MILITARY ACTIVITY:** Enter the name of the departmental project office or laboratory sponsoring (*paying for*) the research and development. Include address.
13. **ABSTRACT:** Enter an abstract giving a brief and factual summary of the document indicative of the report, even though it may also appear elsewhere in the body of the technical report. If additional space is required, a continuation sheet shall be attached.  
 It is highly desirable that the abstract of classified reports be unclassified. Each paragraph of the abstract shall end with an indication of the military security classification of the information in the paragraph, represented as (TS), (S), (C), or (U).  
 There is no limitation on the length of the abstract. However, the suggested length is from 150 to 225 words.
14. **KEY WORDS:** Key words are technically meaningful terms or short phrases that characterize a report and may be used as index entries for cataloging the report. Key words must be selected so that no security classification is required. Identifiers, such as equipment model designation, trade name, military project code name, geographic location, may be used as key words but will be followed by an indication of technical context. The assignment of links, roles, and weights is optional.